

Review

Nitrogen Containing Heterocycles as Anticancer Agents: A Medicinal Chemistry Perspective

Adarsh Kumar ^{1,†}, Ankit Kumar Singh ^{1,†}, Harshwardhan Singh ¹, Veena Vijayan ¹, Deepak Kumar ¹, Jashwanth Naik ¹, Suresh Thareja ¹, Jagat Pal Yadav ², Prateek Pathak ³, Maria Grishina ³, Amita Verma ⁴, Habibullah Khalilullah ⁵, Mariusz Jaremko ⁶, Abdul-Hamid Emwas ⁷ and Pradeep Kumar ^{1,*}

¹ Department of Pharmaceutical Sciences and Natural Products, Central University of Punjab, Ghudda, Bathinda 151401, India

² Pharmacology Research Laboratory, Faculty of Pharmaceutical Sciences, Rama University, Kanpur 209217, India

³ Laboratory of Computational Modeling of Drugs, Higher Medical and Biological School, South Ural State University, 454008 Chelyabinsk, Russia

⁴ Bioorganic and Medicinal Chemistry Research Laboratory, Department of Pharmaceutical Sciences, Sam Higginbottom University of Agriculture, Technology and Sciences, Prayagraj 211007, India

⁵ Department of Pharmaceutical Chemistry and Pharmacognosy, Unaizah College of Pharmacy, Qassim University, Unayzah 51911, Saudi Arabia

⁶ Smart-Health Initiative and Red Sea Research Center, Division of Biological and Environmental Sciences and Engineering, King Abdullah University of Science and Technology, Thuwal 23955-6900, Saudi Arabia

⁷ Core Labs, King Abdullah University of Science and Technology, Thuwal 23955-6900, Saudi Arabia

* Correspondence: pradeepyadav27@gmail.com

† These authors contributed equally to this work.



Citation: Kumar, A.; Singh, A.K.; Singh, H.; Vijayan, V.; Kumar, D.; Naik, J.; Thareja, S.; Yadav, J.P.; Pathak, P.; Grishina, M.; et al. Nitrogen Containing Heterocycles as Anticancer Agents: A Medicinal Chemistry Perspective. *Pharmaceuticals* **2023**, *16*, 299. <https://doi.org/10.3390/ph16020299>

Academic Editors: Antonella Messore, Valentina Noemi Madia and Michael Schmiech

Received: 9 January 2023

Revised: 26 January 2023

Accepted: 28 January 2023

Published: 14 February 2023



Copyright: © 2023 by the authors. Licensee MDPI, Basel, Switzerland. This article is an open access article distributed under the terms and conditions of the Creative Commons Attribution (CC BY) license (<https://creativecommons.org/licenses/by/4.0/>).

Abstract: Cancer is one of the major healthcare challenges across the globe. Several anticancer drugs are available on the market but they either lack specificity or have poor safety, severe side effects, and suffer from resistance. So, there is a dire need to develop safer and target-specific anticancer drugs. More than 85% of all physiologically active pharmaceuticals are heterocycles or contain at least one heteroatom. Nitrogen heterocycles constituting the most common heterocyclic framework. In this study, we have compiled the FDA approved heterocyclic drugs with nitrogen atoms and their pharmacological properties. Moreover, we have reported nitrogen containing heterocycles, including pyrimidine, quinolone, carbazole, pyridine, imidazole, benzimidazole, triazole, β -lactam, indole, pyrazole, quinazoline, quinoxaline, isatin, pyrrolo-benzodiazepines, and pyrido[2,3-d]pyrimidines, which are used in the treatment of different types of cancer, concurrently covering the biochemical mechanisms of action and cellular targets.

Keywords: heterocyclic; anti-cancer; FDA; nitrogen-containing heterocyclic; biological activity

1. Introduction

Carcinoma is the abnormal growth of normal cells that typically grow beyond their original boundaries, invade surrounding areas, spread to other organs, and result in metastasis, which is one of the main causes of cancer-related death, the second most common cause of deaths across the globe [1]. Around 10.0 million cancer-related fatalities (9.9 million excluding squamous cell carcinoma) and 19.3 million new cases of cancer (18.1 million excluding squamous cells carcinoma) were estimated globally by 2020. Up to 25% of cancer cases are caused by cancer-causing illnesses such as hepatitis as well as human papillomavirus infections. The most common malignancies in both genders are breast, lung, stomach, colorectal, thyroid, liver, and ovarian. The most fatal cancers are lung (1.8 million), liver (830,000), stomach (769,000), breast cancer (627,000), and colorectal (935,000). The most commonly diagnosed cancers worldwide are lung (2.2 million), breast (2.09 million), colorectal (1.9 million), prostate (1.28 million), skin (1.04 million), and stomach (1.04 million).

The prevalence of cancer is rising worldwide, burdening people and families emotionally and financially [2–5].

In wealthy nations, cancer has become one of the leading causes of mortality. A DNA mutation can cause cancer to develop. The etiology of the gene can be either adopted or hereditary. Both genetic and epigenetic variables are involved. The co-carcinogenic responses, hormonal impacts, and many other epigenetic variables are tumor promoters. Conversion of protooncogene to oncogene and the inactivation of tumor-suppressing genes are the two genetic factors responsible for cancer. Cancer cells can divide quickly or slowly, as in the cases of plasma tumor cells and Burkitt's lymphoma, respectively. In the cancer cell growth, proliferation is the crucial element, which is very quick compared to the regular cells. When cancerous cells proliferate out of control, alterations occur in the proteins and growth factors, telomerase expression, tumor-associated angiogenesis, and intracellular signaling pathways that regulate apoptosis and cell cycles [6]. Sulfur mustards were utilized in battle throughout the First World War, producing marrow aplasia during that period and later being applied to the chemoprevention. In the last 30–50 years, several other types were developed, including folate analogues, pyrimidine inhibitors, and purine inhibitors. Depending on the type of cancer, different anti-cancer medicines were chosen for the treatment. Surgery, which is similar to plucking a seed from its shell, can eradicate benign tumors, typically referred as nonmalignant [7,8].

Heterocyclic are substances where the ring carbon atom has been replaced by one of the other three elements, oxygen, nitrogen, or sulphur, in the parent scaffold. The existence of the modified atoms as well as the size of the scaffold in the compound affects its physical and chemical properties. Modifications to a molecule's heterocyclic ring structure can alter its anti-inflammatory, antibacterial, anti-tumor, antiviral, and antifungal properties. In nature, nitrogen-containing heterocyclic compounds are widely distributed and serve as the basis for many different substances, including alkaloids, vitamins, hormones, dyes, antibiotics, herbicides, and pharmaceuticals [9–11]. There are few examples of naturally occurring molecules with nitrogen atoms, including morphine, caffeine, nicotine, thiamine, and atropine, known as alkaloids. The number of nitrogen atoms found inside the ring, such as three, four, five, as well as six, is used to categorize these molecules. Pyrrole and azoles are five membered rings containing one nitrogen, while imidazole and pyrazole have two atoms of nitrogen. Pyridine, a six-membered ring with one nitrogen atom, and pyrimidine, a six-membered ring with two nitrogen atoms, are the best examples of nitrogen containing heterocycles [12].

For many years, nitrogen-containing heterocycles have attracted attention of scientists due to their structural variety and biological importance. The present study covers the most recent developments in nitrogen-containing heterocyclic compounds as potential cancer chemotherapeutics. With approximately 60% of unique small-molecules containing a nitrogen heterocyclic, a quick glance through FDA archives demonstrates the structural significance of nitrogen-based heterocycles in drug design. Due to the formation of hydrogen bonds between these heteroatoms and DNA, complexes containing heteroatoms are more stable. In reality, the strength of the binding between DNA and heterocyclic compounds corresponds with the anti-cancer impact [13–15]. Natural products, pharmaceuticals, organic materials, sensitizers, copolymers, dyestuff, dyes and corrosion inhibitors all contain nitrogen heterocycles in their skeleton [16–20].

In addition to their important structural role in herbal drugs, e.g., codeine, morphine, vinblastine, reserpine, procaine, papaverine, emetine, and cardiac glycosides, nitrogen-containing heterocyclic compounds are also widely present in synthetic drugs, e.g., azidothymidine, chlorpromazine, antipyrine, metronidazole, diazepam, captopril, isoniazid, chloroquinine, and barbituric acid [21]. Numerous active medicines and natural compounds contain heterocyclic scaffolds as their fundamental nuclei. According to statistics, $\geq 85\%$ physiologically active molecules are heterocycles or contain one nitrogen atom in their intricate structures [22]. We searched "Nitrogen containing heterocyclic compounds" on ChEMBL (<https://www.ebi.ac.uk/chembl/>, accessed on 22 November 2022), an open

access biological database, and found 2,331,700 compounds on 467 targets. With the help of ChEMBL, we plotted a graph between the molecular weight of nitrogen containing heterocyclic compounds with log P values and color, which indicated the violation of rule of 5 (RO5). LogP values of the reported molecules were directly correlated with their molecular weight (Figure 1). As there are so many molecules violating RO5, to explore the correlation of RO5 with activity, we have plotted a heatmap of 929 nitrogen containing molecules violating RO5 against different biological targets, but certain molecules violating RO5 have biological activities (Figure 2). Drug development commonly employs Lipinski's rule of five. This criterion makes it possible to determine whether a bioactive molecule would likely possess the physical and chemical traits necessary for oral bioavailability. According to the Lipinski rule, certain physicochemical features determine how a medicine will behave in terms of absorption, distribution, metabolism, and excretion. The PChEMBL average value indicates the activity count for particular compounds [23].

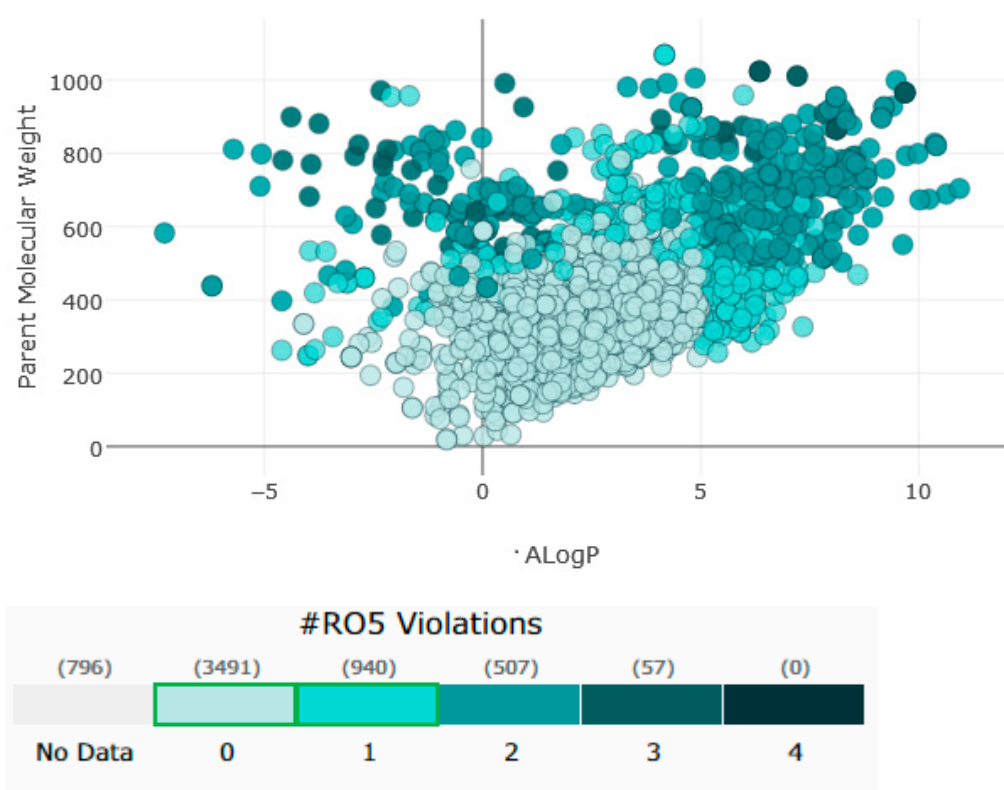


Figure 1. Correlation between molecular weight of nitrogen containing heterocyclic compounds with log P.

Table 1. Nitrogen-containing FDA-approved drugs.

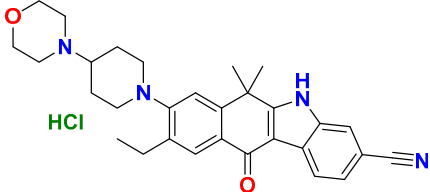
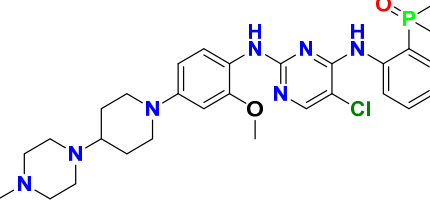
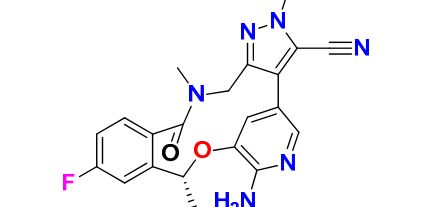
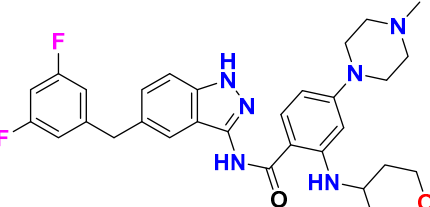
S. No.	Name	Structure	Mode of Action	Drug Target	Approval Year	References
1.	Alectinib Hydrochloride	 The structure shows a central benzimidazole core with a methyl group at position 2, a cyano group at position 5, and a 4-ethylphenyl group at position 7. It is substituted with a 4-(4-morpholinyl)phenyl group at position 4 and a 4-ethylphenyl group at position 7. A green 'HCl' label is placed below the structure.	It prevents the multiplication of cancer cells by blocking the action of abnormal proteins.	Anaplastic lymphoma kinase (ALK) Inhibitor	2015	[24]
2.	Brigatinib	 The structure features a central benzimidazole core with a methyl group at position 2, a chlorine atom at position 5, and a 4-(dimethylphosphoryl)phenyl group at position 7. It is substituted with a 4-(4-morpholinyl)phenyl group at position 4 and a 4-(4-morpholinyl)phenyl group at position 7.	It inhibits the ability of the phosphate group to bind ALK and inhibits the activity of proteins STAT3, A.K.T., ERK1/2, and S6 both in vitro and in vivo.	Anaplastic lymphoma kinase (ALK) Inhibitor	2017	[25]
3.	Lorlatinib	 The structure consists of a central benzimidazole core with a methyl group at position 2, a cyano group at position 5, and a 4-(4-morpholinyl)phenyl group at position 7. It is substituted with a 4-(4-morpholinyl)phenyl group at position 4 and a 4-(4-morpholinyl)phenyl group at position 7.	Inhibits will disrupt the ALK and ROS1-mediated signaling, further inhibiting the growing tumor cells in ALK and ROS1 cells.	Anaplastic lymphoma kinase (ALK) Inhibitor	2018	[26]
4.	Entrectinib	 The structure features a central benzimidazole core with a methyl group at position 2, a cyano group at position 5, and a 4-(4-morpholinyl)phenyl group at position 7. It is substituted with a 4-(4-morpholinyl)phenyl group at position 4 and a 4-(4-morpholinyl)phenyl group at position 7.	It interferes with the growth of cancer cells, which are eventually destroyed.	Anaplastic lymphoma kinase (ALK) Inhibitor	2019	[27]

Table 1. Cont.

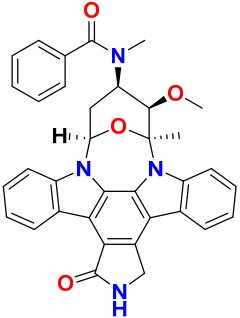
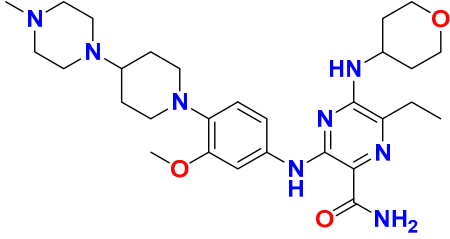
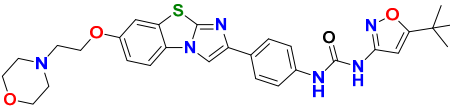
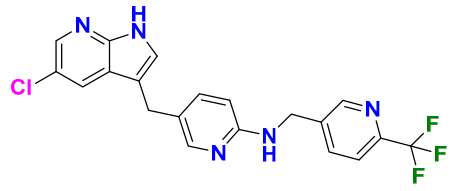
S. No.	Name	Structure	Mode of Action	Drug Target	Approval Year	References
5.	Midostaurin	 The chemical structure of Midostaurin is a complex polycyclic molecule. It features a central indole-like core with a benzimidazole ring system. Attached to this core are a benzamide group, a methoxy group, and a methyl group. The structure is drawn with stereochemistry indicated by wedges and dashes.	It Prevents the multiplication of cancer cells by blocking the action of abnormal proteins.	Fms-like tyrosine kinase (FLT3) inhibitor	2017	[28,29]
6.	Gilteritinib fumarate	 The chemical structure of Gilteritinib fumarate consists of a central pyrimidine ring system. It is substituted with a methyl group, an ethyl group, a primary amide group, and a secondary amide group. The secondary amide is further substituted with a piperazine ring, which is in turn connected to a piperidine ring. A methoxy group is also present on the pyrimidine ring.	Blocks the action of naturally occurring substances that promote cancer cell growth.	Fms-like tyrosine kinase (FLT3) inhibitor	2018	[30]
7.	Quizartinib	 The chemical structure of Quizartinib features a central thiazole ring system. It is substituted with a morpholine ring, a benzimidazole ring, and a pyridine ring. The pyridine ring is further substituted with a methyl group and a trifluoromethyl group.	It inhibits cancer cell proliferation which leads to the death of the cells.	Fms-like tyrosine kinase (FLT3) inhibitor	2018	[31]
8.	Pexidarinib	 The chemical structure of Pexidarinib is a complex molecule with a central pyridine ring system. It is substituted with a chlorine atom, a methyl group, and a trifluoromethyl group. The structure is drawn with stereochemistry indicated by wedges and dashes.	Inhibits the colony-stimulating factor (CSF1)/CSF1 receptor pathway	Fms-like tyrosine kinase (FLT3) inhibitor	2019	[32]

Table 1. Cont.

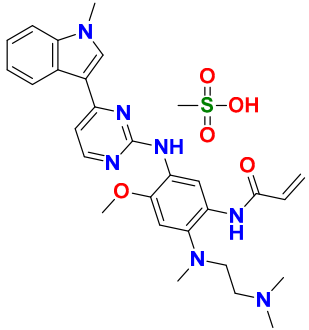
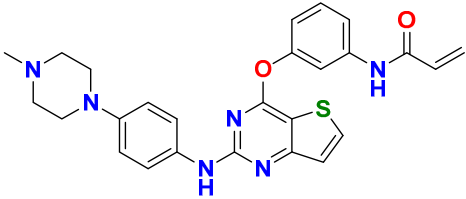
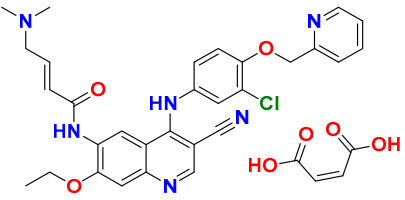
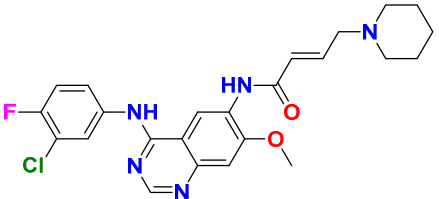
S. No.	Name	Structure	Mode of Action	Drug Target	Approval Year	References
9.	Osimertinib mesylate		The abnormal protein's ability to cause cancer cells to grow is blocked, which may also help tumors get smaller and slow down the spread of cancer cells.	Epidermal growth factor (EGF) receptor inhibitors	2018	[33]
10.	Olmudinib		Restricting the mutant form of E.G.F.R. causes the death of E.G.F.R. expressing tumor cells.	Epidermal growth factor (EGF) receptor inhibitors	2015	[34]
11.	Neratinib maleate		The autophosphorylation is prevented on tyrosine residues receptor, and the Oncogenic signaling was reduced through mitogen-activated protein kinase and Akt pathways.	Epidermal growth factor (EGF) receptor inhibitors	2017	[35]
12.	Dacomitinib		The E.G.F.R. activating mutations like exon 19 deletion or the exon 21 L858R substitution mutation and E.G.F.R. proteins like EGFR/HER1, HER2, and HER4 activities are blocked.	Epidermal growth factor (EGF) receptor inhibitors	2018	[36]

Table 1. Cont.

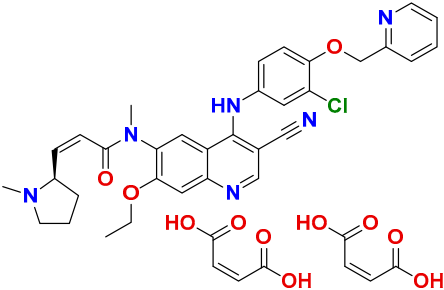
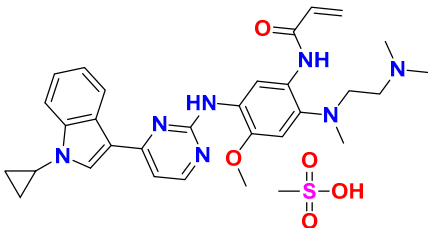
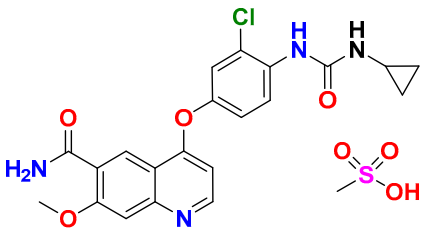
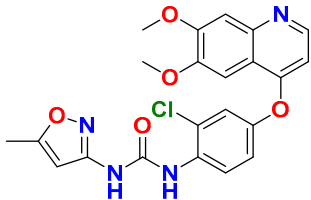
S. No.	Name	Structure	Mode of Action	Drug Target	Approval Year	References
13.	Pyrotinib maleate		Covalently binds to the intracellular kinase domain of HER1, HER2, and HER4 to block downstream signaling pathways, inhibits autophosphorylation, and prevents the creation of homologous/heterodimers of the HER family.	Epidermal growth factor (EGF) receptor inhibitors	2018	[37]
14.	Almonertinib mesylate		It inhibits E.G.F.R. tyrosine kinase targeting EGFR-sensitizing and T790M resistance mutations.	Epidermal growth factor (EGF) receptor inhibitors	2020	[38]
15.	Lenvatinib mesylate		The kinase activities of vascular endothelial growth factor (VEGF) receptors VEGFR1 (FLT1), VEGFR2 (K.D.R.), and VEGFR3 (FLT4) are inhibited.	Vascular endothelial growth factor (VEGF) inhibitors	2015	[39]
16.	Tivozanib		The phosphorylation of V.E.G.F.R. (vascular endothelial growth factor) receptors (V.E.G.F.R.)-1, VEGFR-2, and VEGFR-3, as well as kinases including c-kit and platelet-derived growth factor beta (P.D.G.F.R.), are suppressed.	Vascular endothelial growth factor (VEGF) inhibitors	2021	[40]

Table 1. Cont.

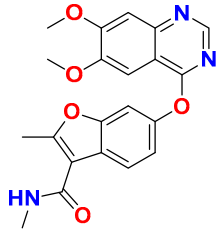
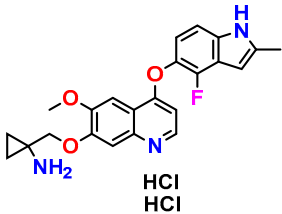
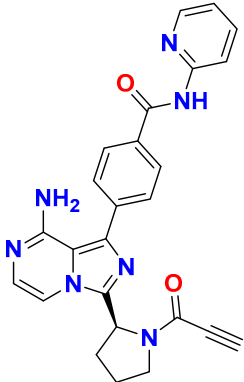
S. No.	Name	Structure	Mode of Action	Drug Target	Approval Year	References
17.	Fruquintinib		It prevents the VEGF from causing the phosphorylation of V.E.G.F.R.s 1, 2, and 3, which may reduce the proliferation, migration, and survival of endothelial cells, the development of microvessels, and the proliferation and death of tumor cells.	Vascular endothelial growth factor (VEGF) inhibitors	2020	[41]
18.	Anlotinib dihydrochloride		It inhibits the development of tumor cells by inhibiting the pathways like PI3K/AKT, RAS/MAPK, and PLCy/PKC by using the receptors: V.E.G.F.R., F.G.F.R., and P.D.G.F.R.	Vascular endothelial growth factor (VEGF) inhibitors	2020	[42]
19.	Acalabrutinib		Bruton Tyrosine Kinase inhibitor that stops B cells from chemotactic, proliferating, moving, and adhesion of B cells	Tyrosine kinase inhibitor(tki)	2017	[43]

Table 1. Cont.

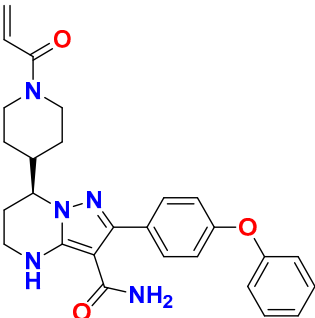
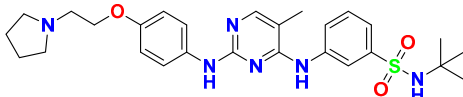
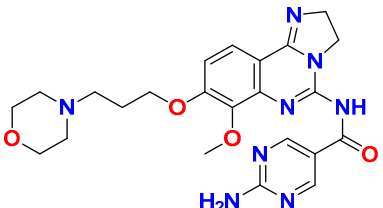
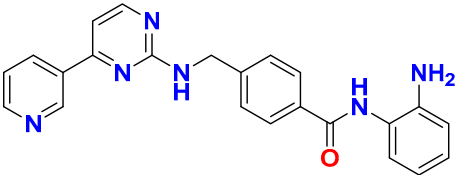
S. No.	Name	Structure	Mode of Action	Drug Target	Approval Year	References
20.	Zanubrutinib		Inhibits the growth and survival of cancerous B cells to shrink the size of the tumor in mantle cell lymphoma	Tyrosine kinase inhibitor(tki)	2021	[44]
21.	Fedratinib		Inhibits cell division and induces apoptosis	Janus kinase 2 (JAK2) inhibitors	2019	[45]
22.	Copanlisib		Apoptosis-induced tumor cell death and primary malignant B cell line growth suppression.	Phosphatidylinositol 3-hydroxy kinase inhibitors	2014	[46,47]
23.	Mocetinostat		Acts by turning on tumor suppressor genes that have been inappropriately turned off	Hydroxamic acid-based hdac Inhibitors (hdaci)	2014	[48,49]

Table 1. Cont.

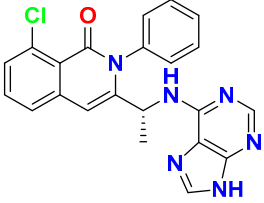
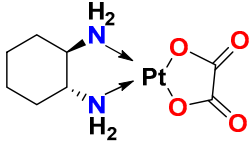
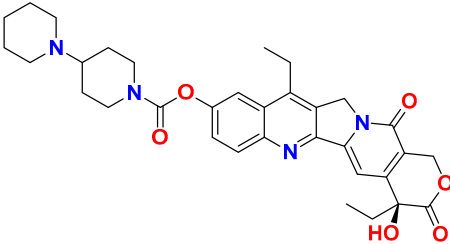
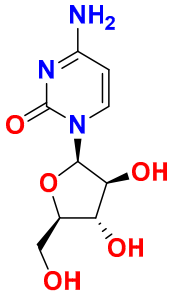
S. No.	Name	Structure	Mode of Action	Drug Target	Approval Year	References
24.	Duvelisib		Inhibit isoform gamma, essential for cytokine signaling and the pro-inflammatory response, and inhibit the isoform delta of PI3K (<i>phosphoinositide 3-kinase</i>), which is required for cell proliferation and survival.	Phosphatidylinositol 3-hydroxy kinase inhibitors	2018	[50]
25.	Oxaliplatin		Inhibits D.N.A. synthesis and transcription by binding preferentially to the guanine and cytosine moieties of D.N.A.	Platinum derivative	2004	[51,52]
26.	Irinotecan		Binds to the topoisomerase I-DNA complex and prevents the D.N.A. strand from relegating, which then forms a ternary complex disrupting the replication fork and moving slowly, leading to breakage of lethal double-stranded DNA.	Topoisomerase I inhibitor	2000	[53,54]
27.	Cytarabine		It prevents cancer cells from generating and repairing the D.N.A., which they require to thrive and proliferate.	Antineoplastic anti-metabolite	1999	[55,56]

Table 1. Cont.

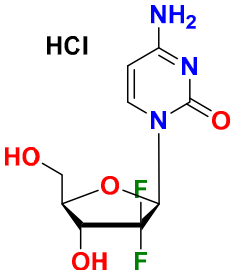
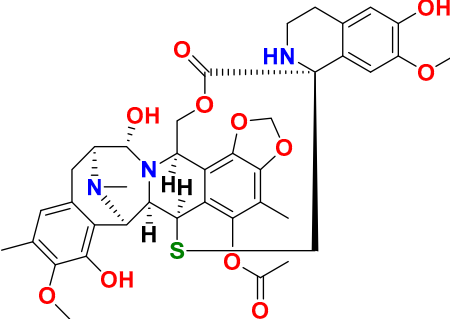
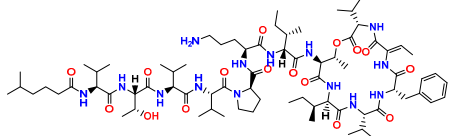
S. No.	Name	Structure	Mode of Action	Drug Target	Approval Year	References
28.	Gemcitabine		Inhibits D.N.A. synthesis	Pyrimidine nucleoside antimetabolite	2011	[57,58]
29.	Trabectedin		Inhibition of trans-activated transcription and the interaction with D.N.A. repair proteins	Alkylating agent	2015	[59,60]
30.	Kahalalide F		Induces oncosis	Lysosomes	2004	[61,62]

Table 1. Cont.

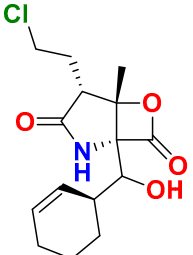
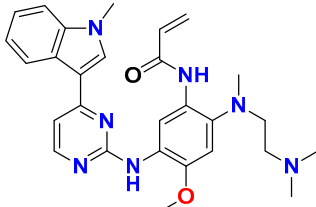
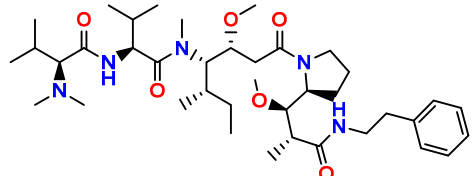
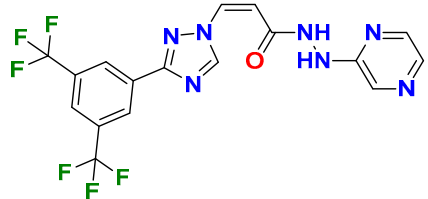
S. No.	Name	Structure	Mode of Action	Drug Target	Approval Year	References
31.	Salinosporamide A		Covalently modifies the threonine residues in the 20S proteasome's active site to decrease proteasome activity.	Inhibitor of the 20S proteasomes	2004	[63]
32.	Osimertinib		Binds to specific E.G.F.R. mutants (T790M, L858R, and exon 19 deletions), which are more prevalent in non-small cell lung cancer (N.S.C.L.C.) following the first-line EGFR-TKI treatment.	Epidermal growth factor receptor (E.G.F.R.) tyrosine kinase inhibitor (T.K.I.)	2015	[64]
33.	TZT1027 (Soblidotin)		Inhibits tubulin polymerization	Inhibit microtubule polymerization	2011	[65]
34.	Selinexor		XPO1 is selectively inhibited, and tumor-suppressing proteins are activated, causing tumor cell death	Inhibiting exportin 1 (XPO1)	2019	[66,67]

Table 1. Cont.

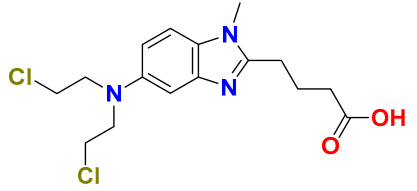
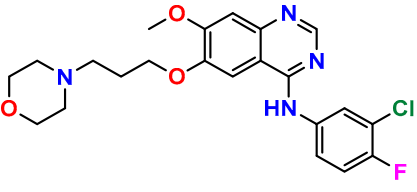
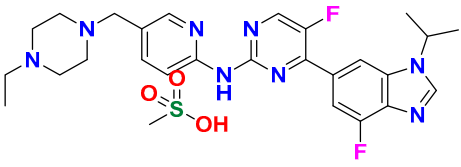
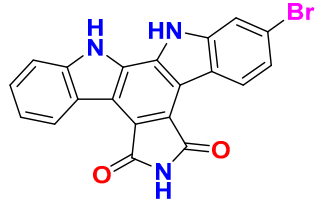
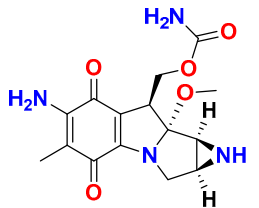
S. No.	Name	Structure	Mode of Action	Drug Target	Approval Year	References
35.	Bendamustine		Eradicates current cancer cells and restricts the development of new cancer cells.	Alkylation	2008	[68]
36.	Gefitinib		It prevents a variety of tyrosine kinases linked to transmembrane cell surface receptors from becoming phosphorylated intracellularly, including those linked to the epidermal growth factor receptor (EGFR-TK).	Epidermal growth factor receptor tyrosine kinase inhibitors (EGFR-tkis)	2003	[69]
37.	Abemaciclib		The action of an abnormal protein is blocked, which causes the cancer cell's signals to multiply	Blocks the activity of CDK4 and CDK6 proteins (CDK4/6)	2017	[70,71]
38.	Ribociclib		Cell-cycle progression is blocked by acting directly on the cyclin D–CDK4/6–p16–Rb pathway	Cyclin-dependent kinase 4 and cyclin-dependent 6 (CDK 4 and CDK 6) Inhibitor	2018	[72]
39.	Mitomycin C		Causes cross-linking and inhibition of D.N.A. synthesis and function	Double-stranded D.N.A. alkylating agent	1974	[73]

Table 1. Cont.

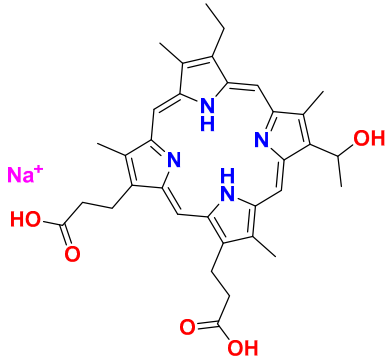
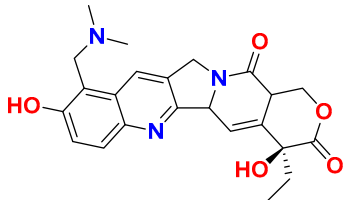
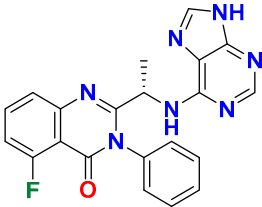
S. No.	Name	Structure	Mode of Action	Drug Target	Approval Year	References
40.	Porfimer		When activated by laser light, a cytotoxic activity that depends on oxygen and light causes the release of thromboxane A2, which in turn causes vascular necrosis and oxygen-free radicals.	Photodynamic therapy agent High-affinity immunoglobulin gamma Fc receptor I antagonist	2003	[74]
41.	Topotecan		D.N.A. damage occurs by prevention of topoisomerase from relegating cleaved D.N.A. strand	Novel topoisomerase-1 inhibitor	1996	[75]
42.	Idelalisib		Prevents proliferation and induces apoptosis in cell lines derived from malignant B-cells and in primary tumor cells	PI3K inhibitor	2014	[76,77]

Table 1. Cont.

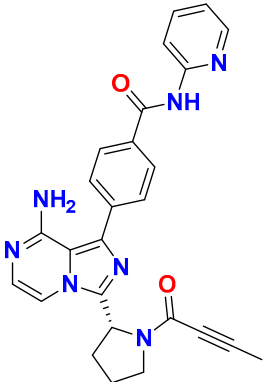
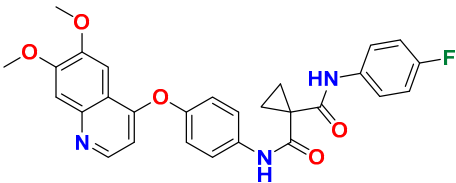
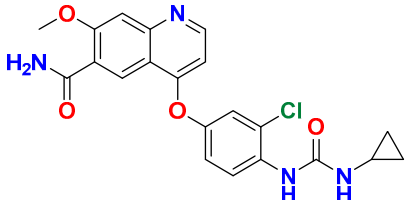
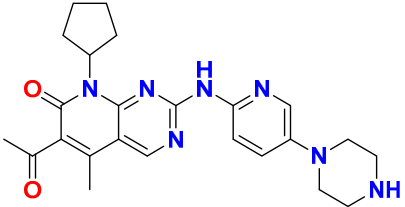
S. No.	Name	Structure	Mode of Action	Drug Target	Approval Year	References
43.	Acalabrutinib		It inhibits B.C.R. signaling by reduced phosphorylation of PLC γ 2.	Bruton tyrosine kinase (btk) inhibitor	2017	[78]
44.	Cabozantinib		Resistance of V.E.G.F.R. inhibitor via the c-MET axis is decreased by inhibiting V.E.G.F.R. and c-MET	Tyrosine kinase inhibitor	2016	[79,80]
45.	Lenvatinib		The kinase activities of vascular endothelial growth factor (VEGF) receptors VEGFR1 (FLT1), VEGFR2 (K.D.R.), and VEGFR3 (FLT4) are inhibited.	Multi-receptor Tyrosine Kinase Inhibitor.	2018	[81,82]
46.	Palbociclib		Blocking cell cycle progression from G1 into S phase and inhibits the phosphorylation of retinoblastoma (Rb) protein,	Proteins cyclin-dependent kinase 4 and 6 (CDK4 and CDK6) Inhibitor	2016	[83,84]

Table 1. Cont.

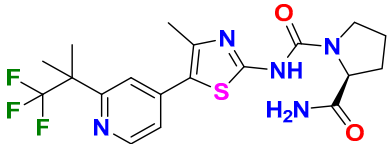
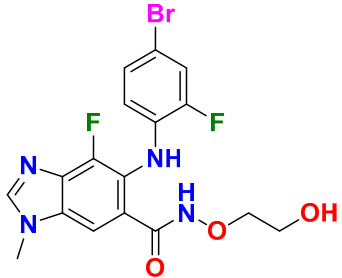
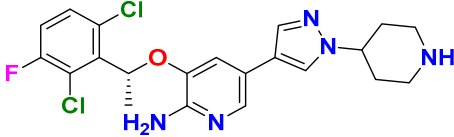
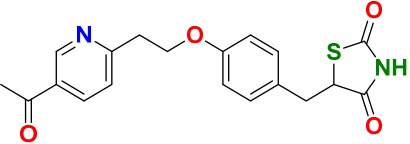
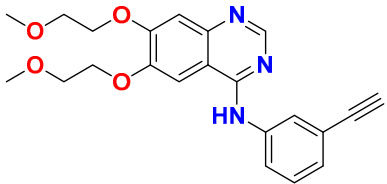
S. No.	Name	Structure	Mode of Action	Drug Target	Approval Year	References
51.	Alpelisib		Blocks the catalytic subunit of PI3K, class I PI3K p110, a lipid kinase involved in several biological processes, including proliferation, survival, differentiation, and metabolism	Phosphatidylinositol 3-kinase (PI3K) inhibitor	2019	[94]
52.	Binimetinib		The activation of MEK1/2-dependent effector proteins and transcription factors is prevented by inhibiting MEK1/2	Mitogen-activated protein kinase kinase 1, Dual specificity mitogen-activated protein kinase kinase 2 Inhibitor	2018	[95,96]
53.	Crizotinib		Blocks certain chemical messengers that tell cells to grow.	Small-molecule kinase inhibitor ALK, c-MET, and ROS1	2022	[97,98]
54.	Dactinomycin		D.N.A. intercalation and the stabilization of DNA-topoisomerase I and II cleavable complexes	Potent transcription inhibitor	2009	[99]
55.	Erlotinib		The intracellular phosphorylation of tyrosine kinase associated with the epidermal growth factor receptor (E.G.F.R.) is inhibited	Inhibition of epidermal growth factor receptor (E.G.F.R.)	2004	[100]

Table 1. Cont.

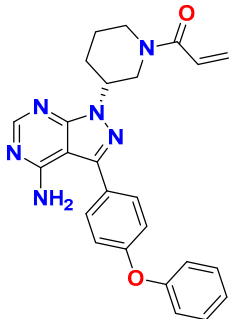
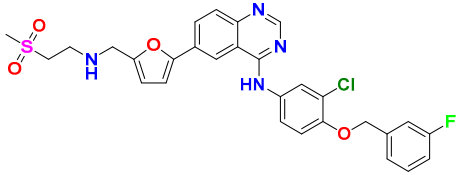
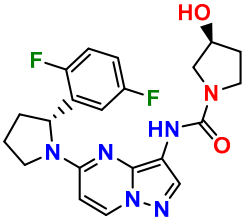
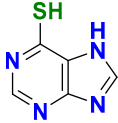
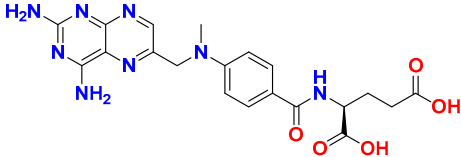
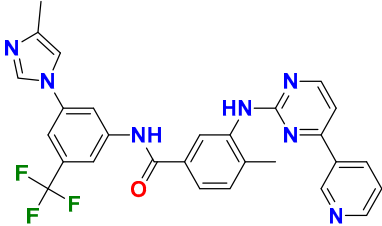
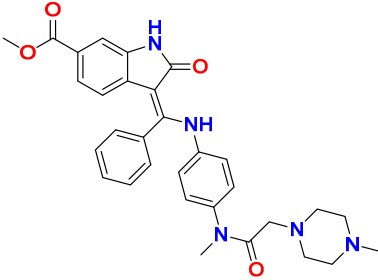
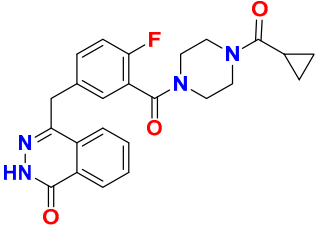
S. No.	Name	Structure	Mode of Action	Drug Target	Approval Year	References
56.	Ibrutinib		It inhibits Btk's enzyme activity by forming a covalent bond with a cysteine residue (CYS-481) at the active site.	Bruton tyrosine kinase inhibitor	2022	[101,102]
57.	Lapatinib		It works by competitively binding to the intracellular ATP-binding site of the receptor, inhibiting the tyrosine kinase domains of the human epidermal growth factor receptor (HER)-2 and the epidermal growth factor receptor.	HER2 and E.G.F.R. antagonist	2007	[103]
58.	Larotrectinib		The activity of T.R.K. proteins is disrupted, which is caused by fusion in a family of genes known as N.T.R.K.	T.R.K. (Tropomyosin Receptor Kinase) inhibitor	2018	[104,105]
59.	Mercaptopurine		De novo purine synthesis is inhibited and acts as an antiproliferative agent by interfering with protein, R.N.A. and D.N.A. synthesis and induces apoptosis.	Hypoxanthine-guanine phospho ribosyl transferase, Amido phospho ribosyl transferase, Inosine-5'-monophosphate dehydrogenase Inhibitor	2014	[106]

Table 1. Cont.

S. No.	Name	Structure	Mode of Action	Drug Target	Approval Year	References
60.	Methotrexate		The enzymes responsible for nucleotide synthesis are aminoimidazole carboxamide ribonucleotide transformylase (A.I.C.A.R.T.), dihydrofolate reductase, thymidylate synthase, and amido phosphor ribosyl transferase are inhibited.	Thymidylate synthase and Dihydrofolate reductase Inhibitors	1999	[107,108]
61.	Nilotinib		Stabilizes the Abl protein's kinase domain's inactive conformation by binding to it.	Tyrosine kinase inhibitor	2007	[109]
62.	Nilutamide		The action of androgens of testicular and adrenal origin that stimulate the growth of normal and malignant prostatic tissue is blocked	Androgen receptor antagonist	2016	[110]
63.	Olaparib		Blocks the repair of single-strand D.N.A. breaks by inhibiting poly(ADP-ribose) polymerase.	Poly (ADP-ribose) polymerase (PARP) inhibitor	2014	[111,112]

3. Current Advances in Nitrogen Containing Heterocycles as Anticancer Agents

3.1. Pyrimidine Derivatives as Anticancer Agents

Pyrimidines gained popularity in the history of organic chemistry as “m-Diazine” which is the product of uric acid catabolism. Brugnatelli discovered the first pyrimidine derivative, alloxan, in 1818 while oxidising uric acid with nitric acid. The heterocyclic six membered aromatic ring of pyrimidine contains nitrogen atoms in 1st and 3rd position. The melting and boiling temperatures of pyrimidine are 22.5 °C and 124 °C, respectively [113,114].

Fathalla et al. (2012) synthesized 10 pyrimidine derivatives and evaluated their antitumor activity against a liver cancer (HepG2) cell line by a comparison with the well-known anticancer drugs 5-Fluorouracil and Doxorubicin. While comparing the synthesized compounds, growth inhibition effectiveness was shown on the tested tumor cell line at doses between 1 and 10 µg/mL. The most potent compound in this study was found to be compound **1** with the IC₅₀ value of 3.56 µg/mL, whereas doxorubicin and 5-fluorouracil were having IC₅₀ values 3.56 µg/mL and 5 µg/mL, respectively [115]. Ahmed et al. (2020) synthesized and evaluated the anti-tumor activity of 16 nitrogen heterocyclic compounds bearing a pyrimidine moiety. The newly developed pyrimidine derivatives were tested for in vitro anti-proliferative activity against human liver (HepG2), breast (MCF7), and normal fibroblast (WI-38) cell lines, and their efficacy was compared to Doxorubicin. Among all the tested compounds, compound **2** showed excellent anticancer activity with IC₅₀ values of 7.36, 10.76, and 6.7 µM respectively, whereas IC₅₀ values of doxorubicin were 4.5, 4.1, and 6.7 µM (WI-38) respectively [116]. Gupta et al. (2022) studied the anticancer activity of spiroisoquinoline-pyrimidine derivatives against the MCF-7 cancer cell line. Out of these, compound **3** having an ethoxy group from the acetylene molecule was found to be the most potent cytotoxic agent with an IC₅₀ value of 98.8 µM as compared to the reference Doxorubicin. An MTT assay was carried out at the concentration of 50 µM and it showed 60% of cell viability with control doxorubicin having 100% cell viability [117]. Al-Issa (2013) synthesized fused pyrimidines and tested them in vitro anti-tumour activity against human cancer cell line HEPG2. Out of these compounds, the most potent anticancer activity was shown by the compound **4** with the IC₅₀ value of 17.4 µg/mL as compared to the standard drug doxorubicin having an IC₅₀ value 1.2 µg/mL [118]. Osmania et al. (2022) synthesized a new pyrimidine-triazole derivatives and carried out studies on its anticancer effect. A total of 10 novel Pyrimidine-Triazole derivatives were synthesized in this study and they were evaluated against three cancer cell lines; A549, MCF-7, and NIH3T3. IC₅₀ values were calculated at 24 h and 48 h (incubation time). Two compounds, namely compound **5a** and **5b**, were found to be potent anticancer agents. Compounds **5a** and **5b** have the IC₅₀ values of 1.573 µM and 3.698 µM after 48 h on MCF-7 cell lines respectively. The selective index of these compounds at the end of incubation period was 28.59 and 5.51, respectively. The control was Cisplatin with the IC₅₀ value of 49.23 µM (48 hr) and Doxorubicin at 0.958 µM (48 h) against the MCF cell line, respectively. The aromatase enzyme inhibition effects of the compound **5a** and **5b** is also calculated having the IC₅₀ values of 0.082 and 0.198 µM [119]. Qin et al. (2015) synthesized fifteen 2,4-diaminopyrimidines and evaluated their biological activity as selective Aurora A kinase inhibitors. Their cytotoxic activity was tested against five cell lines. The most potent compound reported in this study was compound **6** with IC₅₀ values of 3.6 µM (HCT-8), 0.5 µM (A-549), 0.9 µM (HeLa), and 2.4 µM (Hep-G2). VX680 was used as the standard, having IC₅₀ of 44.6 µM (HCT-8), 19.4 µM (A-549), 27.3 µM (HeLa), and 63.4 µM (Hep-G2). Molecular docking studies revealed that compound **6** formed a major interaction with Aurora A, which showed 35-fold greater selectivity for Aurora A than for Aurora B. Additionally, compound **6** caused HeLa cells to arrest in the G2/M cell cycle. The IC₅₀ values of compound **6** were 0.012 and 0.043 µM against Aurora A and Aurora B respectively whereas that of standard VX-680 were 0.261 and 0.453 µM respectively [120]. Filho et al. (2021) synthesized 6-ferrocene/heterocycle-2-aminopyrimidine and 5-ferrocene-

1H-Pyrazole derivatives by microwave-assisted Atwal reaction and carried out docking, machine learning, and anti-proliferative activity studies of these agents. The compound **7** showed the potent anticancer activity. It was tested on 4 cancer cell lines like HCT116, PC3, HL60, and SNB19 with IC_{50} values of 56.99, 33.56, 70.26, and 85.11 μM respectively. The docking studies revealed that the compound **7** is the most active compound having the binding energy of -6.3 Kcal/mol with targeted protein (PDB:4HLW) [121].

El-Deen et al. (2022) designed and synthesized pyridothienopyrimidine derivatives and evaluated their anticancer and antimicrobial activity. The cytotoxic activity of newly synthesized compounds was evaluated against three cell lines, MCF-7, HepG-2, and WISH. The compounds that showed potent activity were examined as EGFR kinase inhibitors. The most potent anticancer agent reported in this study was compound **8** with IC_{50} values of 1.17, 1.52, and 417.55 μM against the cell lines HepG-2, MCF-7, and WISH, respectively. It is compared with the control drug Doxorubicin with IC_{50} values of 2.85, 3.58, and 432.10 μM against the cell lines HepG-2, MCF-7, and WISH, respectively. In terms of in vitro enzymatic inhibitory activity against EGFR kinase, compound **8** showed IC_{50} of 7.27 nM as compared to control Erlotinib with IC_{50} value of 27.01 nM [122]. Al-Anazi et al. (2022) synthesized pyrazoline and pyrimidine derivatives as novel epidermal growth factor receptor (EGFR) inhibitors and tested their anticancer property. All the synthesized compounds showed good anticancer activity. Among them the compound **9** showed the most potent activity against MCF-7 cell line with the IC_{50} value of 5.5 μM and selective index 18.18 as compared to tamoxifen standard with IC_{50} value of 26.95 μM [123].

El-Metwally et al. (2021) synthesized thieno pyrimidine-based derivatives as potent VEGFR-2 kinase inhibitors and evaluated their anti-cancer properties using MTT against the HepG2, HCT-116, and MCF-7 human cancer cell lines using sorafenib as a positive control. The most potent derivative reported was compound **10** with IC_{50} value 0.23 μM against the MCF-7 cell line which is similar to the control sorafenib with IC_{50} value 0.23 μM [124].

Madia et al. (2021) designed and synthesized pyrimidine-based analogues and evaluated their anticancer activity against HT-29, U-87 MG, MDA-MB231, CAL27, and FaDu cancer cell lines. Each of synthesized compounds showed excellent anticancer activity. Among them, compound **11** showed excellent activity at 24 and 48 h time intervals with EC_{50} values of 10.2, 22.0, 18.0, 9.7, and 26.2 and 5.4, 7.5, 7.9, 4.3, and 8.5 μM , respectively with control RDS 3442 (EC_{50} values of 51.8, 75.2, 34.8, 54.2, and 69.3 at 48 h respectively) [125].

All the reported pyrimidine derivatives (Figure 3 (1–11)) were acting as anticancer agents. The most potent compound among them was compound **10**, having the lowest IC_{50} value of 0.23 μM against MCF-7 cell line. It has a hydrazine moiety joined by phenyl amino linkage and pyrimidine with benzothiophene nucleus which may be responsible for its excellent activity.

3.2. Quinoline Derivatives as Anticancer Agents

Quinoline is a nitrogen containing heterocyclic aromatic compound, also known as 1-aza-naphthalene or benzopyridine. Its molecular weight is 129.16 and molecular formula is C_9H_7N . The log P value is 2.04 while the pK_b and pK_a values are 4.85 and 9.5, respectively. Quinoline is a weak tertiary base and with acids it can produce salt and exhibits reactions akin to those of pyridine and benzene. Numerous naturally occurring chemicals (Cinchona Alkaloids) and pharmacologically active molecules with a wide range of biological activities include the quinoline nucleus in their structure. Diverse pharmacological activities (anticonvulsant, analgesic, cardiotoxic, antibacterial, antifungal, anti-inflammatory, and anti-malarial) of quinoline have been reported [126].

Hamdy et al. (2019) conducted anticancer study on quinoline based heterocycles targeting Bcl-2. Out of these, Compound **12** showed excellent activity in MDA-MB-231, HeLa, KG1a, and Jurkat with the IC_{50} values of 0.54, 1.42, 1.21, and >100 μM respectively. This compound showed the IC_{50} value of 0.15 μM against Bcl-2 compared with Gossypol (IC_{50} value of 0.60 μM). Compound **12** had sub-micromolar anti-proliferative activity in cancer cell lines that express Bcl-2, as well as a sub-micromolar IC_{50} value in an ELISA

experiment using the Bcl2-Bim peptide [127]. Mathada et al. (2022) studied the anticancer effect of quinoline and its derivatives. Hence, 62 compounds were synthesized in this study. Out of these, the most potent compound was found to be compound **13**, which showed a potent anticancer effect against three cell lines, MDA-MB-231, HeLa, and SMMC-7721 with IC_{50} values of 0.12, 0.08, and 0.34 μ M respectively. Etoposide was used as standard drug with IC_{50} values of 5.26, 2.98, and 3.48 μ M respectively. Compound **13** had a unique capacity to induce apoptosis in HeLa cells, halt the cell cycle at the G₀/G₁ phase, elevate intracellular ROS (Reactive Oxygen Species) levels, and decrease mitochondrial membrane potential. Additionally, it had the ability to significantly reduce MEK1 kinase activity and disrupt the Ras/Raf/MEK/ERK transduction pathway [128].

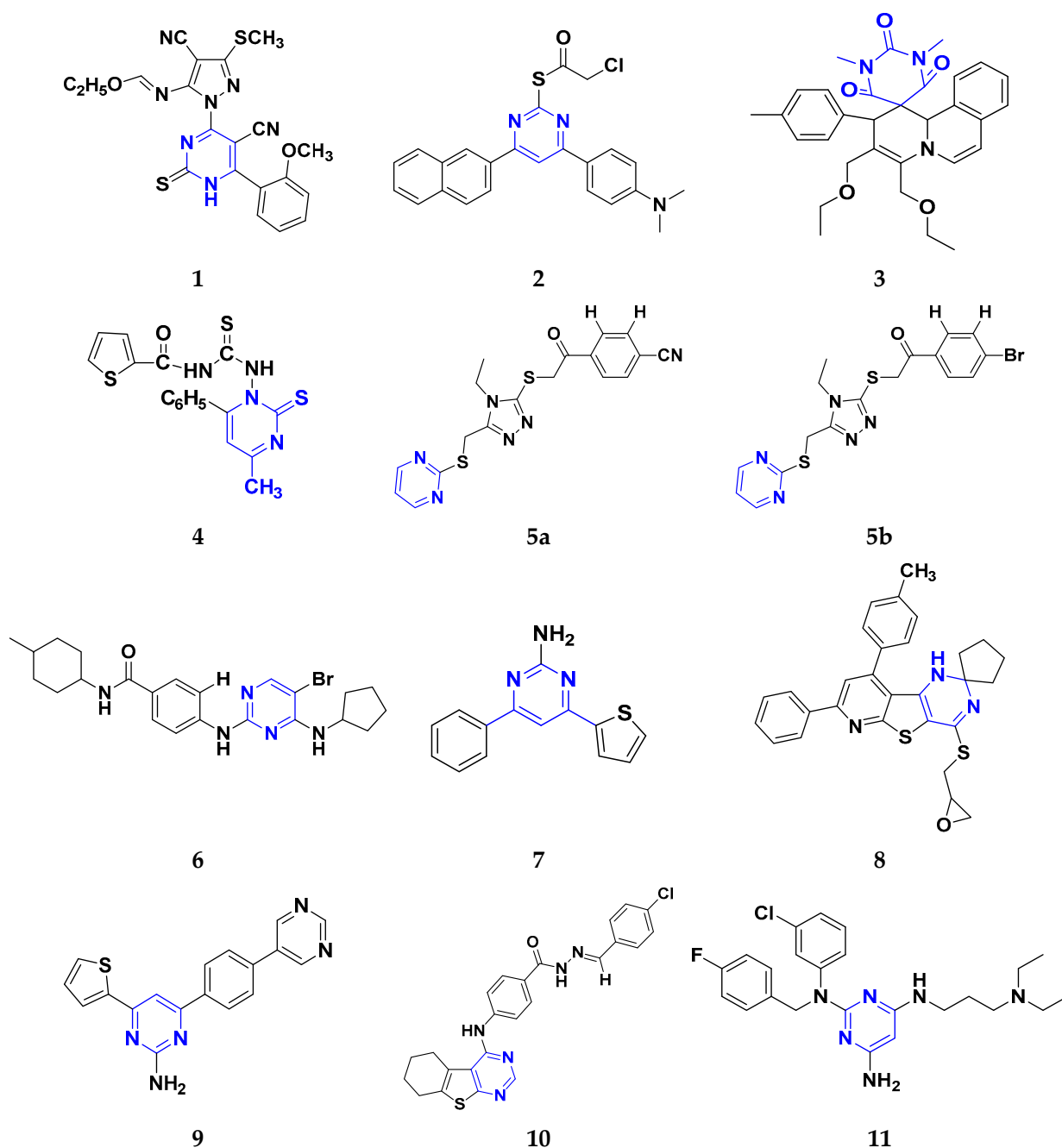


Figure 3. Pyrimidine derivatives (1–11) as anticancer agents.

Katariya et al. (2020) performed the studies on anticancer, antimicrobial activities of quinoline based hydrazone analogues. Nine compounds out of all the tested compounds showed significant anti-cancer activity at 10 μM . These compounds were then screened at 10-fold dilutions of five different concentrations (0.01, 0.1, 1, 1, and 100 μM) with GI_{50} values ranging from 0.33 to 4.87 μM and LC_{50} values ranging from 4.67 μM to >100 μM . The most active molecule, compound **13**, had a mean graph midpoint (MG-MID) GI_{50} value of 1.58 μM , which was significantly lower than commercially available standards Bendamustine and chlorambucil (60 and 52 μM , respectively). The IC_{50} value of compound **14** was 132 μM against the NIH/3T3 cell line, which was significantly higher than the GI_{50} values of compound **14** against the NCI 60 cancer cell lines, which demonstrated that compound **14** was highly selective for cancer cells at concentrations that are lower than the effective concentration against healthy cell lines [129].

George et al. (2019) synthesized the new derivatives of quinoline, i.e., 4,5-dihydropyrazoles as EGFR inhibitors and evaluated their anti-proliferative activity. The newly synthesized compounds were tested against HeLa, MCF-7, and DLD1 cancer cell lines as well as normal fibroblast WI-38. Eight compounds showed potent activity towards the DLD1 cell line and it was safe to normal cell lines. The most active compound in this study was compound **15**, with IC_{50} values of 0.227, 0.136, 1.277, and >94.5 μM against the cell lines MCF-7, HeLa, DLD1, and WI-38, and it was compared to the control drug CHS 828 with the IC_{50} values of 0.018, 0.040, 2.315, and >134.71 μM respectively. Compound **15** showed the EGFR inhibitory activity with IC_{50} value of 31.8 nM as compared to the control Gefitinib 29.16 nM [130]. Koprulu et al. (2021) had conducted anticancer activity and molecular docking studies of quinoline derivatives. The cytotoxic activity of synthesized piperazine substituted quinoline derivatives were tested against three cell lines, namely rat glioblastoma (C6), human cervical cancer (HeLa), and human adenocarcinoma (HT29). The docking studies revealed that compound **16** was the most potent compound for metastatic cancer treatment due to its binding affinity to PLC γ 1. The IC_{50} values of compound **16** were 100, 144.8, and 117.6 μM against the cell lines, C6, HeLa, and HT29. Further, 5-Fluoro Uracil was used as the standard drug with IC_{50} values of 163, 469.6, and 501.2 μM [131].

Ramya et al. (2018) synthesized and evaluated anticancer potential of curcumin inspired 2-chloro/phenoxy quinoline analogues. This study described the synthesis of twenty novel 2-chloro/phenoxyquinoline derivatives inspired by curcumin. The cytotoxic activity of the acquired novel chemical entities toward various tumor cell lines was examined in vitro. The most active compound **17** showed potential cytotoxicity against different cell lines HeLa, HGC, NCI-H460, DU-145, PC-3, and 4T1 with IC_{50} values of 5.41, 8.73, 3.96, 3.99, 3.12, and 1.81 μM respectively. The reference drug curcumin had the IC_{50} values of 17.11, 33.15, 18.65, and 18.65 μM against the cell lines NCI-H460, DU-145, PC-3, and 4T1, respectively. Additionally, study of ROS levels, DAPI staining, AO-EB labelling, and annexin binding assay showed that the promising compound **16** may cause apoptosis in PC-3 cells and G2/M cell cycle arrest [132].

Upadhyay et al. (2018) conducted the synthesis and screening of pyrano[3,2-c]quinolones derivatives. One pot multicomponent condensation was carried out between malononitrile, 2,4-dihydroxy-1-methylquinoline, and substituted aromatic aldehydes to create a number of pyrano[3,2-c]quinoline based structural analogues. The compounds were accessed for their cytotoxic and anti-inflammatory activity. Out of these, compound **18** was found to be the most potent anticancer agent and showed 81–53% anti-proliferative inhibition at 1 μM concentration against all cell lines, including ACHN, Panc-1, HCT-116, H-460, and Calu-1, with IC_{50} values of 0.1, 1.0, 0.3, 0.3, and 0.5 μM respectively. Flavopiridol, having the IC_{50} values of 71, 78, 71, 88, and 74 μM , and gemcitabine, with 73, 74, 73, 71, and 79 μM , respectively, were used as standard [133].

Hagras et al. (2021) designed, synthesized, and conducted docking studies and anti-proliferative evaluation of newly discovered quinolines. The most effective anti-tubulin polymerization agents are colchicine binding site inhibitors. In order to exhibit the same fundamental pharmacophoric characteristics as colchicine binding site inhibitors, novel

quinoline compounds have been developed and synthesized. Using colchicine as a positive control, the synthesized compounds were evaluated *in vitro* against three human cancer cell lines; MCF-7, HepG-2, and HCT-116. The most potent compound **19** have the IC₅₀ values of 1.89, 1.43, and 4.21 μM against the cell lines HePG2, HCT-116, and MCF-7 respectively. The control drug colchicine with IC₅₀ values of 7.4, 9.3, and 10.4 μM, respectively, and its effect on cell cycle distribution were evaluated. The outcomes showed that compound **19** had the ability to stop the cell cycle at the G2/M phase. A double-staining test with annexin V and PI was performed to investigate the apoptotic effect of the synthesized compounds. Compound **19** caused HepG-2 cells to apoptosis thirteen times more frequently than control cells [134]. Mirzaei et al. (2019) synthesized novel quinoline chalcone hybrids and conducted studies on the structure–activity relationship and docking studies for their anticancer potential as active tubulin inhibitors. Four different human cancer cell lines, including A2780/RCIS (Cisplatin-resistant human ovarian carcinoma), A2780 (human ovarian carcinoma), normal Huvec cells, MCF-7 (human breast cancer cells), and MCF-7/MX (Mitoxantrone-resistant human breast cancer cells), were used to test the cytotoxic activity of synthesized substances. The most potent compound reported in this study was compound **20** with IC₅₀ values of 2.32, 2.615, 4.96, 2.32, and 4.44 μM against the cell lines A2780, A2780/RCIS, MCF-7, MCF-7/MX, HUVEC respectively. It is compared with the standard drug CA-4 with IC₅₀ values of 0.24, 0.22, 0.43, and 1.49 μM against the cell lines A2780, A2780/RCIS, MCF-7, and MCF-7/MX, respectively [135]. Chate et al. (2018) investigated novel spiro-pyrimido[5,4-b]quinoline-10,50-pyrrolo[2,3-d]pyrimidine derivatives as promising anticancer agents. By using the MTT assay, the newly synthesized compounds' anticancer effects were assessed *in vitro* against the A431, PC-3, MCF-7, and MCF-10A cancer cell lines. Out of these, the most potent was compound **21**, having an IC₅₀ value of 36.25 μM for MCF-10A (normal breast epithelial cell lines), indicating five times more selectivity for MCF-7 cancer cells with the IC₅₀ value of 7.82 μM. Sunitinib was used as a control having IC₅₀ values of 6.48, 7.25, 20.66, and 34.55 μM against the cancer cell lines A-41, MCF-7, PC-3, and MCF-10A, respectively [136].

While evaluating the above reported quinoline derivatives (Figure 4 (12–21)), most of the compounds were evaluated with their cytotoxic activity commonly against HeLa, MCF-7, and HCT-116 cells. Compounds **13**, **15**, and **18** were reported to be potent anticancer compounds but the most potent one among them was compound **13** with the lowest IC₅₀ value of 0.08 μM on HeLa cells, 0.12 μM on MDA-MB-231, and 0.34 μM on SMMC-7721, having a steroid nucleus directly attached with quinoline along with a hydrazine chain. This also demonstrated the ability to cause apoptosis in HeLa cells.

3.3. Carbazole Derivatives as Anticancer Agents

A polycyclic aromatic hydrocarbon called carbazole has a broad aromatic system and a central nitrogen atom that exhibits substantial electron delocalization. It consists of a five-membered nitrogen-containing ring sandwiched between two six-membered benzene rings. It has an indole-like structure, but at the indole position 2–3, a second benzene ring is fused to the five-membered ring. When creating electron donor-electron acceptor (D-A) chemical dyes, carbazole is frequently used as a conjugated bridge [137].

Murali et al. (2017) studied the creation of hetero annulated isoxazolo-, pyrido-, and pyrimido carbazoles, also screening them for *in vitro* anticancer activity. By cyclo condensation with the appropriate reactants (hydroxylamine hydrochloride, malononitrile, and guanidine nitrate), the newly synthesized heterocycles isoxazolo-, pyrido-, and pyrimido-carbazoles were produced from the readily available 2-(3'-bromo-4'-methoxybenzylidene)-2,3,4,9-tetrahydro-1H-carbazol. All the synthesized substances were tested for *in vitro* cytotoxicity against the A-549 and MCF-7 human cancer cell lines. Compound **22** demonstrated substantial activity against MCF-7 with the IC₅₀ value of 20 μM as compared to cisplatin IC₅₀ value of 18 μM. All other compounds showed moderate to powerful activity and consequent apoptotic cell death, which was demonstrated by AO/EB and DAPI of fluorescence microscopy analysis [138]. Wang et al. (2011) designed and synthesized

substituted 11H-benzo[a] carbazole-5-carboxamides as novel anticancer agents and tested them against human cancer A549 and HCT-116 cell lines. The most potent derivative was compound **23** with IC_{50} value 8.2, 9.5 μ M against the cancer cell lines A549, and HCT-116 respectively. Amonafide was used as the standard with IC_{50} values 8.1 μ M and 15.3 μ M, respectively [139]. Debray et al. (2010) synthesized N-ethoxycarbonyl-N-arylguanidines by the montmorillonite K-10 catalyzed cyclization, which provides access to pyrimido[4,5-c]carbazole and pyrimido[5,4-b]indole derivatives. Further, 3-aminocarbazole and 3-aminoindole were converted into two novel heterocycles, pyrimido[4,5-c]carbazole and pyrimido[5,4-b]indole, respectively. With the aid of montmorillonite K-10 clay as a catalyst and microwave irradiation, the essential Friedel–Crafts intramolecular cyclization was accomplished. The micromolar IC_{50} of the pyrimido[4,5-c]carbazole derivative was significant against cancer cell lines. The most potent compound in this study was found to be compound **24** with the IC_{50} values 17 and 17 μ M against the cancer cell lines HL60 N and HL60 MX2, respectively. Etoposide is used as a reference with IC_{50} values of 1.3 μ M and 11.9 μ M [140].

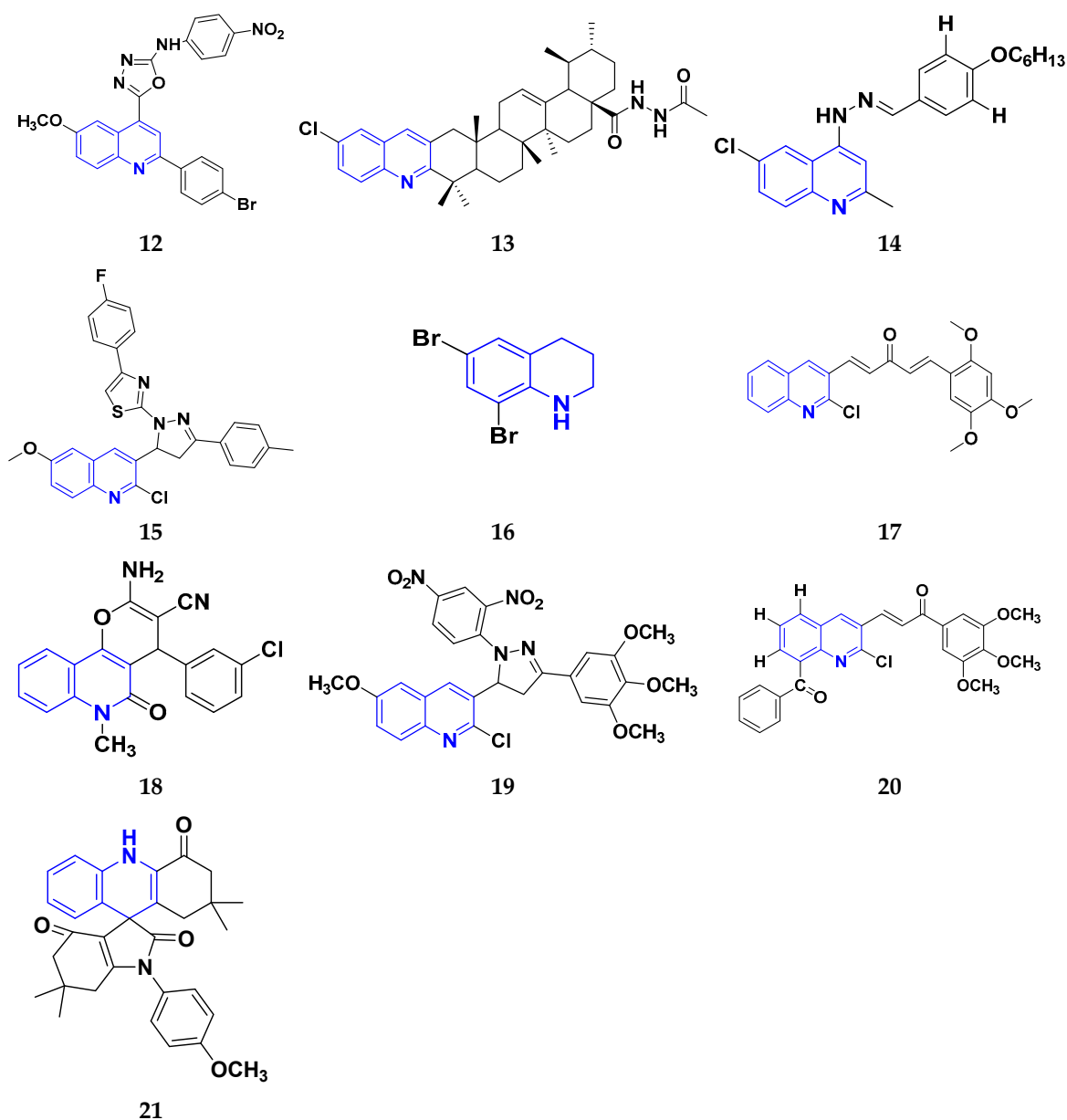


Figure 4. Quinoline derivatives (12–21) as anticancer agents.

Sun et al. (2017) synthesized novel carbazole sulfonamide derivatives and evaluated their anti-proliferative activity and aqueous solubility as an antitumor agent. A number of novel carbazole sulfonamide derivatives were produced by the current optimization of IG-105 on the carbazole-ring. Each compound's anti-proliferative effectiveness was tested on HepG2 cells. When tested for anti-proliferative activity against MIA PaCa-2 (pancreatic cancer), MCF-7 (breast cancer), and Bel-7402 (hepatocellular/liver cancer), compounds that had shown action superior or equivalent to that of IG-105 against HepG2 were found to be effective. Five of the seven substances were chosen for further investigation and discovered to have IC_{50} values against the four cell lines that were comparable to those for IG-105. The activity of two compounds, compound **25a** and **25b** against HepG2 and MCF-7 (IC_{50} values of 0.01 and 0.07 μM) was close to that of the positive controls podophyllotoxin and CA-4. The most potent compound out of these two was Compound **25a** with IC_{50} value against HEPG2 was 0.012 μM as compared to the controls podophyllotoxin with IC_{50} value 0.003 μM and CA-4 with IC_{50} value of 0.002 μM respectively [141]. Arya et al. (2018) performed eco-compatible synthesis of highly functionalized pyrido[2,3-a] carbazole derivatives and tested them for their cytotoxic effects on cancer cell lines MCF-7 and A549. The result of this study revealed compound **26** as the potent anticancer compound with lowest IC_{50} values of 45 μM and 50 μM against MCF-7 and A549 while the control drug Ellipticine presented IC_{50} values of 73 μM and 65 μM , respectively [142]. Padmaja et al. (2014) tested the anticancer activity of novel pyrano[3,2-c]carbazole derivatives which induce cell death by the inhibition of tubulin polymerization. A facile one-pot, three-component reaction using malononitrile-ethyl cyanoacetate, aromatic aldehydes, and 4-hydroxycarbazoles, catalyzed by trimethylamine was used to synthesize pyrano[3,2-c]carbazole derivatives. Investigations were performed to test their ability to inhibit the proliferation of several cancer cell lines, including K562, MDA-MB-231, HeLa, and A549. The most potent anticancer agent was compound **27** with IC_{50} values of 0.43, 1.13, 3.41, 6.12, and 69.24 μM against the cell lines MDA-MB 231, K562, A549, HeLa, and L929, respectively. Combrestatin A-4 (CA-4) was used as the control. This compound causes apoptosis by preventing tubulin polymerization and G2/M phase arrest of the cell cycle [143]. Patel et al. (2021) synthesized and characterized coumarin carbazole based functionalized pyrimidines, evaluated the anticancer effect, and performed molecular docking studies. The synthesized compounds were evaluated against three cell lines (HeLa, NCI-H520, and NRK-52E). Compound **28a** and **28b** were reported to be most active because of their ability to cause apoptosis and cell cycle arrest. Both of these molecules demonstrated high binding affinity towards CDK2 protein. Compound **28a** was the most potent anticancer agent with IC_{50} values of 12.59 μM , 11.26 μM , and 28.37 μM against the cell lines HeLa, NCI-H520, and NRK-52E respectively. It was compared to the control Cisplatin with IC_{50} values of 7.75, 10.41, and 12.93 μM and 5-Fluorouracil with IC_{50} values of 55.72, 8.36, and 46.68 μM , respectively [144]. Huang et al. (2021) performed the synthesis of novel carbazole derivatives as selective and potent anticancer drugs, as well as performed their biological evaluation and structure–activity relationship studies. The in vitro cytotoxic effects of two series of carbazole compounds against the three cell lines A875, HepG2, and MARC145 were assessed. In this study, compared to the control 5-fluorouracil, the results showed that some of these carbazole derivatives had much better cytotoxic effects against the examined cell lines. Particularly, the carbazole acylhydrazone compounds **29a** and **29b** showed strong inhibitory effect against cancer cells, but essentially no activity against normal cells. Particularly, compound **29a** showed significantly selective proliferation inhibition on cancer and normal cell lines with the selectivity index up to 13, and it had a stronger inhibitory effect on the A875 with IC_{50} value of 7.65 μM and HepG2 cell lines with IC_{50} value of 8.16 μM compared to the normal cells line MARC145 with IC_{50} value of > 105 μM . The control 5-Fluorouracil had IC_{50} values of 72.33, 81.94, and 77.56 μM against A875, HepG2, and MARC145 cell lines, respectively [145].

Chen et al. (2018) synthesized racemic and chiral carbazole aminoalcohols and tested their anticancer potential. It was found that the topoisomerase I was inhibited due to a

number of reasons, e.g., substitution site, heterocycle, chirality, and length of alkyl chain. MDA-MB-231, HCT116, and A549 cancer cell lines were used as test subjects and carbazole amino alcohols with potent topo I inhibitory activities, such as pyrrolidine derivative and propyl- to pentyl- amine derivatives, demonstrated good anticancer activities. The most potent compound reported in this study was compound **30** with broad spectrum anti-tumor activity against 15 cancer cell lines. The IC_{50} values were 7.9, 4.6, 2.8, 7.5, 3.9, 3.4, 3.8, 2, 4.8, 1.6, 1.5, 1.7, 1.7, 1.7, and 2.2 μM against A549, HCT116, MDA-MB-231, HeLa, H3122, BT549, BEL7402, 3AO, HO-8910, Rh30, Pfeiffer, Molm13, OC1-AML2, Jurkat, and HL60 cell lines, respectively [35].

Vairavelu et al. (2014) performed solvent-free synthesis of heteroannulated carbazoles using grinding conditions and a number of new carbazole analogues. Templates for isoxazolo, pyrido, pyrazolo, and pyrimido were developed and synthesized in high yield. The synthesized compounds were tested in vitro for their anticancer potential. Compound **31** was the most potent anticancer compound with IC_{50} values of 0.37 μM and 15.12 μM against HeLa and AGSb cell lines respectively. Ellipticine was used as the control with IC_{50} values of 4.12 and 7.33 μM , respectively [146].

Among the above-mentioned carbazole derivatives (Figure 5 (22–31)), the most potent one was compound **25a** having a pyridine ring joined by sulphonamide linkage and substituted with 2,5-dimethoxy group, having the lowest IC_{50} value of 0.012 μM against the HEPG2 as compared to the control podophyllotoxin with IC_{50} value of 0.003 μM and CA-4 with IC_{50} value of 0.002 μM .

3.4. Pyridine Derivatives as Anti-Cancer Agents

Pyridine has the chemical formula $\text{C}_5\text{H}_5\text{N}$ and is a fundamental heterocyclic organic molecule. The word “pyridine” is taken from Greek and combines the words “idine” and “pyr,” which both refer to aromatic bases. Picoline, the first pyridine base, was discovered by Anderson in 1846. It took quite some time for Wilhelm Korner and James Dewar to discover its structure. It resembles the well-known and fundamental aromatic molecule benzene in many ways, but with one C-H group replaced by an atom of Nitrogen. Like benzene, pyridine possesses a conjugated system of six delocalized electrons distributed around the heterocyclic ring. The molecule satisfies the Huckel requirements for aromaticity and is planar in nature [147].

Gomha et al. (2018) performed the studies on anti-tumor activity through the Synthesis of some new pyridine-based heterocyclic compounds. By the reaction of 7-(pyridin-4-yl)-2-thioxo-2,3-dihydropyrido[2,3-d] pyrimidin-4(1H)-one and 2-cyano-N-(1-(pyridin-4-yl)ethylidene)-acetohydrazide with hydrazonoyl halides, 5-amino-N-(1-(pyridin-4-yl)ethylidene)-1H-pyrazole-4-carbohydrazides and 8-(pyridine-4-yl)pyrido[2,3-d][1,2,4]triazolo[4,3-a]pyrimidin-5(1H)-ones were synthesized. The anti-cancer activity of the synthesized compounds was tested against the HEPG2 cell line. The most potent compound reported in this study was compound **32**, with an IC_{50} value of 0.97 μM against the HEPG2 cell line Doxorubicin is used as the standard with an IC_{50} value of 0.74 μM [148]. Fayed et al. (2019) designed, synthesized, and performed molecular modeling studies of coumarin derivatives. The synthesized compounds were evaluated for their cytotoxic activity against different cell lines; HCT-116, MCF-7, A549, and HepG-2. The most potent compound in this study was compound **33** with IC_{50} values of 1.11, 6.44, 4.51, and 7.18 μM against the cancer cell lines MCF-7, HCT-116, HepG-2, and A549, respectively. 5-Fluorouracil was the standard with IC_{50} values of 7.76, 8.78, 8.15, and 7.65 μM , respectively. Compound **33** induced cell cycle arrest in the G2/M phase and apoptosis. Caspase-3 is used for stimulating apoptosis [149]. Nagender et al. (2016) synthesized novel hydrazone and azole-functionalized pyrazolo[3,4-b]pyridine derivatives. With the key intermediate ethyl 2-(3-amino-6-(trifluoromethyl)-1H-pyrazolo[3,4-b]pyridin-1-yl)acetate, a variety of pyrazolo[3,4-b]pyridine compounds were synthesized. The reaction was carried out with hydrazine hydrate followed by isothiocyanate, acid chloride, and different aldehydes to form 1,2,4 triazoles, oxadiazoles, hydrazones, and thiadiazoles. All the synthesized compounds were screened for anti-cancer activity. With an IC_{50} value of 3.2 μM , compound **34** with the

trifluoromethylthio group demonstrated excellent action against the lung cancer cell line (A549) compared with the control 5-Fluorouracil with an IC_{50} value of 1.7 μ M [150].

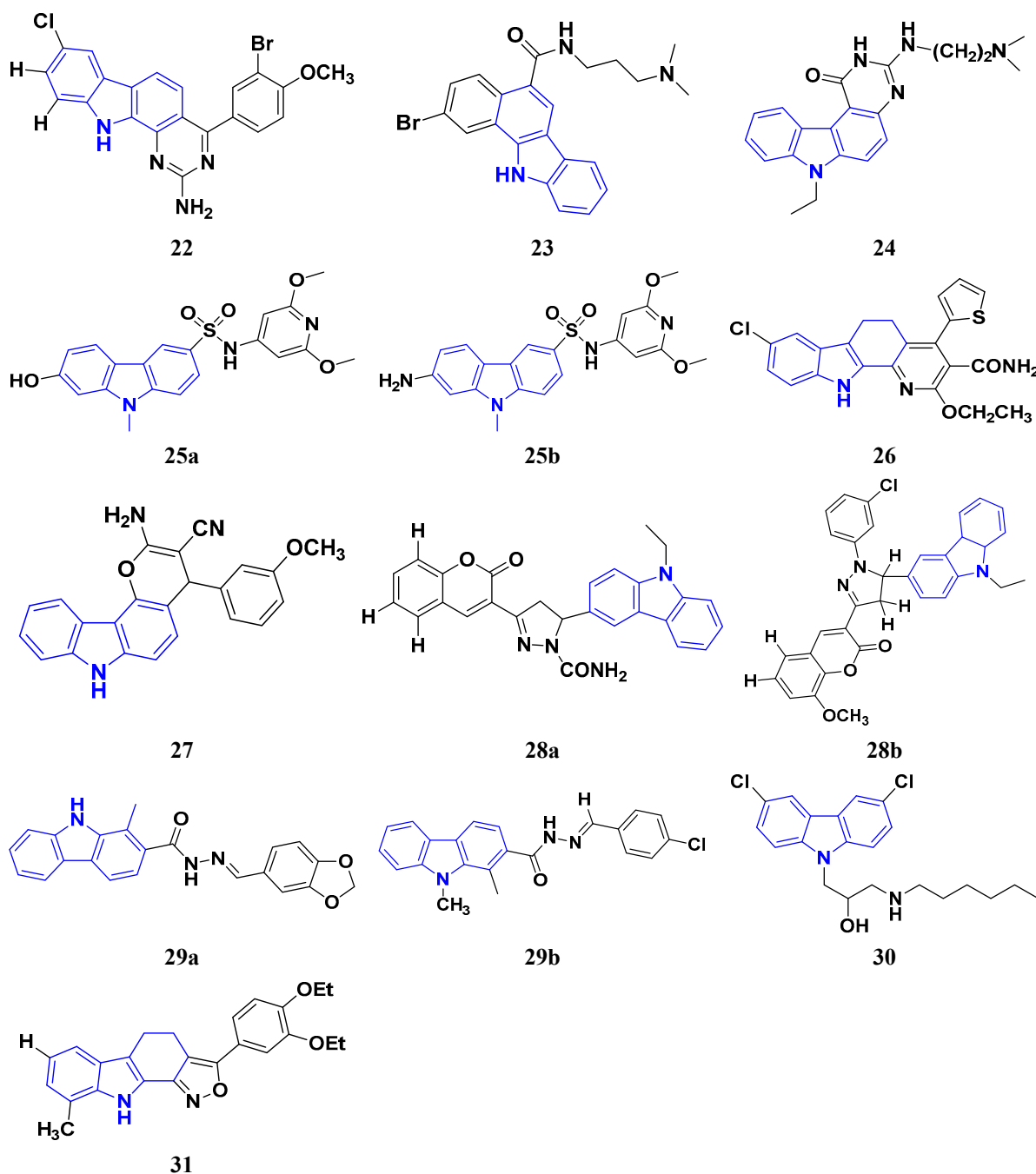


Figure 5. Carbazole derivatives (22–31) as anticancer agents.

El-Naggar et al. (2018) conducted the synthesis and biological evaluation of pyridine-urea derivatives as anti-cancer drugs. All the synthesized compounds were tested for their *in vitro* antiproliferative activity in breast cancer against the MCF-7 cell line. Two compounds, **35a** with IC_{50} values of 0.22 μ M (48 h) and 1.88 μ M (72 h) and **35b** with IC_{50} values of 0.11 μ M (48 h) and 0.80 μ M (72 h), were reported to present potent anti-cancer activity against the MCF-7 cell line. The most potent compound was compound **35b** with the lowest IC_{50} value, while compared to the reference drugs, doxorubicin presented IC_{50} values of 1.93 μ M (48 h) and 1.07 μ M (72 h) and sorafenib with IC_{50} values of 4.50 μ M (48 h) and 1.71 μ M (72 h) respectively [151].

Dinda et al. (2014) carried out a study on the cytotoxicity of pyridine-wingtip substituted annelated N-heterocyclic carbene complexes of silver (I), gold (I), and gold (III). Three new compounds were synthesized from 1-methyl-2-pyridin-2-yl-2H-imidazo[1,5-a]pyridin-4-ylum chloride. The synthesized complexes were tested for their cytotoxicity against HepG2 (human hepatocellular carcinoma), A549 (human lung adenocarcinoma), HCT 116 (human colorectal carcinoma), and MCF-7 (human breast adenocarcinoma) cells. Compound **36** was the most potent antiproliferative agent with IC_{50} values of 4.91, 5.08, 5.23, and 5.18 μM against the cell lines HepG2, HCT-116, A549, and MCF-7, respectively. Cisplatin was used here with IC_{50} values of 4.31, 4.89, 6.12, and 4.42 μM , respectively [152]. El-Gohary et al. (2019) synthesized novel pyrazolo[3, 4-b]pyridine analogs, screened their anti-cancer potential, and performed molecular modeling. An in vitro anti-cancer assay toward MCF-7, HepG2, and Hela cancer cells and in vivo anti-cancer assay over E.A.C. in mice were carried out. The most potent compound was compound **37**, with IC_{50} values of 3.63, 3.11, and 4.91 μM against the cell lines HepG2, MCF-7, and Hela, respectively. Doxorubicin was used as the reference with IC_{50} values of 4.3, 3.97, and 5.17 μM , respectively. According to molecular modeling studies, it was reported that the synthesized compounds bind to DNA through intercalation similar to doxorubicin [153].

Sangani et al. (2014) designed, synthesized, and evaluated the molecular modeling of pyrazole-quinoline-pyridine hybrids as a potential class of antibacterial and anti-cancer drugs. A one-pot multicomponent reaction was carried out using a base-catalyzed cyclo condensation reaction, and a new series of pyrazole-quinoline-pyridine hybrids were synthesized. All the compounds synthesized tested for in-vitro anti-cancer and antimicrobial activity. The most potent compound with the lowest cytotoxicity was compound **38**, compared to reference drug Erlotinib with IC_{50} values of 0.13, 0.12, and 0.032 μM , against the cell lines A549, HepG2, and E.G.F.R. respectively. Compound **38** showed three hydrogen bonds and one $-\pi$ cation interaction with a minimum binding energy of -54.6913 kcal/mol in the molecular docking studies with the catalytic pocket of protein [154]. Elzahabi (2011) synthesized and characterized some benzazoles bearing pyridine moiety in a search for novel anti-cancer agents. Thirteen new benzazole compounds were synthesized as potential anti-cancer agents. The National Cancer Institute (NCI), U.S.A. chose four derivatives of the produced compounds to be tested for their anti-cancer potential against a panel of 60 cancer cell lines at a single high dose. Compounds 4-[p-chlorophenyl]pyridine and 4-[p-methoxyphenyl]pyridine were chosen for further testing at five doses after exhibiting a broad and moderate anti-cancer activity against 41 tumor cell lines belonging to the nine subpanels employed. The compounds **39a** and **39b** showed excellent activity in HOP-92 cells with GI_{50} values of 0.275 μM and 2.65 μM , respectively. Regarding colon cancer, compound **39a**'s GI_{50} value against HCT116 was 3.47 μM , and the most sensitive cell line in this subpanel was KM12 towards compound **39b** with GI_{50} 4.79 μM . The most sensitive lines for compounds **39a** and **39b** were SF-539 and SNB-75, belonging to C.N.S. cancer cell lines with GI_{50} 2.07 μM and 2.36 μM , respectively [155].

Zheng (2014) researched the design, synthesis, and biological evaluation of novel combretastatin-A4 pyridine-bridged analogs as anti-cancer drugs. The synthesized compounds potentially suppressed cell growth and survival, stopped the cell cycle, and prevented angiogenesis and the development of blood vessels, similar to CA-4 (combretastatin-A4). The IC_{50} values of compound **40a** against three cancer cell lines were 0.0031, 0.089, and 0.0038 μM against MDA-MB-231, A549, and HeLa, respectively, and for compound **40b** were 0.0046, 0.044, and 0.0014 μM respectively. The reference compound used was combretastatin-A4 with IC_{50} values of 0.0028, 0.0038, and 0.0009 μM , respectively [156]. Abbas et al. (2015) synthesized novel pyridines having an imidazole moiety. The one-pot multicomponent reaction of 5-acetyl imidazole, substituted benzaldehyde (or terephthaldehyde), malonitrile (or ethyl cyanoacetate or diethyl malonate), and ammonium acetate was carried out to produce a novel series of pyridine and bipyridine derivatives. Some recently synthesized compounds were tested for their anti-cancer activities against the human breast cell line (MCF-7) and liver carcinoma cell line (HEPG2) with the reference

Doxorubicin IC₅₀ values of 0.46 μ M and 0.42 μ M, respectively. The most potent compound was compound **41**, with IC₅₀ values of 1.7 and 6 μ M, respectively [157]. Ivasechko (2022) synthesized novel pyridine-thiazole hybrid molecules as potential anti-cancer agents and evaluated their anti-cancer activity against several kinds of tumors, e.g., carcinomas of the breast, lung, colon, glioblastoma, and leukemia. Two compounds showed the highest anti-cancer activity. The most potent compound reported was compound **42**, with an IC₅₀ value of 2.79 μ M against the MCF-7 cell line. Doxorubicin was standard with an IC₅₀ value of 1.04 μ M against the MCF-7 cell line [158].

Among the above-reported potent anti-cancer compounds (Figure 6 (32–42)) having a pyridine moiety, the most active compound which showed the best cytotoxic activity was compound **40a** (a diaryl compound joined by pyridine ring. Diaryl rings were substituted with methoxy group on different positions). It showed the lowest IC₅₀ value of 0.0031 μ M, 0.089 μ M, and 0.0038 μ M against the three human cancer cell lines MDA-MB-231, A549, and HeLa, respectively.

3.5. Imidazole Derivatives as Anticancer Agents

Heinrich Debus synthesized the first Imidazole in 1858 by reacting glyoxal and formaldehyde in the presence of ammonia. Derivatives of Imidazole are now widely used in many treatments and have recently attracted much attention. Various medicinal properties of imidazole-based hybrid molecules have been reported, especially as antitumor, anti-diabetic, anti-HIV, anti-mycobacterial, anti-inflammatory, analgesic, and anti-protozoal activities [159].

Liu et al. (2015) synthesized carbazole-imidazole-based carbazole derivatives and tested them for anticancer activity against various cell lines: HL-60, SMMC-7721, A549, MCF-7, and SW480. Compound **43** demonstrated potent activity among the synthesized carbazole derivatives, with IC₅₀ values of 0.51, 2.38, 3.12, 1.40, and 2.48 μ M, whereas control cisplatin (DDP) had IC₅₀ values of 1.32, 6.24, 11.83, 15.17, and 12.95 μ M, respectively. Furthermore, Compound **43** caused cell cycle arrest in SMMC-7721 cells at IC₅₀ of 0.51 μ M [160].

Ruzi et al. (2021) synthesized imidazole derivatives having ethyl 5-amino-1-N-substituted imidazole-4-carboxylate building blocks as anticancer agents. Compound **44** showed the best anticancer activity with HeLa, HT-29, A549, HCT-15, and MDA-MB-231 cell lines with IC₅₀ values of 0.81, 1.77, 15.22, 17.92, and 5.48 μ M. Reference drug Doxorubicin presented IC₅₀ values of 0.1, 0.03, 1.1, 0.27, and 0.51 Mm, respectively [161]. Singh et al. (2021) synthesized and reported C₆-substituted benz[4,5]imidazo[1,2- α]quinoxaline derivatives and performed their anticancer evaluation. Compound **45** showed excellent anticancer activity at IC₅₀ values of 14.62, 4.78, 1.55, and 1.04 μ M against MDA-MB-231, MDA-MB-486, MCF-7, and MCF12A cell lines, respectively, whereas control cisplatin had IC₅₀ values 3.26, 1.43, and 4.23 μ M against MDA-MB-231, MDA-MB-486, and MCF-7 cell lines, respectively [162]. Yang et al. (2012) synthesized various novel hybrids of 2-phenylbenzofuran and Imidazole. Among them, compound **46** displayed good in vitro activity against different cancer cell lines, including SMMC-7721, SW480, MCF-7, A549, and HL-60, with IC₅₀ values of 1.65, 3.38, 5.87, 10.93, and 2.49 μ M, respectively, whereas control cisplatin (DPP) had IC₅₀ values of 8.86, 15.92, 1.65, 11.68, and 1.81 μ M respectively. Compound **46** demonstrated good anticancer activity with more excellent cytotoxic activity than standard DPP [163]. Song et al. (2012) synthesized different novel hybrids with 2-substituted benzofuran and imidazole. In vitro anticancer activities of synthesized hybrids were tested against a panel of human tumor cell lines, such as the ovarian carcinoma cell line (Skov-3), leukemia (HL-60), and breast carcinoma (MCF-7). Compound **46** was found to be more selective than standard DPP. Compound **47** showed more potent activity at IC₅₀ values of 9.5, 8.4, and 11.8 μ M with standard drug Cisplatin (DDP) (IC₅₀ values of 8.9, 5.5, and 13.0 μ M respectively) [164].

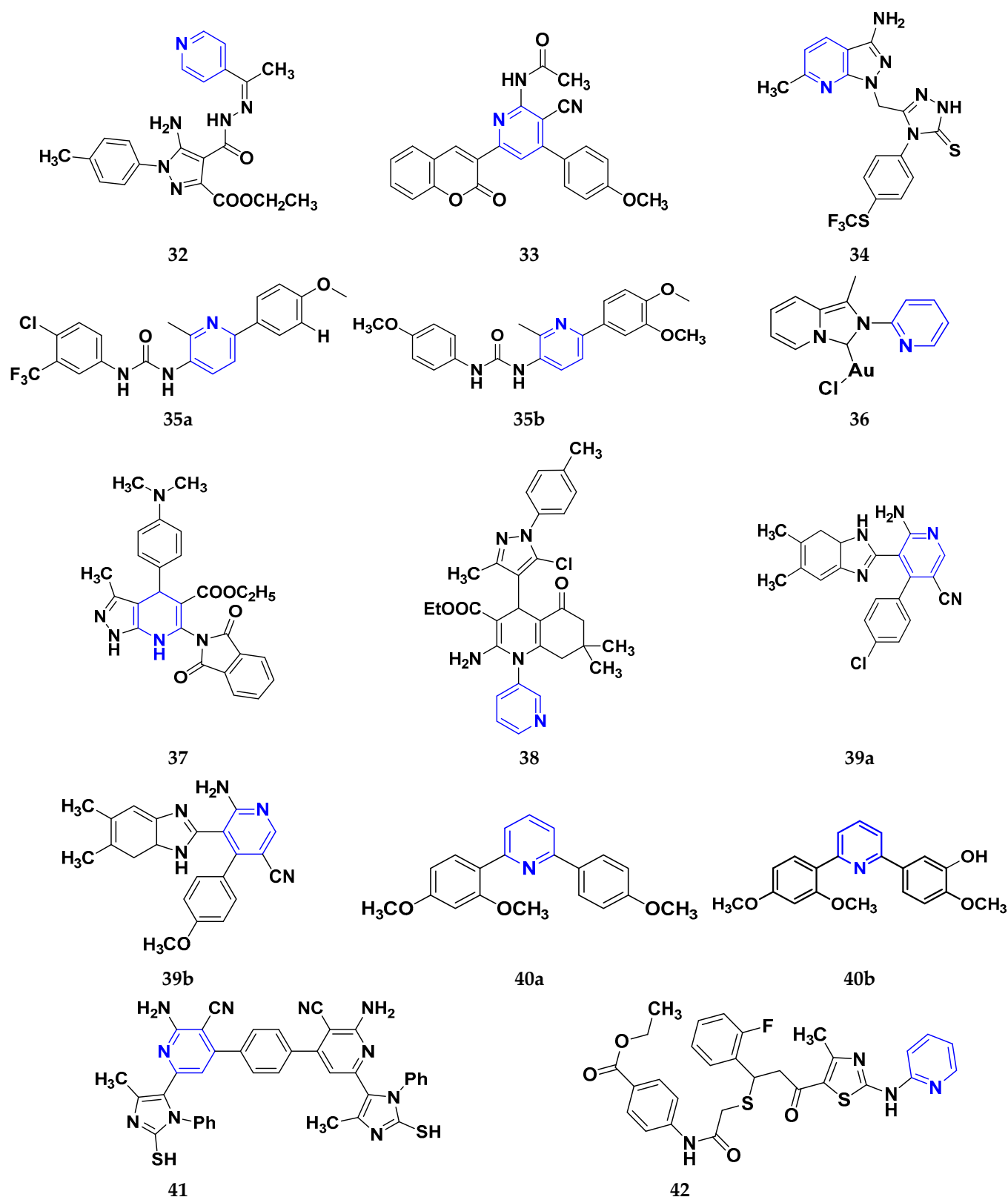


Figure 6. Pyridine derivatives (32–42) as anticancer agents.

The design, synthesis, and anti-proliferative evaluation of novel imidazole-thione linked benzotriazole derivatives against MCF-7, HL-60, HCT-116 and HUVEC cell lines were reported by Khayyat et al. (2021). Anticancer activity screening results revealed that

compound **48** was the most promising anticancer agent having IC₅₀ values of 3.57, 0.4, 2.63 and 118.9 μM, respectively. CA-4 was used as a reference drug with IC₅₀ values of 0.58, 0.77, 0.24, and 13.6 μM, respectively [165]. Quinazoline-based imidazole derivatives were synthesized and screened for their anticancer activity against epidermal growth factor receptor (EGFR) and HT-29 cell lines (normoxic and hypoxic conditions) by Kumar et al. (2022). Most of the synthesized compounds displayed potent anticancer activity. Among them, compound **49** showed excellent activity with IC₅₀ values 0.47 and 2.21 μM, respectively, with control gefitinib IC₅₀ values 0.45 μM against EGFR, and 3.63 μM and 5.21 μM against Normoxia and Hypoxia in HT-29 cells, respectively [166]. Kalra et al. (2021) synthesized imidazole and purine-derived derivatives as anticancer agents. These are tested for antiproliferative activity against different cancer cell lines, including MDA-MB-231, T47D, MCF-7, A549, and HT-29 by MTT assay. Compound **50** had IC₅₀ values of 36.7, 9.96, 5.17, 2.29, and 3.29 μM, respectively, whereas control, Erlotinib, had IC₅₀ values 5.46, 9.80, >30.00, 1.04, and 4.63 μM, respectively. Compound **50** showed the most potent anticancer activity against A549 cell lines with an IC₅₀ value of 2.29 μM [167].

Taheri et al. (2020) synthesized and reported imidazole derivatives of anticancer importance. The imidazole derivatives showed a good cytotoxic effect on MCF-7, HT-29, and HeLa cell lines. The order of cytotoxic effect of the compounds on various cell lines was MCF7 > HT-29 > HeLa. Compound **51** showed the most potent activity at IC₅₀ values of 2.5, 5.36 and 4.03 μM, respectively. Doxorubicin was used as positive control with the IC₅₀ values 1.4 μM, 0.7 μM, and 0.9 μM respectively [168]. Oskuei et al. (2021) synthesized new imidazole chalcone derivatives and performed MTT assays against four cancer cell lines, including A549, MCF-7, HEPG2 and MCF-7/MX. Among them, compound **52** showed significant cytotoxicity with IC₅₀ values of 7.05, 9.88, 20.2, and 3.86 μM with control combretastatin having IC₅₀ values 0.86, 0.43, 0.63, and 1.49 μM respectively [169]. Wang et al. (2013) synthesized the novel 2-benzylbenzofuran and imidazole derivatives and compared their activity against various cancer lines, namely HL-60, A549, SW480, MCF-7, and SMMC-7721. Compound **53** showed potent cytotoxic activities among the synthesized molecules with IC₅₀ values of 1.02, 3.57, 3.55, 2.29, and 3.09 μM with Control DDP (IC₅₀ values of 3.10, 13.61, 12.32, 10.64 and 14.75 μM). Among the synthesized compounds, imidazole, 2-methyl-imidazole, or 2-ethyl-imidazole scaffolds showed weak cytotoxic activities. Compound **53** showed the selectivity towards the MCF-7 and SMMC-7721 with IC₅₀ values of 1.02 and 3.09 μM) [170].

Du et al. (2021) synthesized and reported new series of 1,3,4-oxadiazole based imidazole based heterocyclic hybrids as anti-cancer agents. Among them, compound **54** showed the highest anticancer activity against HepG2, SGC-7901, and MCF-7 cell lines with IC₅₀ values of 0.7, 30.0, and 18.3 μM. Standard drug, 5-Fluorouracil had IC₅₀ values of 22.8, 28.9, and 16.7 μM respectively [171]. The above-reported anticancer compounds (Figure 7 (43–54)) have an imidazole moiety, which showed the best cytotoxic activity against representative cell lines. Furthermore, compound **49** showed the lowest IC₅₀ value of 0.47 μM against epidermal growth factor receptor, whereas the control drug, gefitinib, had an IC₅₀ value of 0.45 μM. Compound **49** had a quinazoline ring which was substituted with substituted aromatic ring joined by amino linkage.

3.6. Benzimidazole Derivatives as Anticancer Agents

Benzimidazole consists of benzene fused to the 4,5-positions of the imidazole ring. It is known as benzimidazole or benzoglyoxaline. The resonance in benzimidazole demonstrates its amphoteric nature and indicates that an electrophilic attack will occur either at N-1 or in the benzene ring [172]. Various studies have revealed that substituted benzimidazoles and heterocycles can easily interact with biopolymers, having pharmacological activity with lower toxicities. Because of the fused nitrogen nuclei, benzimidazoles are structural isosteres of nucleobases and readily interact with biomolecular targets, eliciting a wide range of biological activities, such as anti-inflammatory, antiulcer, anti-hypertensive, anthelmintic [173], and anticancer properties. For example, nocodazole, benzimidazole

containing antineoplastic drug works by depolymerizing microtubules to achieve its effects [174].

Shao et al. (2014) synthesized and reported novel pyrimidine-benzimidazole derivatives with anticancer properties against MCF-7, MGC-803, EC-9706, and SMMC-7721 cancer cell lines. Compound 55 showed excellent anticancer activity against cancer cell lines with IC_{50} values of 1.40, 1.07, 2.79, and 19.28 μM respectively. The standard drug 5-flourouracil had IC_{50} values of 7.12, 3.45, 8.07, and 15.08 μM respectively [175]. Husain et al. (2012) designed and synthesized two series of compounds having benzimidazole rings merged with triazole-thiadiazole and trizolothizdiazole. The synthesized compounds showed good anticancer activity against CCRF-CEM, HL-60 (T.B.), MOLT-4, RPMI-8226, and S.R cell lines. Compound 56 showed good anticancer activities against leukemia cell lines having $\log_{10}GI_{50}$, $\log_{10}TGI$, and $\log_{10}LC_{50}$ values 6.58, 6.01, and 4.00 μM , respectively [176].

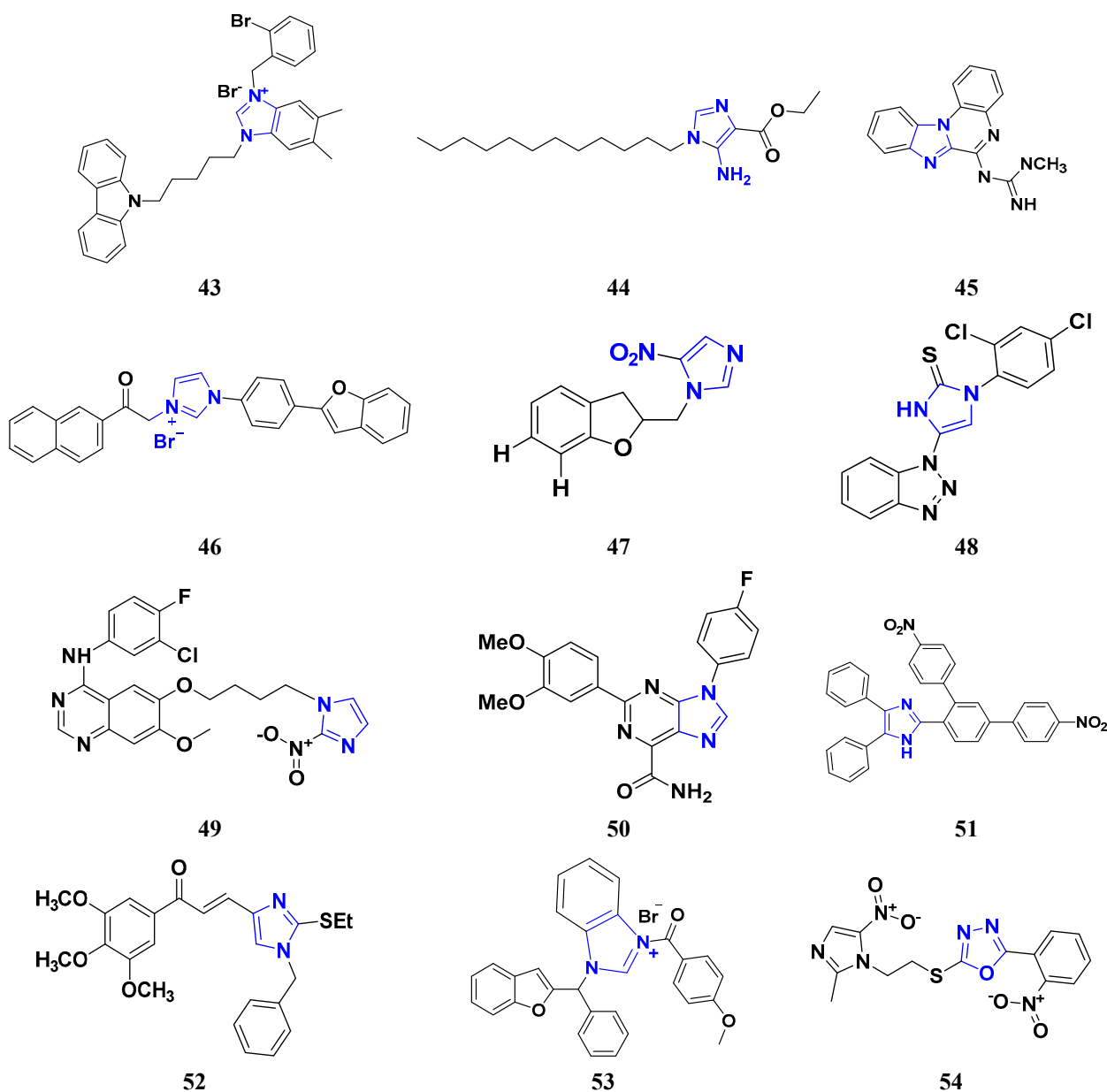


Figure 7. Imidazole derivatives (43–54) as anticancer agents.

Sana et al. (2021) synthesized cinnamide derived pyrimidine-benzimidazole having growth inhibitory effects against five cancer cell lines, including A549, PC-3, HeLa, MDA-

MB-231, and L132. Among the synthesized compounds, molecules **57** exhibited potent activity at IC_{50} values of 2.21, 3.15, 7.29, 5.71, and 69.25 μM , respectively, while the control Nocodazole had IC_{50} values 2.39, 1.96, 3.48, 2.13, and N.D. (for L132), respectively [177]. Sireesha et al. (2020) synthesized benzoxazole-linked β -carbolines by combining two anticancer fragments. Compound **58** showed the most promising anticancer activity against a panel of cell lines, MCF-7, A549, colo-205, and A2780 with IC_{50} values of 0.092, 0.72, 0.34, and 1.23 μM , respectively, while the control etoposide had IC_{50} values of 2.11, 3.08, 0.13, and 1.31 μM respectively [178]. Shi et al. (2014) synthesized and screened quinazoline-4-amines with benzimidazole analogs to have anticancer activity as dual inhibitors of c-Met and VEGFR-2. Compound **58** displayed the most potent inhibitory activity against c-Met and VEGFR-2 with IC_{50} values of 0.05 μM and 0.02 μM . Moreover, compound **59** showed potent activity against cancer cell lines, namely MCF-7 and Hep-G2, at IC_{50} of 1.5 and 8.7 μM , respectively. Furthermore, it also interacted at the ATP-binding site of c-Met and VEGFR-2 [179].

Romero-Castro et al. (2010) synthesized 2-aryl-5(6)-nitro-1H-benzimidazole derivatives by one multicomponent reaction and evaluated their anticancer potential against K562, HL60, MCF7, MDA231, A549, HT29, K.B., and HACAT cancer cell lines. Compound **60** showed anticancer activity against representative cell lines at IC_{50} of 4.9, 2.1, 8.0, 4.0, 0.028, 1.8, 3.0, and 22.2 μM respectively whereas standard drug carboplatin had IC_{50} values of 1.5, 0.3, 8.9, 2.6, 0.05, 0.9, 4.1, and 0.6 μM respectively [180]. Sivaramakarthykeyan et al. (2020) synthesized benzimidazole-pyrazole hybrids and evaluated their anticancer activity against various cancer cell lines. Most of the synthesized compounds demonstrated potent anticancer activity. Compound **61** had potent anticancer activity against SW1900, AsPC1, and MRCS with IC_{50} values of 30.9, 32.8, and 80.0 μM , respectively, whereas control gemcitabine had IC_{50} values of 35.09, 39.27, and 54.17 μM , respectively [181].

Perin et al. (2021) synthesized a new series of acrylonitrile derivatives from aromatic aldehydes and N-substituted-2-cyanoethyl benzimidazole and tested their anticancer activity on various human cancer cell lines, such as Htert rpe-1, Capan-1, HCT-116, NCI-H460, DND-41, HL-60, K-562, MM.1S, and Z-138. Compound **62**, with both cyano and isobutyl substituents attached to the benzimidazole moiety, demonstrated good anticancer activity with IC_{50} values of 4.3, 0.3, 0.6, 0.4, 0.2, 0.3, 2.1, 1.5, and 0.4 μM , respectively, with standard docetaxel, which had IC_{50} values of 0.0553, 0.0088, 0.0017, 0.0024, 0.0125, 0.0072, 0.0152, 0.0118, and 0.0142 μM respectively. Furthermore, It was tested and found not to affect normal cells [182].

Wu et al. (2015) synthesized benzimidazole-2-substituted phenyl and pyridinepropyl ketene derivatives and tested their cytotoxicity on three cancer cell lines, i.e., MCF-7, HepG2, and HCT116. The synthesized compound **63** showed potent anticancer activity at IC_{50} values of 9.80, 0.75, and 0.03 μM , respectively, with control drug 5-Fluorouracil with IC_{50} values of 222.6, 174.5, and 56.96 μM , respectively [183]. Holiyachi et al. (2016) synthesized coumarin benzimidazole hybrids from the 4-formylcoumarins by using N-sulphonation and N-methylation reactions. Among them, compound **64** showed excellent anticancer activity against HeLa and HT29 cell lines at LC_{50} and GI_{50} of 10, 20, 40, and 80 $\mu M/mL$, respectively [184]. Tahlan et al. (2018) synthesized heterocyclic 1H-benzimidazole derivatives and tested them for anticancer activity against a cancer cell line (HCT116) using the SRB method. Their results were similar to standard 5-fluorouracil. Compound **65** exhibited the anticancer activity at an IC_{50} value of 4.12 μM , with control 5-fluorouracil (IC_{50} value of 7.69 μM) [185]. Yuan et al. (2019) synthesized 6-amide-2-aryl benzoxazole/benzimidazole derivatives and tested them in vitro against tumor cells and by inhibiting VEGFR-2 kinase. Among them, compound **66** showed good potent anticancer activity. It showed good anticancer activity against VEGFR-2, EGFR, and different cell lines, including; HUVEC, HepG2, A549, and MDA-MB-231 at IC_{50} values 102.8, 58.3, 1.47, 2.57, 73.81, and 57.32 μM with control sorafenib (IC_{50} values 103.6, 57.8, 5.35, 2.41, 7.62, and 17.38 μM , respectively) [186]. The above-reported anticancer compounds (Figure 8 (55–66)) had a benzimidazole moiety, which showed the best cytotoxic activity against representative cell lines. Furthermore,

compound **59** (having the quinazoline ring and a substituted aromatic ring) showed the lowest IC_{50} value of 0.02 μ M against VEGFR-2 with the control drug gefitinib.

3.7. Triazole Derivatives as Anticancer Agents

Triazole has been used in pharmaceuticals, agrochemicals, artificial materials, artificial acceptors, supramolecular ligands, and biomimetic catalysts. Heterocyclics have received particular attention due to their diverse pharmacological activities. The triazole ring is an essential five-membered heterocycle with three nitrogen atoms [187]. When creating new drug molecules, the triazole ring is a crucial isostere of imidazole, oxazole, pyrazole, and thiazole moieties. Many triazole-based derivatives have been extensively prepared and investigated for biological activities, which is one of the most active areas in new drug research and development [188]. Kurumurthy et al. (2019) synthesized pyrimidine based triazole derivatives and assessed their anticancer activity. Most of the synthesized compounds showed potent anticancer activity. Among them, compound **67** showed excellent activity against various cell lines, including U₉₃₇, THP-1, and Colo205 cells, having IC_{50} values of 6.20, 11.27, and 15.01 μ g/mL with control etoposide having IC_{50} values of 17.94, 2.16, and 7.24 μ g/mL respectively [189].

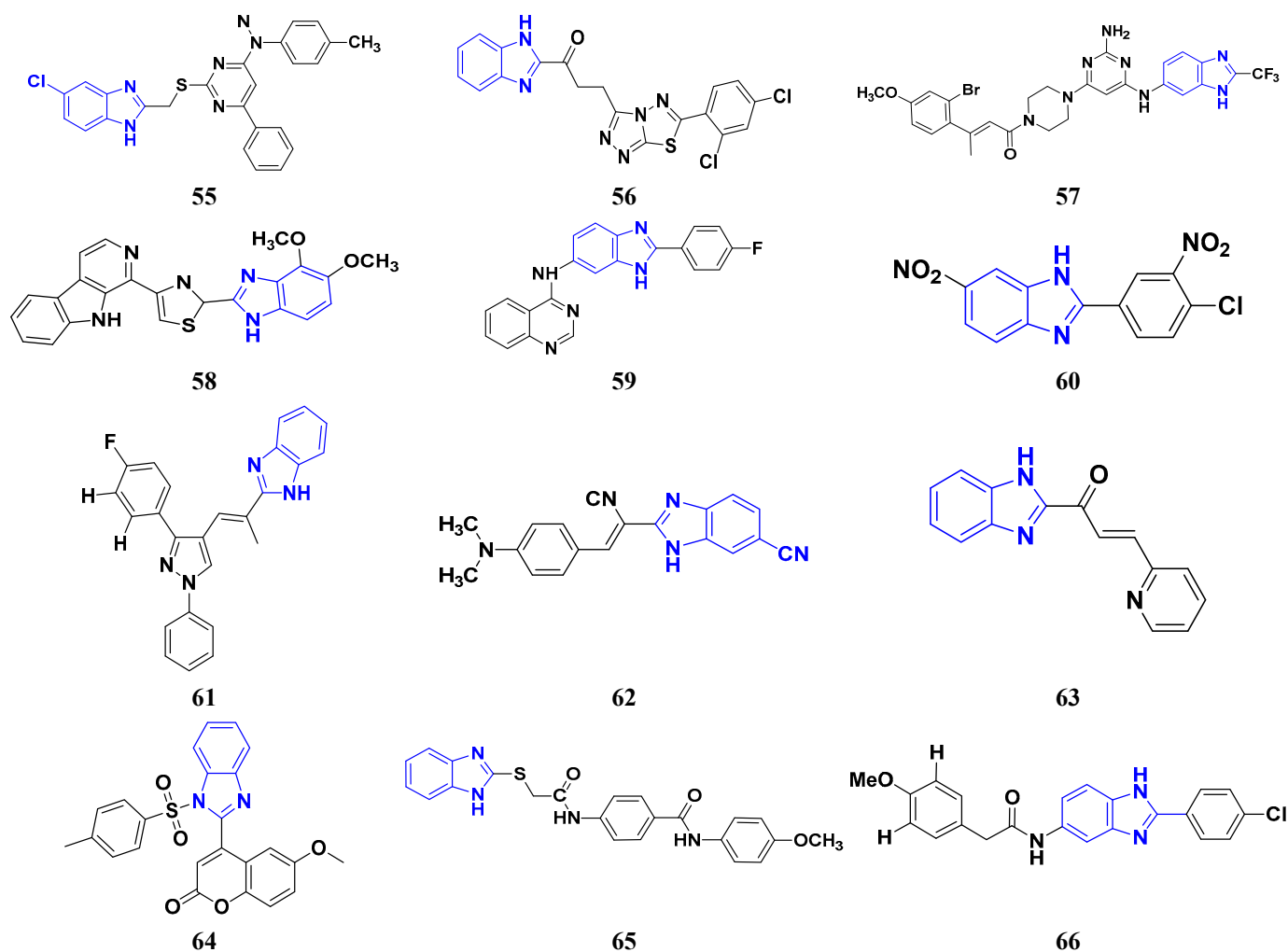


Figure 8. Benzimidazole derivatives (55–66) as anticancer agents.

Al-Blewi et al. (2021) designed and synthesized new imidazole derivatives with good anticancer properties based on the triazole pharmacophore. Four cancer cell lines, including Caco2, HTC116, HeLa, and MCF-7, were used for anticancer assessment. From all synthesized compounds, the recombinant click adducts triazole (compound **68**) was

found to be the most potent with the IC_{50} values of 4.67, 16.78, 6.87, and 0.38 μM , respectively, with standard doxorubicin (IC_{50} values of 5.17, 5.64, 1.25 and 0.65 μM respectively). Furthermore, it showed excellent activity against MCF-7 cell line IC_{50} of 0.38 μM and was more potent than the control drug, doxorubicin (IC_{50} 0.65 μM) [190]. Bozorov et al. (2019) synthesized 1,2,3-triazole-linked isoxazole-benzothiazole-benzoxazole hybrids and tested them for anticancer activity against HeLa, A549, and HEK-293 cells. Compound **69** showed potent activity with IC_{50} values of 1.768 and 2.594 μM , and it was not toxic to normal cells. Compound **69** showed cell cycle arrest in the sub G1 cell cycle phase with 49.43% of cells. Moreover, compound **69** (42.58%) demonstrated significant and enhanced apoptotic activity in the sub-G1 phase of HeLa cells [191]. Djemoui et al. (2019) synthesized triazole-benzimidazole-based chalcone derivatives as anticancer agents and evaluated them against T47-D, MDA-MB-231, and PC3 cell lines. The cytotoxic effects of triazole-benzimidazole-chalcone hybrid compound **70** were shown at >100, >100, and 5.64 μM , respectively. Compound **70** produced better cytotoxicity in PC3 cell lines. Control, doxorubicin, had IC_{50} values 0.13, 1.51, and 0.73 μM , respectively [192].

Suryanarayana et al. (2021) designed and synthesized novel 1,2,3-triazole-containing dinitrophenylpyrazoles and evaluated them as anticancer agents. These novel molecules were examined for anticancer activity against three tumor cell lines, namely human epithelial colorectal adenocarcinoma (CECA), cervical carcinoma (HeLa), and breast adenocarcinoma (MCF-7). Compound **71** showed potent activity at IC_{50} values 08, 06, and 12 μM , respectively, whereas control combretastatin-A4 had IC_{50} values of 10, 9 and 11 μM , respectively [193]. Chandrashekar et al. (2016) synthesized triazole- myrrhanone hybrids and tested them for anticancer activity against various cell lines, including A549, HeLa, MCF-7, DU-I45, and HepG2. Among them, compound **72** demonstrated good anticancer activity with IC_{50} values of 06.16, 07.76, 09.59, 08.83, and 09.52 μM . Control doxorubicin had IC_{50} values 2.818, 2.570, 1.135, 1.412, and 3.013 μM , respectively [194].

Najafi et al. (2014) synthesized and assessed the in vitro cytotoxic activity of novel triazole- isoxazole derivatives anticancer activity. Most of the synthesized compounds display good anticancer properties. Compound **73** proved effective against MCF-7 and T47D with IC_{50} values of more than 100 and 27.7 μM , respectively, whereas control etoposide had IC_{50} values 7.5 and 7.9 μM , respectively [195]. Duan et al. (2013) synthesized 1,2,3-triazole and dithiocarbamate hybrids and explored their anticancer activity. Most of the synthesized compounds demonstrated good anticancer activity. Among them, compound **74** demonstrated potent activity against four cell lines, i.e., MGC-803, MCF-7, PC-3, and EC-109, with IC_{50} values of 0.73, 5.67, 11.61, and 2.44 μM , respectively. Control, 5-fluorouracil had IC_{50} values of 7.01, 7.54, 27.07, and 3.34 μM , respectively [196]. Kumbhare et al. (2015) synthesized and assessed the anticancer activity of triazole thiazole hybrids against various cell lines. Most of the synthesized compounds displayed potent anticancer activity. Compound **75** exhibited potent activity against four cell lines, i.e., MCF-7, A549, A375, and MCF-10A, at IC_{50} values of 2.12, 5.48, 4.7, and 29.33 μM , respectively. Control, doxorubicin, had IC_{50} values 0.12, 3.13, 7.2, and 24.0 μM and paclitaxel had IC_{50} values 2.58, 4.9, 8.0, and 38 μM respectively [197].

Ying et al. (2015) synthesized and reported triazole pyrimidine urea hybrids as anticancer agents. Most of the synthesized compounds displayed potent anticancer activity. Among them, compound **76** displayed potent activity against four cell lines, i.e., EC-109, MCF-7, MGC-803, and B16-F10, with IC_{50} values of 2.96, 3.11, 3.60, and 4.55 μM , respectively. Standard drug, 5-fluorouracil had IC_{50} values 11.61, 9.12, 8.43, and 1.43 μM , respectively [198].

Above reported triazole compounds (Figure 9 (67–76)) showed the best cytotoxic activity against representative cell lines among their own series. Furthermore, compound **68** (having nitro substituted aromatic ring and imidazole ring joint by ethylene bridge with sulphur linkage) showed the lowest IC_{50} value, 0.38 μM , against MCF-7 cell lines as compared to standard drug, doxorubicin, having IC_{50} 0.65 μM .

3.8. β -Lactam Derivatives as Anticancer Agents

“ β -lactams” represent the most well-known class of antibiotics. Since the 1920s, various new penicillin compounds have been developed, along with related beta-lactam families, including cephalosporins, cephamycins, monobactams, and carbapenems. Every new class of beta-lactam has been created to either deal with particular resistance mechanisms that have emerged in the targeted bacterial population or to broaden the spectrum of activity to encompass more bacterial species. Bacterial enzymes, which hydrolyze the beta-lactam ring and leave the drug inert, represent the main cause of resistance to beta-lactams [199]. Banik et al. (2003) synthesized beta-lactam-based heterocyclic derivatives and evaluated their anti-neoplastic activity on nine representative cell lines. All the synthesized compounds showed good anticancer activity when tested on BRO, MCF-7, MDA-231, OVCAR, SKOV, PC-3, HL-60, K-562, and HT-29 cell lines. Among them, compound 77 showed potent activity at IC_{50} values 10.84, 9.81, 11.98, 4.17, 6.88, 16.32, 3.64, 4.33, and 5.66 μ M, respectively. Among the tested cell lines, compound 77 showed excellent activity against HL-60 cell lines with IC_{50} values at 3.64 μ M. Cisplatin was used as a reference drug with IC_{50} values 7.66, 10.05, 12.33, 3.99, 5.99, 4.66, 1.66, 2.33, and 16.99 μ M, respectively [200].

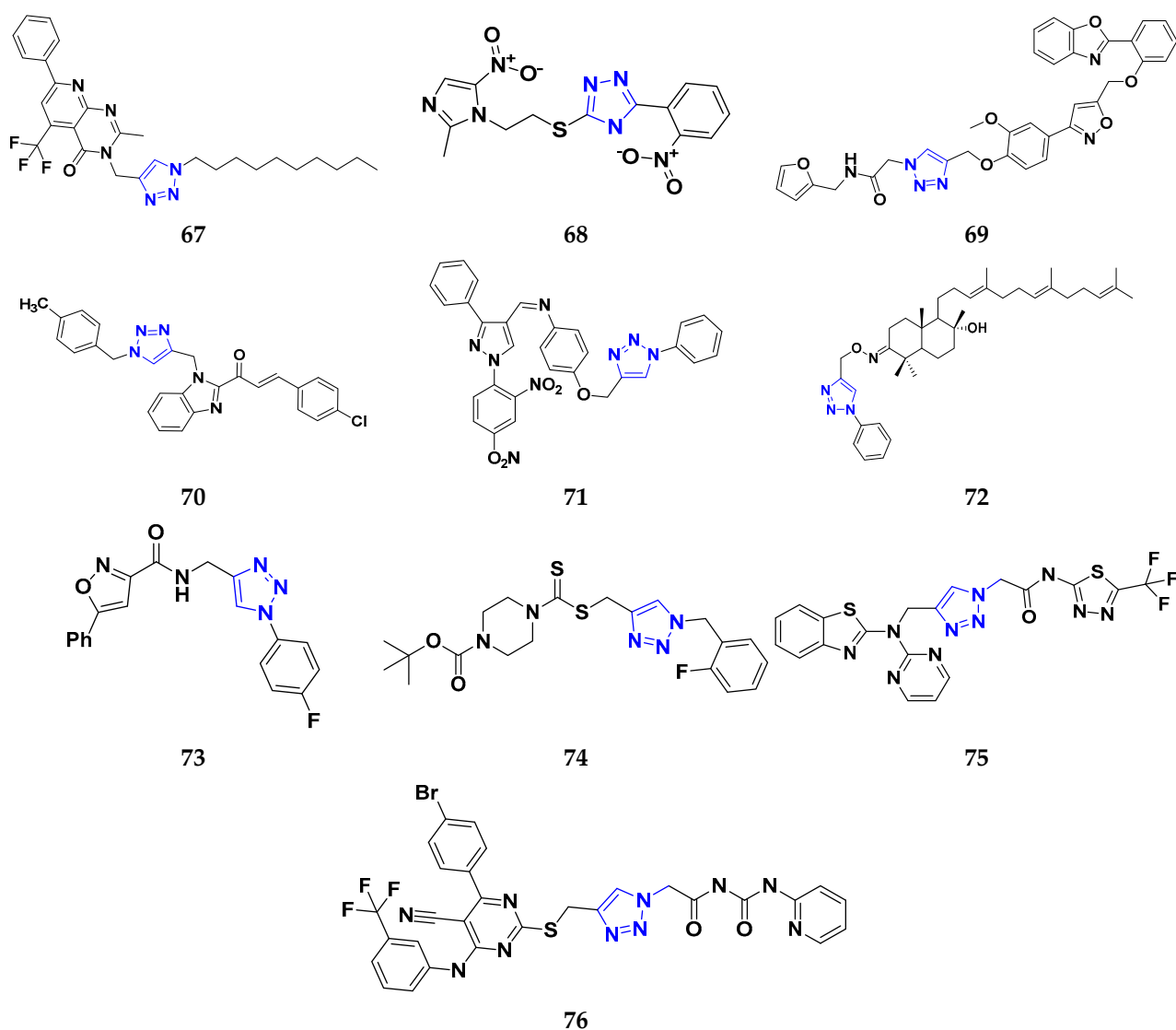


Figure 9. Triazole derivatives (67–76) as anticancer agents.

Borazjani et al. (2020) synthesized beta-lactams-based heterocyclic derivatives and evaluated their anticancer activity on three representative cell lines. All the synthesized

compounds showed potent anticancer activity against MCF-7, TC-1, and HepG2 cell lines. Among them, compound **78** showed good anticancer activity at IC_{50} values of 131.52, 85.34, and >1000 μM respectively. Among the tested cell lines, compound **78** showed potent activity against TC-1 cell lines with IC_{50} value 85.34 μM . Gemcitabine was used as a reference drug with IC_{50} values 191.57, 153.25, and 215.01 μM , respectively [201]. Nagaraju Payili et al. (2018) synthesized and evaluated anticancer activity of beta-lactam based derivatives. Utilizing the MTT assay and in vitro antiproliferative activity, newly synthesized molecules were evaluated. Out of the 14 quinone bearing carbamyl-lactam-lactam hybrids synthesized, compound **79** exhibited excellent anticancer activity against the B16F10 cell line. However, the experiments also revealed that the carbamyl derivative with a methyl group at the piperidine rings on the 4-position displayed better activity with IC_{50} value 24.40 μM [202]. Ranjbari S. et al. (2020) synthesized beta-lactam-based heterocyclic derivatives and evaluated their anticancer activity on four representative cell lines. All the synthesized compounds showed potent anticancer activity against SW1116, HepG2, MCF-7, and HEK-293 cell lines. Among them, compound **79** showed potent anticancer activity at IC_{50} values 1.53, >100 , >100 , and >100 μM respectively. Among the tested cell lines, compound **80** showed most potent activity against SW1116 cell lines with IC_{50} value 1.53 μM . Doxorubicin is used as a reference drug with IC_{50} 6.9, 7.3, 5.5, and 6.1 μM respectively [203].

Fabian E. Olazaran et al. synthesized beta-lactams-based heterocyclic derivatives and evaluated their anticancer activity on three representative cell lines. All the synthesized compounds showed potent anticancer activity when tested on SiHa, B16F10, and CHANG cell lines. Among the synthesized compounds, compound **81** showed potent activity at IC_{50} value 0.07, 1.21, and > 10.0 μM respectively. Among the tested cell lines, compound **81** showed strong activity against SiHa cell lines with IC_{50} value 0.07 μM . Vincristine was used as reference drug with IC_{50} values 0.01, 0.01, and 0.01 μM , respectively. Furthermore, compound **81** showed induction of apoptosis [204]. Rashidi et al. performed MTT assay for newly synthesized compounds in which cell viability was determined at fixed concentrations of 2 and 4 $\mu\text{g}/\text{mL}$, all compounds showed moderate to high cytotoxic activity in MCF-7 cell lines. Among them, compound **82** showed good % cell viability of 21.19 and 27.35% with control 2,4-D (80.40 and 53.10% respectively) [205]. Fu et al. (2017) synthesized beta-lactams-based heterocyclic derivatives and evaluated their anticancer activity on three representative cell lines. All the synthesized compounds showed potent antineoplastic activity when tested on MGC-803, MCF-7, and A549 cell lines. Among them, compound **83** showed most potent activity at IC_{50} values 0.106, 0.421, and 0.507 μM respectively. Among the tested cell lines, compound **83** showed potent activity against MGC-803 cell lines with IC_{50} value 0.106 μM . Fosbretabulin (CA-4P) was used as a control with IC_{50} values 0.015, 0.023, and 0.033 μM respectively [206]. Gupta et al. (2015) designed and synthesized beta-lactam based heterocyclic derivatives, evaluated their anticancer activity on three representative MCF-7, MDA-MB- 231, and NCI60 cell lines. Among the synthesized compounds, compound **84** showed potent anticancer activity against MCF-7 cell lines with IC_{50} value 7 μM . The control used was Combretastatin A-4 with IC_{50} value 0.015 μM respectively [207].

Banik et al. synthesized beta-lactam-based heterocyclic derivatives and evaluated their anticancer activity on seven representative cell lines. All the synthesized compounds showed potent anticancer activity when tested on BRO, MDA-231, SKOV-3, PC-3, HL-60, K-562, and HT-29 cell lines. Among them, compound **85** showed good anticancer activity at IC_{50} value 6.1, 0.8, 6.8, 1.4, 0.7, 1.1, and 0.7 μM respectively. Among the tested cell lines, compound **85** showed excellent activity against HT-29 cell lines with IC_{50} value 0.7 μM . Cisplatin was used as a control with IC_{50} values 7.66, 12.33, 5.99, 4.66, 1.66, 2.33, and 16.99 μM , respectively [208].

Miriam Carr et al. (2010) designed and synthesized beta-lactams-based heterocyclic derivatives and evaluated their anti-proliferative activity on two representative cell lines. All the synthesized compounds showed good anticancer activity when tested on MCF-7

and MDA-MB-231 cell lines. Among them, compound **86** showed potent activity at IC_{50} values 0.017 and 0.054 μM , respectively. Among the tested cell lines, compound **86** showed the most potent activity against MCF-7 cell lines with IC_{50} value 0.017 μM . 2(CA-4) was used as a control with IC_{50} values 0.0031 and 0.043 μM , respectively. Additionally, the most potent compound **86** exhibited anti-proliferative action at nanomolar doses. Like CA-4, compound **105** inhibited tubulin polymerization, leading to a G2/M phase cell cycle arrest in human MCF-7 breast cancer cells [209]. In summary, the above reported beta-lactam derivatives (Figure 10 (77–86)) were acting as anticancer agents. The most potent compound among them was compound **86** with 3- hydroxy-4-methoxyphenyl-1-3,4,5-trimethoxyphenyl terminal moiety, having the lowest IC_{50} value of 0.017 μM against MCF-7 (breast cancer) cell line.

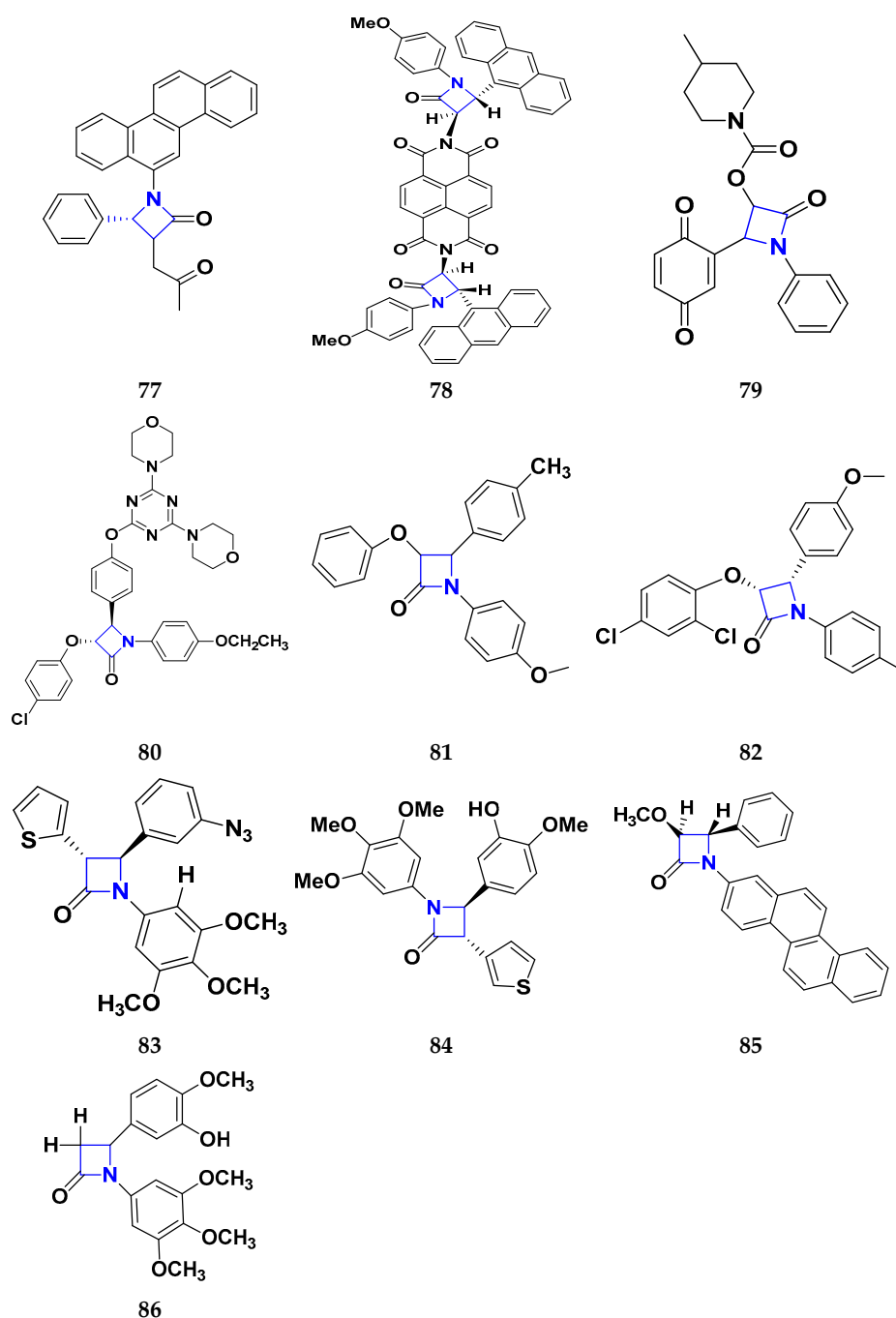


Figure 10. β -lactam derivatives (77–86) as anticancer agents.

3.9. Indole Derivatives as Anticancer Agents

Benzene and pyrrole rings are fused to form the heterocyclic molecule known as indole. A.V. Baeyer and C.A. Knop identified the compound, indole, as the fundamental component of the naturally occurring dye indigo. Indole was detected in coal tar by R. Weissgerber in 1910. It has an m.p. between 52 and 54 °C and a b.p. of 254.7 °C. It is an opaque solid. It is readily soluble in most solvents, including benzene, diethyl ether, and ethanol. Additionally, it is volatile in steam, barely soluble in cold water, and miscible in hot water. Since indole comes from a natural source and is a component of orange blossom oil and jasmine oil, it is found in many perfumes, has been used for a long time to mask unpleasant odors, and has crucial role in the synthesis of the amino acid, tryptophan [210].

Singla et al. (2018) designed and synthesized indole-based derivatives and evaluated their anticancer activity on using T47D cell line. Among them, compound **87** showed good anticancer activity against T47D cell lines with IC₅₀ value 3.8 µM, compared to the control drug, bazedoxifene, with IC₅₀ value 16.43 µM. These experiments showed that methyl and dimethyl-substituted compounds were more active than aryl-substituted ones. It was confirmed that compound **87** inhibited the expression of the ER-α mRNA in the T47D cells [211]. Cihan-Ustundag et al. (2015) synthesized indole-based derivatives and evaluated their anticancer activity on nine representative cell lines. All the synthesized compounds showed potent anticancer activity when tested on CCRF-CEM, A549/ATCC, COLO 205, SF-268, LOX IMVI, IGROV1, 786-0, PC-3, and MCF7 cell lines. Among them, compound **88** showed the most potent activity at GI₅₀ values of 0.033, 0.034, 0.018, 1.32, 0.028, 0.032, 0.031, 0.034, and 0.029 µM, respectively. Among the tested cell lines, compound **88** showed potent activity against COLO 205 (Colon cancer) cell lines with GI₅₀ value 0.018 µM. 5-fluorouracil used was a control and had GI₅₀ values 10.0, 0.20, 0.16, 1.58, 0.25, 1.26, 0.79, 2.51, and 0.079 µM respectively [212]. He et al. (2019) synthesized indole-based derivatives and evaluated their anticancer activity on five representative cell lines. All the synthesized compounds showed potent anticancer activity against PC3, MGC803, EC109, WPMY-1, and GES-1 cell lines. Among them, compound **89** showed good activity at IC₅₀ value 0.14, 2.94, 3.99, 9.85, and 9.23 µM respectively. Among the tested cell lines, compound **89** showed excellent activities against PC3 cell lines with IC₅₀ value 0.14 µM. Cisplatin was used as a control and had IC₅₀ values 5.44, 1.82, 4.21, 17.25, and 19.02 µM respectively. Furthermore, apoptosis was successfully induced, and PC3 cell proliferation and colonization were effectively inhibited by compound **89**. It did not affect the cell cycle, but it may drastically reduce invasion and migration by inhibiting the EMT process [213]. Prakash et al. (2017) designed and synthesized indole-based derivatives for their potential anticancer activity on the HeLa cell line using MTT assay. The compound **90** showed potent anticancer activity on tested cell lines. Moreover, compound **90** containing an amino group showed potent activity against (HeLa) cervical cancer cell lines with IC₅₀ value 13.41 µM, whereas control cisplatin had an IC₅₀ value 13.20 µM. The anticancer effectiveness was increased by the amino group in pyrimidine [214].

Imran Ali et al. (2018) designed and synthesized indole based heterocyclic derivatives and evaluated their anticancer activity on HepG2/C3A line. Among them, compound **91** showed anticancer activity at the micellar concentration of 670 µL mL⁻¹. By using Lipinski's "rule of five," drug-likeness properties were predicted. Through interactions and electrostatic attraction, the compound **90** was bound to DNA with a K_b value 1.0 × 10⁵ M⁻¹. Compound **91** had 1.44% DLC (drug loading content) and 14.4% DLE (drug-loading efficiency) [215].

Chen et al. (2018) designed and synthesized indole-based derivatives and evaluated their anticancer activity on five representative cell lines. All the synthesized compounds showed potent anticancer activity when tested on MCF-7, A549, HepG2, HeLa, and 293T cell lines. Among them, compound **92** showed most potent activity at GI₅₀ values 0.09, 0.59, 0.029, 0.034, and >300 µM respectively. Among the tested cell lines, compound **92** showed excellent anticancer activity against MCF-7 cell lines with IC₅₀ value 0.09 µM. CA-4 was used as a reference with GI₅₀ values 0.14, 0.31, 0.17, 0.092, and >300 µM, respectively [216].

Lafayette et al. (2017) synthesized indole-based derivatives and evaluated their anticancer activity on four representative cell lines. All the synthesized compounds showed potent anticancer activity on HL60, K562, T47D, and MCF7 cell lines. Among them, compound **93** showed good anticancer activity at IC₅₀ values 12.78, > 50, 1.93, and > 50 µM respectively. Among the tested cell lines, compound **93** showed most potent activity against T47D cell lines with IC₅₀ value 1.93 µM. Doxorubicin was used as a control and had IC₅₀ values 0.01, 6.25, 4.61, and 2.71 µM respectively [217]. Yali Song et al. (2020) designed and synthesized indole-based derivatives and evaluated their anticancer activity on five representative cell lines. All the synthesized compounds showed potent antineoplastic activity on MCF-7, HeLa, MGC-803, Bel-7404, and L929 cell lines. Among them, compound **94** showed potent activity at IC₅₀ values 25.60, 24.96, 20.54, 21.02, and 105.1 µM respectively. Among the tested cell lines, compound **94** showed most potent activity against Bel-7404 cell lines with the IC₅₀ value 21.02 µM. Etoposide was used as a standard with IC₅₀ values 1.45, 5.35, 11.18, 7.76, and 80.36 µM, respectively. Furthermore, Compound **113** responded by arresting their cell cycle in the G2/M phase [218]. Zohreh Bakherad et al. (2019) design and synthesized indole-based derivatives and evaluated their anticancer activity on four representative cell lines. All the synthesized compounds showed potent anticancer activity when tested on A-549, Hep-G2, T-47D, and MCF-7 cell lines. Among them, compound **95** showed very good activity at IC₅₀ values 25.67, 35, 79, >100, and >100 µM respectively. Among the tested cell lines, compound **95** showed excellent activity against A-549 cell lines with the IC₅₀ value 25.67 µM. Etoposide was used as a standard with IC₅₀ values 1.76, 5.93, 7.1, and 4.96 µM, respectively [219].

Eldehna et al. (2020) designed and synthesized indole based derivatives and evaluated their antiproliferative activity on two representative cell lines. All the synthesized compounds showed very good anticancer activity against MCF-7, and MDA-MB-231 cell lines. Among them, compound **96** showed the most potent activity at IC₅₀ values 0.44 and 1.32 µM respectively. Among the tested cell lines, compound **96** showed excellent anticancer activity against MCF-7 cell lines with the IC₅₀ value 0.44 µM. Staurosporine was used as a reference control and had IC₅₀ values 6.81 and 10.29 µM, respectively [220]. Reddymasu Sreenivasulu et al. (2020) synthesized indole-based derivatives and evaluated their anticancer activity on four representative cell lines. All the synthesized compounds showed potent anticancer activity against A549, MDA-MB231, MCF-7, and HeLa cell lines. Among them, compound **97** showed good activity at IC₅₀ values 3.3, 10.23, 2.6, and 6.34 µM, respectively. Among the tested cell lines, compound **97** showed potent activity against MCF-7 cell lines with the IC₅₀ value 2.6 µM. Doxorubicin was used as a control and had IC₅₀ values 0.36, 0.47, 0.98, and 0.89 µM, respectively [221].

Analyzing the above reported indole-based derivatives (Figure 11 (87–97)) discussed herewith, all compounds act as anticancer agents. The most potent compound among them was the compound **88**, which was modified to change the indole substituents, the indole-2-carboxamide/carbohydrazide moiety, and substitute the aromatic ring for improved anticancer efficacy against colon cancer cell line (COLO 205) at the lowest GI₅₀ value, 0.018 µM.

3.10. Pyrazole Derivatives as Anticancer Agents

The chemical formula for pyrazole is C₃H₄N₂ and it has a five-membered ring structure with three C and two nitrogen atoms nearby. It's conjugate acid's pKa at 25 °C is 2.49, making it a weak base with a pKb of 11.5 (pKa). Ludwig Knorr introduced the word pyrazole in 1883. They are categorized as alkaloids because of their chemical nature and distinct pharmacological effects. The first naturally occurring pyrazole was 1-pyrazolyl-alanine, discovered in 1959 from watermelon seeds. Pyrazoles are reported to have a variety of biological activities, including neuroprotective, anti-fungal, antitubercular, anti-inflammatory, anti-convulsant, anticancer, anti-viral, ACE inhibitory, antiviral, cholecystokinin-1 receptor antagonist, and estrogen receptor (ER) agonistic activity [222].

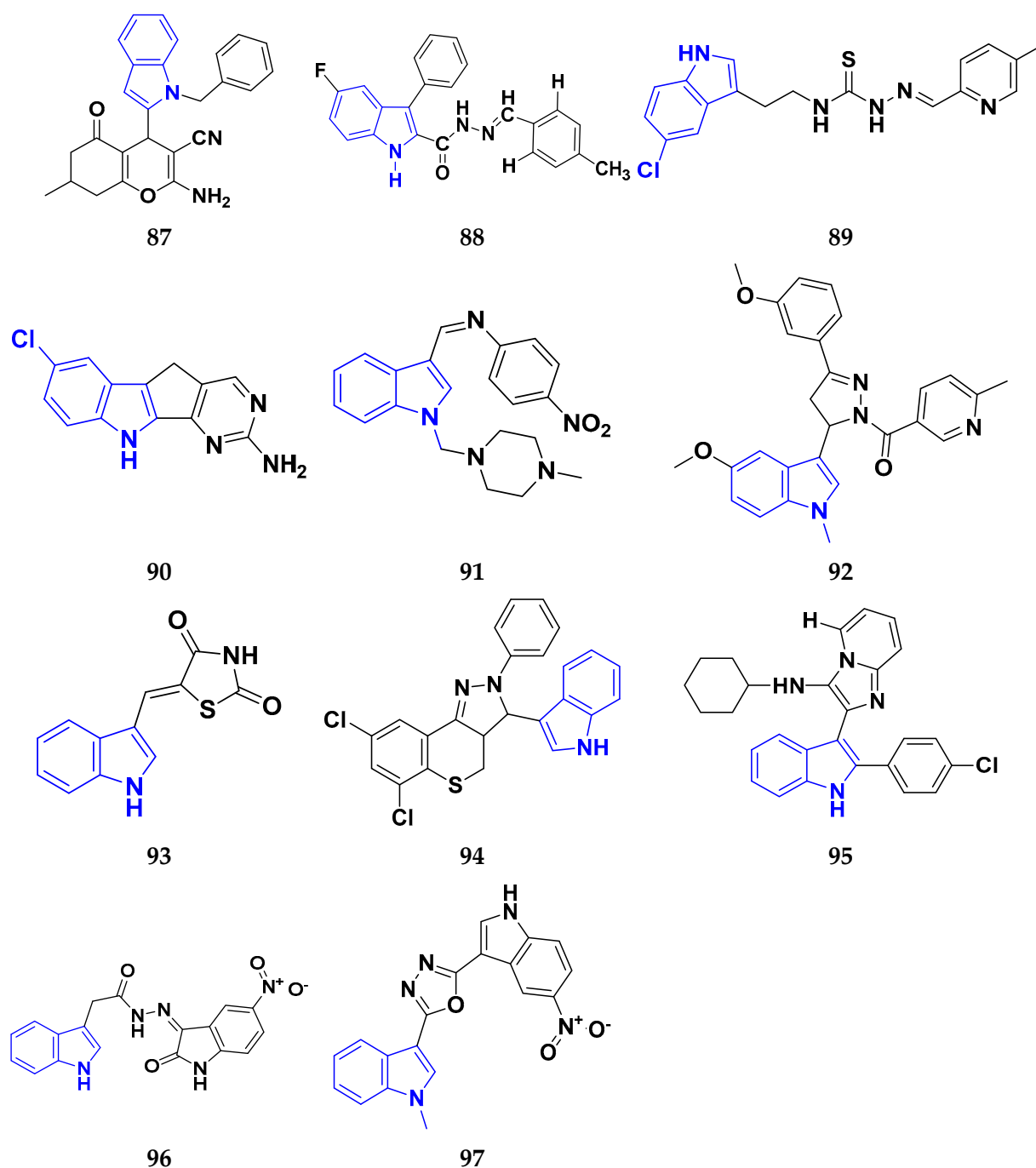


Figure 11. Indole derivatives (87–97) as anticancer agents.

Abdelgawad et al. (2018) designed and synthesized pyrazole-based heterocyclic derivatives and evaluated their antineoplastic activity on two representative cell lines. All the synthesized compounds showed very good anticancer activity against HePG2, and MCF-7 cell lines. Among them, compound 98 showed potent anticancer activity with IC_{50} values 18.23 and 5.23 μ M respectively. Among the tested cell lines, compound 98 showed excellent activity against MCF-7 cell lines with IC_{50} value 5.23 μ M. DOX (doxorubicin) was used as standard and had IC_{50} values 4.50, and 4.70 μ M respectively [223]. Nassar et al. (2017) designed and synthesized pyrazole-based heterocyclic derivatives and evaluated their anti-proliferative activity on three representative cell lines. All the synthesized compounds showed potent anticancer activity against HEPG-2, HCT-116, and MCF-7 cell lines. Among them, compound 99 showed very good anticancer activity with

IC₅₀ values 0.39, 12.96, and 6.97 μM respectively. Among the tested cell lines, compound **99** showed most potent activity against HEPG-2 cell lines with the IC₅₀ value 0.39 μM. DOX (Doxorubicin) was used as standard with IC₅₀ values 4.00, 3.73, and 2.97 μM, respectively [224]. El-Sayed et al. (2019) designed and synthesized pyrazole-based heterocyclic derivatives and evaluated their antineoplastic activity on two representative cell lines. All the synthesized compounds showed good anticancer activity against HepG2, and HeLa cell lines. Among them, compound **100** showed very good activity with IC₅₀ values 5.16, and 4.26 μM respectively. Among the tested cell lines, compound **100** showed most potent activity against HeLa cell lines with IC₅₀ value 4.26 μM. DOX (doxorubicin) was used as standard with IC₅₀ values 4.50 and 5.57 μM, respectively [225]. Omrana et al. (2019) designed and synthesized pyrazole-based heterocyclic derivatives and evaluated their anti-proliferative activity on two representative cell lines. All the synthesized compounds showed potent anticancer activity against HepG2 and VERO-B cell lines. Among them, compound **101** showed good anticancer activity with IC₅₀ values 2.0 and 9.0 μM, respectively. Among the tested cell lines, compound **101** showed most potent activity against HepG2 cell lines with the IC₅₀ value 2.0 μM. DOX (doxorubicin) was used as reference standard with IC₅₀ values 5.5 and 5 μM, respectively [226].

Zhu et al. (2013) designed and synthesized pyrazole-based heterocyclic derivatives and evaluated their anticancer activity on four representative cell lines. All the synthesized compounds showed good anticancer activity against SGC 7901, A549, Raji, and HeLa cell lines. Among them, compound **102** showed most potent activity with IC₅₀ values 2.71, 3.18, 1.09, and 13.52 μM respectively. Among the tested cell lines, compound **101** showed excellent activity against Raji cell lines with the IC₅₀ value 1.09 μM. Cisplatin was used as control with IC₅₀ values 7.56, 17.78, 17.32, and 14.31 μM, respectively [227].

Alam et al. (2016) designed and synthesized pyrazole-based heterocyclic derivatives and evaluated their antineoplastic activity on four representative cell lines. All the synthesized compounds showed very good anticancer activity against HeLa, NCI-H460, PC-3, and NIH-3T3 cell lines. Among them, compound **103** showed good activity with IC₅₀ values 7.98, 8.41, 9.53, and 87.30 μM respectively. Among the tested cell lines, compound **103** showed the most potent activity against HeLa (human cervix) cell lines with the IC₅₀ value 7.98 μM. Etoposide was used as standard control with IC₅₀ values 11.25, 16.63, 23.80, and 90.53 μM respectively [228].

Harras et al. (2018) designed and synthesized pyrazole-based heterocyclic derivatives and evaluated their anti-proliferative activity on three representative cell lines. All the synthesized compounds showed good anti-proliferative activity against HCT116, UO-31, and HepG2 cell lines. Among them, compound **104** showed most potent activity with IC₅₀ values 0.035, 2.24, and 0.028 μM respectively. Among the tested cell lines, compound **104** showed excellent activity against HepG2 cell lines with the IC₅₀ value 0.028 μM. Sorafenib was used as reference standard with IC₅₀ values 0.66, 7.15, and 0.37 μM, respectively. Additionally, biological analysis of compound **104** found that it induced CDK1 expression in HepG2 cells and during the G2/M phase cell cycle arrest [229]. Liu et al. (2019) designed and synthesized pyrazole-based heterocyclic derivatives and evaluated their anti-proliferative activity on four representative cell lines. All the synthesized compounds showed good anticancer activity against MDA-MB-231, MCF-7, HepG-2, and SMMC-7721 cell lines. Among them, compound **105** showed most potent activity with IC₅₀ values 2.41, 2.23, 3.75, and 2.31 μM respectively. Among the tested cell lines, compound **105** showed most potent activity against MCF-7 cell lines with the IC₅₀ value 2.23 μM. Doxorubicin was used as standard with IC₅₀ values 2.24, 0.34, 2.96, and 0.79 μM, respectively [230]. Afif et al. (2019) designed and synthesized pyrazole-based heterocyclic derivatives and evaluated their anticancer activity on five representative cell lines. All the synthesized compounds showed good anti-proliferative activity against A549, MCF-7, HepG-2, Caco-2, and PC3 cell lines. Among them, compound **106** showed potent activity with IC₅₀ values 18.85, 23.43, 23.08, 23.08, and 18.50 μM, respectively. Among the tested cell lines, compound **106** showed the most potent activity against HepG-2 cell lines with the IC₅₀ value 23.08 μM.

5-FU was used as standard with IC_{50} values 83.03, 93.79, 96.89, 112.24, and 82.26 μM , respectively [231].

Bakhotmah et al. (2020) designed and synthesized pyrazole-based heterocyclic derivatives and evaluated their anticancer activity on three representative cell lines. All the synthesized compounds showed potent anticancer activity against HCT-116, Hep-G2, and MCF-7 cell lines. Among them, compound **107** showed very good activity with IC_{50} values 4.13, 5.29, and 6.79 μM respectively. Among the tested cell lines, compound **107** showed the most potent activity against HCT-116 cell lines with the IC_{50} value 4.13 μM . Doxorubicin was used as control drug with IC_{50} values 0.493, 0.467, and 0.469 μM , respectively [232].

Analyzing the above reported pyrazole-based heterocyclic derivatives (Figure 12 (98–107)) discussed herewith, all compounds act as anticancer agents. The most potent compound among them was compound **104** with thioxodihydropyrimidine-4,6(1H,5H)-dione terminal moiety and two substituted aromatic rings, having the lowest IC_{50} value 0.028 μM against HepG2 cell lines. Authors found that these substances downregulated CDK1 expression in HepG2 cells and cell cycle arrest during the G2/M phase.

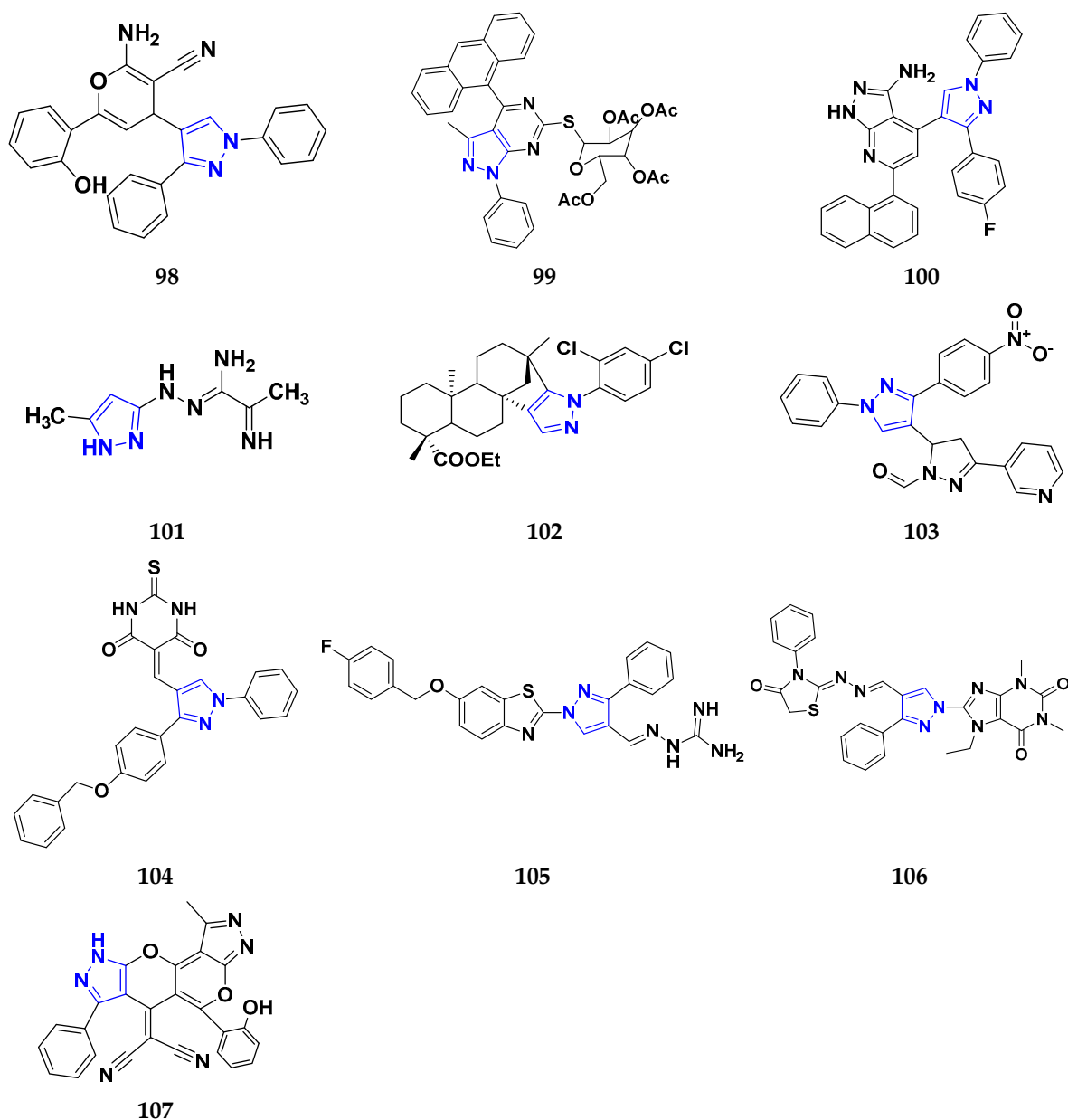


Figure 12. Pyrazole derivatives (98–107) as anticancer agents.

3.11. Quinazoline Derivatives as Anticancer Agents

The parent compound of quinazoline is naphthalene, a manmade organic heterobicyclic compound in which the carbon atoms at positions 1 and 3 have been substituted with nitrogen atoms. It is an azaarene and has an ortho-fused heteroarene. Quinazoline and quinazolinone scaffolds constitute a sizeable class of physiologically active nitrogen heterocyclic compounds. Numerous anticancer drugs are marketed based on these moieties, including gefitinib, erlotinib, lapatinib, afatinib, and vandetanib [233].

Ghorab et al. (2016) designed and synthesized quinazoline-based heterocyclic derivatives and evaluated their antiproliferative activity on four representative cell lines. All the synthesized compounds showed very good anticancer activity when tested on A549, HeLa, LoVo, and MDA-MB-231 cell lines. Among them, compound **108** showed potent activity with IC_{50} values 77.8, 91.5, 96.5, and 77.9 μ M, respectively. Among the tested cell lines, compound **108** showed the most potent activity against A549 cell lines with the IC_{50} value 77.8 μ M. Doxorubicin (DOX) was used as control with IC_{50} values 283.5, 120.7, 374.4, and 26.5 μ M respectively [234].

Chang et al. (2017) synthesized quinazoline-based heterocyclic derivatives and evaluated their anticancer activity on five representative cell lines. All the synthesized compounds showed potent anticancer activity against HepG2, A549, DU145, MCF-7, and SH-SY5Y cell lines. Among them, compound **109** showed potent anticancer activity at IC_{50} values 4.61, 9.50, 6.79, 9.80, and 7.77 μ M, respectively. Among the tested cell lines, compound **109** showed the most potent activity against HepG2 cell lines with the IC_{50} value 4.61 μ M. Gefitinib and QWL-138 were used as controls with IC_{50} values 29.79, 12.08, 8.63, 12.05, 18.21, and 3.06, 6.71, 20.04, 10.54, 8.60 μ M, respectively. Compound **108** induced cell death primarily through apoptosis via a mitochondrial-dependent route and cell cycle arrest in the S phase [235].

Ahmed et al. (2022) synthesized quinazoline-based heterocyclic derivatives and evaluated their anti-proliferative activity on two representative cell lines. All the synthesized compounds showed potent anticancer activity on MCF-7 and HCT116 cell lines. Among the tested compounds, compound **110** showed very good anticancer activity at IC_{50} values 4.43 and 8.23 μ M with control DOX with IC_{50} values 8.09 μ M and 11.26 μ M, respectively. Further, they acted on the G2/M phase of cell cycle [236]. Heba S.A. ElZahabi et al. (2021) synthesized quinazoline-based heterocyclic derivatives and evaluated their anticancer activity on two representative cell lines. All the synthesized compounds showed potent anticancer activity against MCF-7 and A-549 cell lines. Among them, compound **111** showed the most potent activity at IC_{50} values 0.06 and ≥ 100 μ M respectively. Among the tested cell lines, compound **111** showed excellent activity against MCF-7 cell lines with IC_{50} value 0.06 μ M. Doxorubicin and 5-Fluorouracil were used as references with IC_{50} values 0.06, 0.13 and 2.13, 2.36 μ M respectively. Compound **111** boosted apoptotic cell death and induced the arrest of the G1 and pre-G1 phases of the cell cycle [237].

Abdelsalam et al. (2019) synthesized quinazoline-based heterocyclic derivatives and evaluated their anticancer activity on five representative cell lines. All the synthesized compounds showed good antineoplastic activity against HepG2, MCF-7, HCT116, and BHK-21 cell lines. Among them, compound **112** showed the most potent activity at IC_{50} values 24.76, 7.70, 23.66, and >200 μ M respectively. Among the tested cell lines, compound **112** showed excellent activity against MCF-7 cell lines with the IC_{50} value 7.70 μ M. Dox and Erlotinib were used as standards with IC_{50} values 1.95, 1.10, 0.63, and 3.04 and 10.19, 5.06, 13.22, and 19.13 μ M respectively [238].

Hoan et al. (2019) synthesized quinazoline-based heterocyclic derivatives and evaluated their anticancer activity on four representative cell lines. All the synthesized compounds showed good anti-proliferative activity against KB, Hep-G2, Lu, and MCF-7 cell lines. Among them, compound **113** showed potent activity at IC_{50} values > 337 , 2.1, 11.6, and 2.2 μ M respectively. Among the tested cell lines, compound **113** showed the most potent anticancer activity against Hep-G2 cell lines with IC_{50} value 2.1 μ M. Ellipticine was used as standard with IC_{50} values 1.14, 1.14, 1.71, and 1.70 μ M, respectively [239].

Wang et al. (2021) designed and synthesized quinazoline-based heterocyclic derivatives and evaluated their anticancer activity on four representative cell lines. All the synthesized compounds showed potent anticancer activity against H1975, PC-3, MDA-MB231, and MGC-803 cell lines. Among them, compound **114** showed good anticancer activity at IC₅₀ values 2.03, 5.37, 8.16, and 6.25 μM respectively. Among the tested cell lines, compound **114** showed most potent activity against H1975 cell lines with the IC₅₀ value 2.03 μM. Gefitinib was used as standard with IC₅₀ values 9.20, 8.92, 7.12, and 8.19 μM, respectively. Furthermore, compound **114** showed G1 phase mediated cell apoptosis in H1975 cell cycle, which promoted the accumulation of ROS [240].

Zayed et al. (2018) synthesized quinazoline-based heterocyclic derivatives and evaluated their antineoplastic activity on two representative cell lines. All the synthesized compounds showed good anti-proliferative activity against MCF-7 and MDA-MBA-231 cell lines. Among them, compound **115** showed the most potent activity at IC₅₀ value 12.44, and 0.43 μM respectively. Among the tested cell lines, compound **115** showed excellent anticancer activity against MDA-MBA-231 cell lines with the IC₅₀ value 0.43 μM. Erlotinib was used as standard with IC₅₀ 1.14, 2.55 μM respectively [241]. Abuelizz et al. (2017) synthesized quinazoline-based heterocyclic derivatives and evaluated their antineoplastic activity on two representative cell lines. All the synthesized compounds showed good anti-proliferative activity and were tested on HeLa and MDA-MBA-231 cell lines. Among them, compound **116** showed most potent activity at IC₅₀ values 1.85 and 2.33 μM, respectively. Among the tested cell lines, compound **116** showed excellent anticancer activity against HeLa cell lines with the IC₅₀ value 1.85 μM. Gefitinib was used as standard with IC₅₀ values 4.3 and 28.33 μM, respectively [242].

Poudapally et al. (2017) synthesized quinazoline-based heterocyclic derivatives and evaluated their anticancer activity on six representative cell lines. All the synthesized compounds showed good anti-proliferative activity against SKOV3, DU145, THP1, U937, COLO205, and FHC cell lines. Among them, compound **117** showed good activity at IC₅₀ values 9.23, 12.33, 8.17, 6.06, 19.04, and 73.0 μM respectively. Among the tested cell lines, compound **117** showed the most potent activity against U937 cell lines with the IC₅₀ value 6.06 μM. Etoposide was used as standard and had IC₅₀ values 3.84, 6.17, 4.42, 2.89, 5.12, and 49.31 μM respectively [243].

Ewes et al. (2020) synthesized quinazoline-based heterocyclic derivatives and evaluated their anticancer activity on five representative cell lines. All the synthesized compounds showed good antineoplastic activity against HePG2, MCF-7, PC3, HCT-116, and Hela cell lines. Among them, compound **118** showed good antineoplastic activity at IC₅₀ values of 10.30, 8.90, 10.54, 11.47, and 13.41 μM, respectively. Among the tested cell lines, compound **118** showed potent activity against MCF-7 cell lines with the IC₅₀ value 8.90 μM. Doxorubicin was used as standard with IC₅₀ values 4.50, 4.17, 8.87, 5.23, and 5.57 μM, respectively [244].

Analyzing the above reported quinazoline-based heterocyclic derivatives (Figure 13 (108–118)) discussed herewith, all compounds act as anticancer agents. The most potent compound among them was compound **111** with 3-amino-6,8-dibromo-2-methylquinazolin-4(3H)-one terminal moiety, having the lowest IC₅₀ value of 0.06 μM against MCF-7 cell lines.

3.12. Quinoxaline Derivatives as Anticancer Agents

The nitrogen-containing heterocyclic molecule quinoxalines, commonly known as benzopyrazines, has a ring complex composed of a pyrazine ring and a benzene ring [245]. The majority of quinoxaline derivatives are produced synthetically. In quinoxaline, two benzene rings combine, expanding the variety of resonance structures available to these systems. It possesses a zero-dipole moment [246]. Due to the wide range of pharmacological activities that quinoxalines exhibit, they have received a lot of interest. It is regarded as a crucial moiety for anticancer medications. Since the 1980s, when certain quinoxalinone derivatives were produced and investigated for their cytotoxic activity, the screening of quinoxaline as an anticancer scaffold has continued [247]. Ismail et al. (2010) synthesized a

set of quinoxaline 1,4-di-oxides which were tested for their anticancer activities against the U251 (brain tumors) and Hepg2 (liver carcinoma). Among the synthesized compounds, **119** and **120** showed maximum activity against Hepg2 cell lines with IC_{50} values of 0.77 and 0.50 $\mu\text{g}/\text{mL}$, respectively. Tirapazamine was used as standard and its IC_{50} value against HepG2 was 56.6 $\mu\text{g}/\text{mL}$. For carbamate and acid azide derivatives to be cytotoxic, the 7-methoxy (electron-donating group) was important. The activity was decreased when quinoxaline 1,4-dioxide was converted to quinoxaline 4-oxide [248].

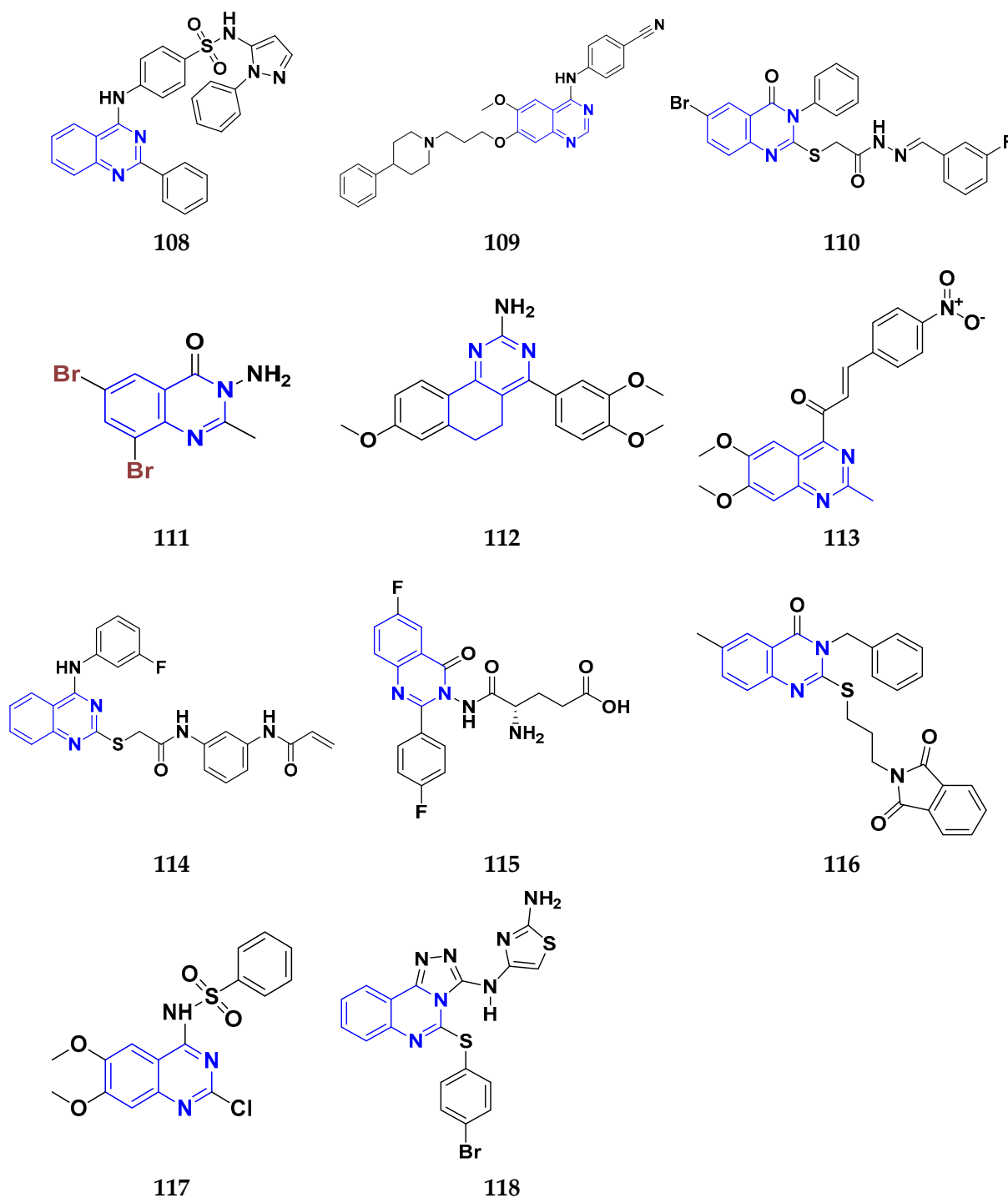


Figure 13. Quinazoline derivatives (108–118) as anticancer agents.

Abbas et al. (2015) synthesized novel quinoxaline derivatives and evaluated their cytotoxicity on NCI-H460, SF-268, and MCF-7 cell lines. Out of the synthesized derivatives, compounds (IC₅₀ value) **121** (0.06), **122** (0.01), **123** (0.02), and **124** (0.08 µg/mL) had maximum cytotoxic activity against MCF-7 cell lines. Doxorubicin was used as a standard drug with IC₅₀ value for NCI-H460 (0.09), SF-268(0.09), and MCF-7(0.04 µg/mL) cells. Compound **121** had enhanced activity because of the presence of the methoxy. The substitution of an *O*-phenyl linker or an *N*-phenyl linker in compounds **123** and **124** showed a strong binding affinity and potency [249].

Desplat et al. (2016) prepared novel ethyl pyrrolo quinoxaline-carboxylate derivatives and tested their anticancer activity on five leukemia cells, i.e., Jurkat, K562, U937, HL60, and U266. Compounds A6730 and LY-294002 were used as standard. The standard drug A6730 with IC₅₀ of 8 µM and two derivatives **125** (IC₅₀ value of 4 µM) and **126** (IC₅₀ value of 3 µM) showed excellent activity against U937 cell line. Substitution at the 4th position by a benzylpiperidinyl fluorobenzimidazole group and in the 1st position by a phenyl group produced an active analogue [250]. Newahie et al. (2019) designed and synthesized three series of quinazoline derivatives and evaluated their cytotoxicity against panel of cell lines, including HepG2, HCT116, and MCF-7 cells. From the second series, compound **127** had IC₅₀ values of 25.7, 7.8, and 60.3 µM. From third series, compound **128** had IC₅₀ values of 22, 2.5, and 9 µM. From the first series, compound **129** had IC₅₀ values of 10.0, 4.4, and 5.3 µM, respectively. Doxorubicin was used as standard with IC₅₀ value of 1.2, 0.62, and 0.9 µM for HepG2, HCT116, and MCF-7 cells respectively. They also tested some of the compounds for WI-38 cell lines and found that **129** was the most active with greater selectivity for WI-38 cell lines. Compound **129** had a phenyl ring attached to another ring which enhanced activity [251]. Ahmed et al. (2020) prepared new quinoxaline derivatives and tested their cytotoxicity on HepG2, HCT-116, and MCF-7 cells by MTT bioassay using erlotinib and doxorubicin as reference drugs. For given cell lines, compounds **130**, (IC₅₀ = 2.51, 4.22 and 2.27 µM), **131** (IC₅₀ = 1.32, 1.41 and 1.18 µM), and **132** (IC₅₀ = 1.72, 1.85 and 1.92 µM) had maximum cytotoxicity with control erlotinib with IC₅₀ values of 1.63, 1.57, and 1.49 µM and doxorubicin with IC₅₀ value of 1.41, 0.90, and 1.01 µM, respectively [252].

Alsaif et al. (2021) synthesized new triazolo quinoxaline derivatives and tested them for anticancer activity against HepG2 and MCF-7 cell lines. Standard drug sorafenib had IC₅₀ values against HepG2 (3.51µM) and MCF-7 (2.17µM). Some of the triazolo quinoxaline derivatives, i.e., **133**, **134**, **135**, and **136**, presented comparable activity with reference drug sorafenib against HepG2 cell lines with IC₅₀ values of 4.1, 8.4, 7.8, and 9.7 µM, respectively. The capability of the synthesized substances to inhibit VEGFR-2 was further evaluated. Compound **133** was the most potent VEGFR-2 inhibitor, with the IC₅₀ value of 3.4 nM, which is close to sorafenib (standard drug) with the IC₅₀ value of 3.2 nM [253]. Khaled El-Adl et al. (2021) prepared new quinoxaline-one derivatives and tested their anticancer activity against HCT-116, MCF-7, and HepG-2 cell lines. Doxorubicin and sorafenib were used as positive controls. Against synthesized compounds, HCT-116 was the most sensitive cell line. The highest level of cytotoxicity was displayed by compounds **137** and **139** toward the examined cell lines. Compound **138** was the most active derivative with IC₅₀ values against HepG-2 (5.30 µM), MCF-7 (2.20 µM), and HCT-116 (5.50 µM). In comparison to doxorubicin (IC₅₀ value of 8.28, 7.67 and 9.63 µM respectively) compounds **138** and **140** showed better anticancer effects against tested cells. In comparison to the hydrophobic and electron-donating groups of other derivatives, the distant benzyl moiety in compound **138** demonstrated better activity [254]. Hajri et al. (2016) synthesized quinoxaline-2-carboxylate and quinoxalin-one derivatives and evaluated their anticancer activity against U87-MG and A549 cell lines. The most cytotoxic arylethynyl derivatives, **141** and **142**, both had the IC₅₀ value of 3.3 µM. The antiproliferative effect of quinoxaline was due to the presence of the ethynyl group at third position in quinoxaline molecule. The compounds **141**, **142**, and **143**, with no modification on the aromatic group, addition of a methyl group in the 4th position, or a fluorine atom in the 3rd position, showed maximum activity against both U87-MG and A549 cell lines. Compound **143**, containing a fluorine atom in the 3rd position, exhibited a

good anticancer activity against the A549 and U87-MG cells [255]. Analyzing the above reported quinoxaline-based heterocyclic derivatives (Figure 14 (119–143)), all compounds act as anticancer agents. The most potent compound among them was compound **122** in which the quinoxaline ring was substituted at N-1 atom by acetohydrazide moiety and bromine, having the IC_{50} value of 0.01 $\mu\text{g}/\text{mL}$ against MCF-7 cell line.

3.13. Isatin Derivatives as Anticancer Agents

Isatin is an endogenous substance found in animals that has a number of pharmacological features, such as anticancer action [256]. In the present era of medicine, there are many challenges that affect human health, especially when it comes to tumors. As a result, new treatments that target tumor cells specifically will inevitably need to be introduced to the armory for treating these malignancies [257]. Aziz et al. (2017) prepared a few sets of isatin-based benzoazine heterocyclic rings, such as isatin- quinoxaline, quinazoline, and phthalazines hybrids. They used three human cancer cell lines, i.e., HT-29, ZR-75, and A-549, for testing the cytotoxicity of all the synthesized compounds. A majority of the synthesized molecules showed potent cytotoxic activity. Sunitinib was used as standard drug with an average IC_{50} value of 8.11 μM . Among synthesized compounds, **144** showed maximum anticancer activity with average IC_{50} value of 5.53 μM [258].

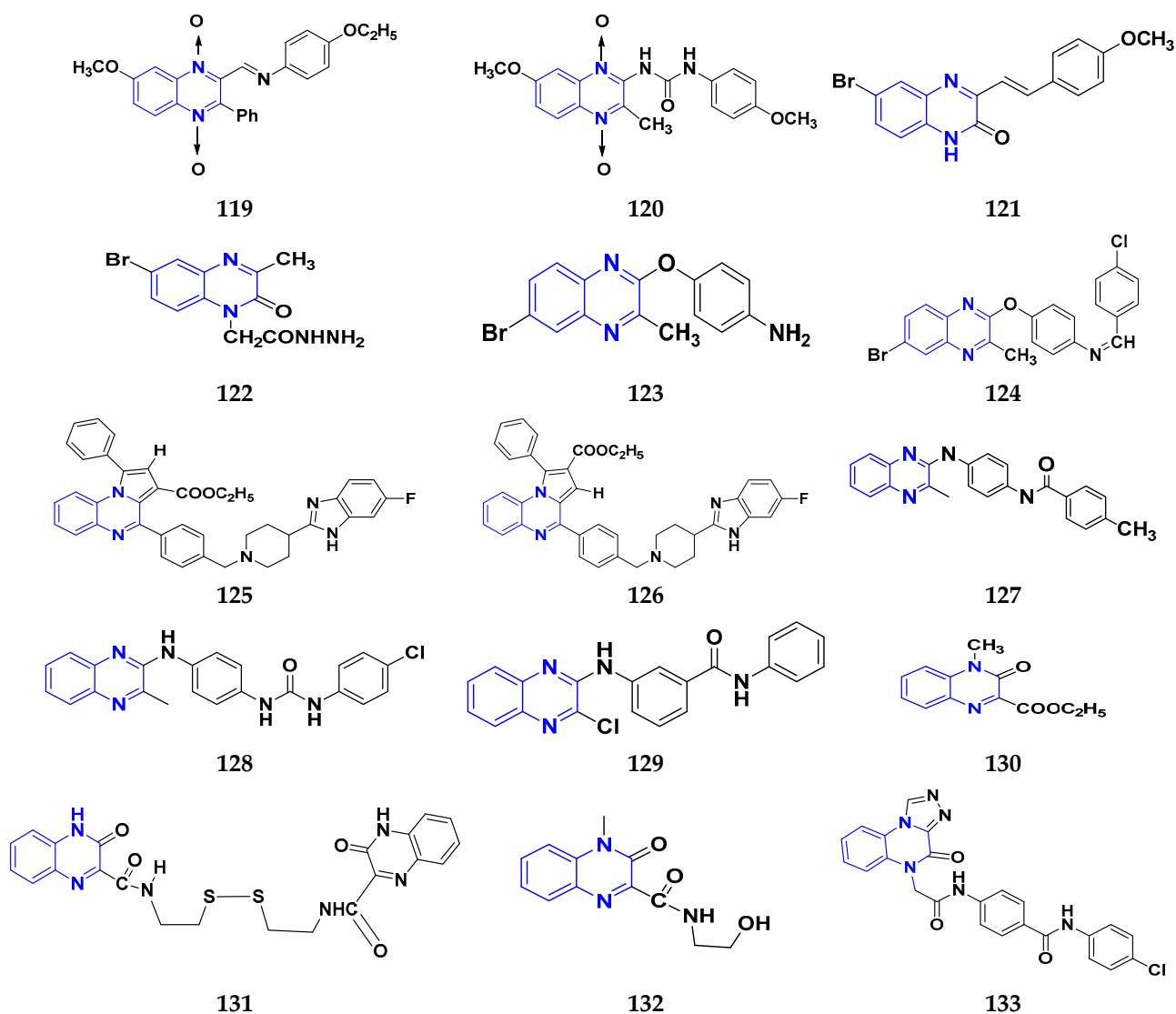


Figure 14. Cont.

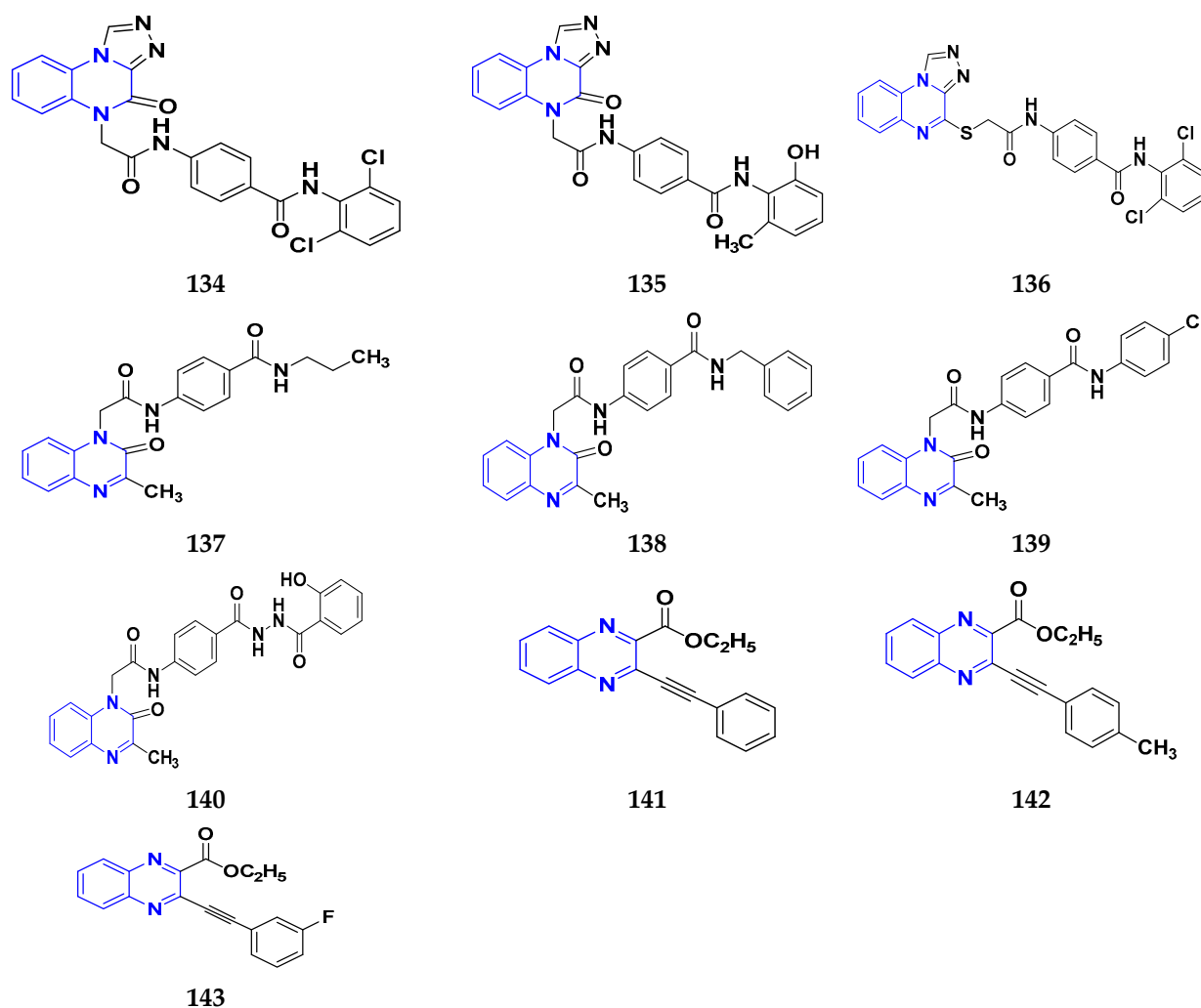


Figure 14. Quinoxaline derivatives (119–143) as anticancer agents.

Meleddu et al. (2018) produced isatin-dihydropyrazole derivatives and tested their ability to prevent the growth of tumor cells in different types of human cancer cell lines, namely IGR39 (melanoma), lung carcinoma (A549), glioblastoma (U87), breast adenocarcinoma (MCF-7), invasive ductal carcinoma (BT474), non-small cell lung carcinoma (H1299), BxPC-3 (pancreatic adenocarcinoma) ovarian cancer (SKOV-3), and fibroblast. Among the synthesized compounds, **145** showed maximum activity with EC_{50} values of 0.18, 0.14, 0.23, 0.31, and 0.10 μM against A549, IGR39, U87, MCF-7, and BxPC-3 cell lines. Sunitinib was used as the positive control and was having EC_{50} values of 0.90, 0.96, 2.5, 1.36, 1.54, and 0.30 μM for BT474, MCF-7, BxPC-3, SKOV-3, and H1299 fibroblast, respectively [259]. Eldehna et al. (2015) synthesized isatin-pyridine derivatives and evaluated their anti-proliferative effect on three human tumor cancer cell lines: lung cancer (A549), hepatocellular carcinoma (HepG2), and breast cancer (MCF-7). A majority of the synthesized compounds showed good antiproliferative activity. The synthesized compound **146** showed maximum activity with IC_{50} values of 10.8, 6.3, and 8.7 μM , respectively. Doxorubicin was used as a reference drug having IC_{50} values of 7.6, 6.1, and 6.9 μM for A549, MCF-7, and HepG2 [260]. Wabli et al. (2020) synthesized isatin-indole derivatives and evaluated their anticancer efficacy against HT-29 (colon), ZR-75 (human breast), and A-549 (lung) cell lines. A majority of the prepared compounds show potent cytotoxicity. The most active compound was **147** with IC_{50} values of 0.74, 0.76, and 2.02 μM against ZR-75, A-549, and HT-29 respectively. Sunitinib was used as standard drug with IC_{50} values of 10.14, 8.31, and 5.87 μM for HT-29, ZR-75, and A-549, respectively [261]. Panga et al. (2016) synthesized

isatin-benzoic acid derivatives and evaluated them *in vitro* for anticancer activity against HeLa and MCF-7 cell lines. The synthesized compounds showed good anticancer activity towards both the cells. Compound **148** showed the highest activity towards both cell lines having IC_{50} values of 9.28 and 14.89 μM and Vinblastine was used as positive control here with IC_{50} values of 4.02 and 7.14 μM , respectively [262]. Eldehna et al. (2021) synthesized isatin-thiazolo benzimidazole derivatives and evaluated their cytotoxic activity against MDA-MB-231 and MCF-7 breast cancer cell lines by using sulforhodamine B colorimetric (SRB) assay. The compound **149** shows good anticancer activity with IC_{50} values of 6.50 and 2.02 μM against MDA-MB-231 and MCF-7 cell lines, respectively. Compound **150** with IC_{50} values of 2.60 and 3.01 μM respectively shows better anticancer activity than standard drug staurosporine, having IC_{50} values of 4.29 and 3.81 μM , respectively [257].

All the above reported isatin-based heterocyclic derivatives (Figure 15 (144–150)) were observed to act as anticancer agents. The most potent compound among them was compound **145** with the EC_{50} value of 0.1 μM against the BxPC-3 cell line, which contained diazole with 2-naphthyl group and 4- CH_3 substituent ring for optimal antiproliferative activity.

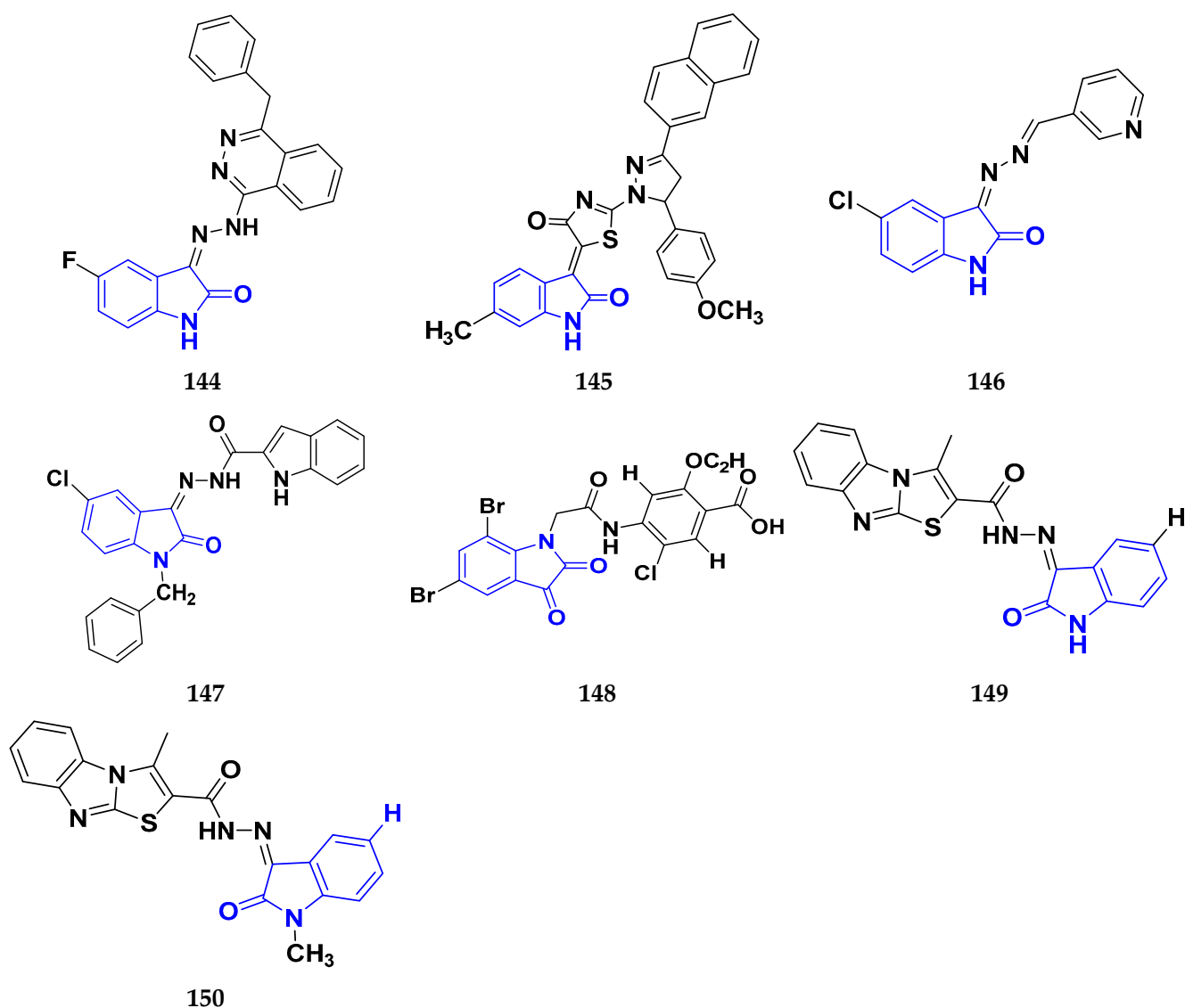


Figure 15. Isatin derivatives (144–150) as anticancer agents.

3.14. Pyrrolo-Benzodiazepines Derivatives as Anticancer Agents

Many actinomycetes species naturally produce or contain pyrrolo-benzodiazepines (PBD) derivatives. PBD binds covalently to DNA, inhibiting transcription factors and DNA replication, thus slowing cellular growth [263]. Bose et al. (2012) synthesized pyrrolo-benzodiazepine derivatives and evaluated the cytotoxic activities of the synthesized compounds against HL-60 (human promyelocytic leukemia), THP-1 (human acute monocytic leukemia), U-937 (human histiocytic lymphoma), A-549 (lung carcinoma), and Jurkat (Human T-cell leukemia) cell lines. The most active compound was **151** with IC₅₀ values of 0.49, 4.13, 3.44, and 6.58 μM against THP-1, HL-60, U-937, and Jurkat cell lines. THP-1, U-937, HL-60, and Jurkat leukemia cell lines were all cultivated in RPMI-1640, while A-549 was grown in Dulbecco's Modified Eagle Medium (DMEM). Etoposide used as reference drug had IC₅₀ values 2.16, 17.94, 1.83, and 5.35 μM against THP-1, U-937, HL-60, and Jurkat cells [264].

Kamal et al. (2012) synthesized pyrrolo-benzodiazepine conjugated with benzimidazole derivatives. The synthesized compounds were evaluated for antiproliferative activity in human cancer cell lines of the prostate, skin, lung, colon, and by using the MTT assay. A majority of the synthesized derivatives showed good anticancer activity. Compound **152** showed maximum activity with IC₅₀ values of 1.21, 1.72, 1.05, and 1.52 μM against Colo-205, A431, A549, and PC-3, respectively. Doxorubicin was used as the positive control and had IC₅₀ values of 1.69, 0.03, 1.02, and 2.51 μM [265]. Chen et al. (2013) synthesized the new series of pyrrolo-benzodiazepine-triazole derivatives and their anticancer activity was evaluated on A375 cells. Most of the synthesized derivatives showed potent cytotoxic activity. On A375 cells, compound **153** showed a greater inhibitory effect with the IC₅₀ value of 2.2 μM [266]. All the above reported Pyrrolo-benzodiazepines-based heterocyclic derivatives (Figure 16 (**151–153**)) discussed herewith were observed to act as anticancer agents. The most potent compound among them was compound **151** with the IC₅₀ value of 0.49 μM against THP-1, containing a fluorine analogue which may have a role in cell-permeability, which was generally enhanced by fluoro compounds.

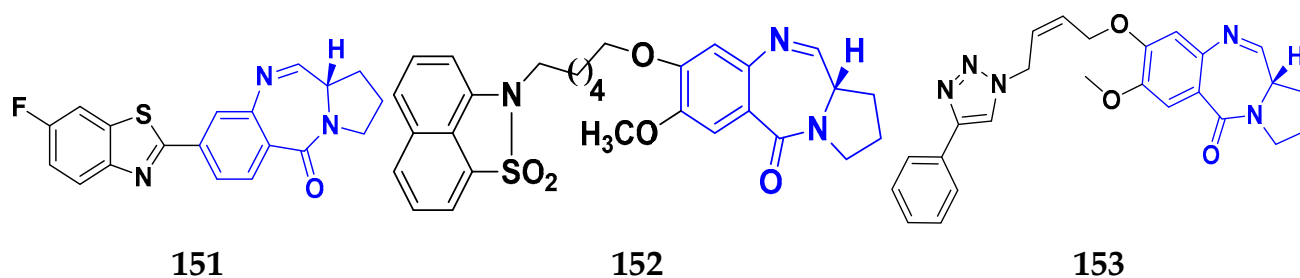


Figure 16. Pyrrolo-benzodiazepines derivatives (**151–153**) as anticancer agents.

3.15. Pyrido[2,3-d] Pyrimidine Derivatives as Anticancer Agents

Purines, quinazolines, pteridines, and pyrido-pyrimidines are examples of bicyclic nitrogen-containing heterocyclic compounds that are well-known pharmacophores in medicinal chemistry. Examples of commercial medications with a bicyclic main structure include the tyrosine kinase inhibitors gefitinib and erlotinib, and both are quinazoline derivatives. Both of them are used to manage non-small cell lung cancer. Pyrido[2,3-d]pyrimidines have been studied extensively as quinazoline analogs [267] Pyrido[2,3-d]pyrimidines have shown antitumor, antibacterial, CNS depressive, anticonvulsant, antipyretic, and analgesic effects [268]. Kumar et al. synthesized isoxazole/triazole attached 7(trifluoromethyl) pyrido[2,3d] pyrimidine compounds and evaluated their cytotoxicity against PANC1, HeLa, A549, and MDA MB-231 cells. A majority of the synthesized derivatives showed potent anticancer activity. Compounds **154** and **155** showed good antiproliferative activity against A549 and PANC-1 cell lines. Compound **154** had GI₅₀ values of 0.86 and 0.02 μM against A549 and PANC-1 cell lines, respectively, and compound **155** had the GI₅₀ value of 0.03

and 0.73 μM against A549 and PANC-1 cell lines, respectively. Nocodazole was used as a standard drug with IC_{50} values 0.08 and 0.029 μM , respectively [269].

Hou et al. (2016) prepared a series of new pyrido[2,3-*d*] pyrimidine derivatives and tested their cytotoxic activity on five human cancer cell lines: BT-474, SK-BR-3, A549, MCF-7, and MDA-MB-231. Most of the prepared compounds showed potent anticancer activity. Compound **156** showed good activity with IC_{50} values of 1.63, 17.17, 29.73, 13.47, and 7.11 μM against MCF-7, SK-BR-3, A549, BT-474, and MDA-MB-231 cell lines which were comparable to standard gefitinib with IC_{50} values of 25.37, 4.92, 24.25, 0.53, and 37.82 μM , respectively [270].

Banda et al. (2018) synthesized the pyridopyrimidine derivatives and tested them for anticancer activities in four types of human cancer cell lines. The anticancer activity was tested against Colo205, B16F10, U937, and THP-1. Most of the derivatives showed cytotoxic activities against all cells at concentrations lower than 100 $\mu\text{g}/\text{mL}$. Compound **157** was found to be the most effective of these derivatives since it had an IC_{50} value of 19 $\mu\text{g}/\text{mL}$ against B16F10 cell line. Further, 5-Fluorouracil was used as a reference drug which showed IC_{50} value of 4.03, 9.82, 0.87 and 0.54 $\mu\text{g}/\text{mL}$ against Colo205, B16F10, U937 and THP-1 cell lines respectively [271]. Behalo et al. (2017) produced new series of pyrido[2,3-*d*] pyrimidine derivatives and tested their anticancer activity against two cell lines: PC-3 and MCF-7. Most of the synthesized derivatives displayed potent anticancer activity. It was found that compounds **158** and **159** had the strongest cytotoxic effect against the PC-3 cell lines with IC_{50} values of 9.47 and 10.34, respectively. 5-Fluorouracil was used as a standard drug, having IC_{50} values of 4.91 and 4.73 $\mu\text{g}/\text{mL}$ for PC-3 and MCF-7 [272]. Elzahabi et al. (2018) synthesized substituted pyrido[2,3-*d*] pyrimidines and evaluated their antiproliferative activity against five tumor cell lines, PC-3, HepG-2, MCF-7, A549, and HCT-116. Most of the compounds displayed good anticancer activity. Against HCT-116, HepG-2, PC-3, and A549, compound **160** demonstrated strong anticancer activity with IC_{50} values of 7, 0.3, 6.6, and 9.6 μM , respectively, and reference drug doxorubicin had IC_{50} values of 12.8, 0.6, 6.8, and 0.087 μM , respectively [273].

Faidallah et al. (2016) prepared pyrido[2,3-*d*] pyrimidines and evaluated their cytotoxic activity against three human cancer cell lines HepG2, MCF-7, and HT29. Most of the synthesized derivatives showed potent anticancer activity. Many of the compounds showed good anticancer activity. Compounds **161** (with LD_{50} = 64.6, 6.4 and 25.2 μM), **162** (with LD_{50} = 70.1, 7.9 and 28.8 μM), and **163** (with LD_{50} = 71.2, 8.91 and 26.9 μM) presented comparable anticancer activity to that of doxorubicin with the LD_{50} value of 3, 4, and 40 μM [274]. Warhi et al. (2022) prepared pyrido[2,3-*d*] pyrimidines derivatives and assessed their anticancer activity against Hepg2 and MCF-7 cell lines. The majority of compounds showed potent anticancer activity. Compound **164** demonstrated comparable activity against the MCF-7 and HepG2 cell lines with IC_{50} values of 6.22 and 19.58 μM , respectively, while the control Taxol had IC_{50} values 8.48 μM and 14.60 μM , respectively [275].

Ding et al. (2022) prepared a series of DHA (dihydroartemisinin) and ARS (artesunate) containing pyrrolo(pyrido)[2,3-*d*] pyrimidine derivatives and tested their antiproliferative activity against MDA-MB-436 and T-47D cell lines. Many of the synthesized compounds showed potent anticancer activity. Among synthesized compounds, **165** displayed maximum anticancer activity towards MDA-MB-436 and T-47D with IC_{50} values of 10.52 and 3.02 μM . Ribociclib was used as positive control with IC_{50} values 24.35 and 4.81 μM , respectively [276].

All the Pyrido[2,3-*d*]pyrimidine based heterocyclic derivatives (Figure 17 (154–165)) discussed herewith were observed to act as anticancer agents. The most potent compound among them is compound **163** with GI_{50} of 0.02 μM against PANC-1, due to the presence of an ethyl group at the C-2 position and substituted aromatic ring with fluorine group.

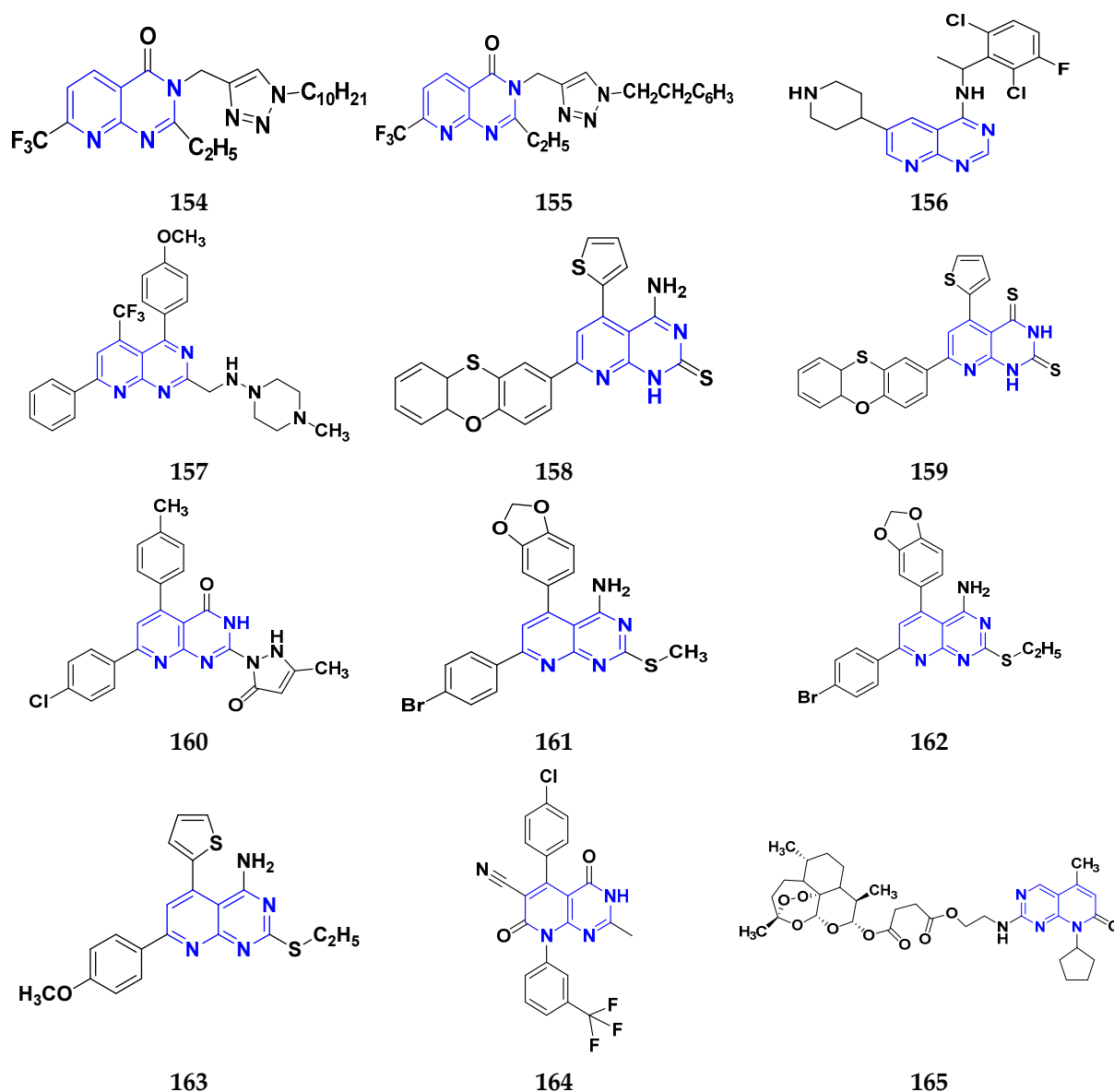


Figure 17. Pyrido[2,3-d]pyrimidine derivatives (154–165) as anticancer agents.

4. Conclusions

Heterocyclic systems have earned their place as true pillars of medicinal chemistry owing to their innate ingenuity, adaptability, and outstanding physicochemical potencies. The majority of natural products and pharmaceuticals that are currently prescribed contain the primary heterocyclic systems. Nitrogen heterocycles stand out among them because about 60% of the FDA-approved pharmaceuticals are nitrogen-based heterocycles. The current study deduced that chemically synthesized nitrogen-containing heterocycles (pyrimidine, quinolone, carbazole, pyridine, imidazole, benzimidazole, triazole, β -lactam, indole, pyrazole, quinazoline, quinoxaline, isatin, pyrrolo-benzodiazepines, and pyrido[2,3-d]pyrimidines) are important and versatile molecules against the different forms of cancer. The spectrum of nitrogen-based molecules used in medicine is expanding every day and their numerous analogues offer a promising and significant route for the discovery of medications with a variety of biological applications.

In vitro studies compiled herewith revealed that imidazole, pyridine, quinoxaline, β -lactam, quinazoline, and isatin majorly act against breast cancer (MCF-7), pyrimidine and pyrazole derivatives against liver cancer (HepG2), quinoline and triazole derivatives against

cervical cancer (HeLa), carbazole, indole, and pyrrolo-benzodiazepines derivatives against lung cancer (A549), and bezimidazole and pyrido[2,3-d]pyrimidine against colorectal cancer (HCT-116).

Particularly, pyridine derivative compound **39a** showed excellent anticancer activity on all tested cell lines, including MDA-MB-23, A549, and HeLa cell lines at IC₅₀ values of 0.0031, 0.089, and 0.0038 μ M, respectively. Further, Compounds **10**, **13**, **25a**, **49**, **59**, **68**, **86**, **88**, **104**, **111**, **122**, **145**, **151**, and **164** also showed potent anticancer activity on MCF-7, HeLa, HepG2, EGFR, VEGFR-2, MCF-7, MCF-7 Colo-205, HepG2, MCF-7, MCF-7 BxPc3, THP-1, and PANC-1 at concentration of 0.23, 0.8, 0.012, 0.47, 0.02, 0.38, 0.017, 0.018, 0.028, 0.06, 0.01, 0.1, 0.49, and 0.02 μ M to nM range respectively. Among these potent compounds, compounds **10**, **68**, **86**, **111**, and **122** showed excellent activity against the breast cancer (MCF-7 cell line).

The compiled studies confirm the potential of nitrogen heterocyclic molecules in cancer treatment. The reported promising compounds from every scaffold present excellent activity against the different cell lines and kinase inhibitory assay which could be used in the structural based design of efficacious nitrogen-based anticancer drugs.

Author Contributions: Conceptualization: P.K., M.G. and M.J.; data collection: V.V., D.K., J.N. and J.P.Y.; writing the manuscript: A.K. and A.K.S.; sketching of figures: P.P. and H.S.; data interpretation: S.T. and A.-H.E.; writing, review and final editing of the manuscript: A.V. and H.K. All authors have read and agreed to the published version of the manuscript.

Funding: The APC was funded by King Abdullah University of Science and Technology (KAUST), Thuwal, Jeddah, Saudi Arabia.

Institutional Review Board Statement: Not applicable.

Informed Consent Statement: Not applicable.

Data Availability Statement: All the data given in this manuscript has been taken from published research articles, given in the list of references and are available online.

Acknowledgments: The authors are thankful to Central University of Punjab and DST-FIST, India and South Ural State University, Russia for providing infrastructural facilities for the successful completion of this study.

Conflicts of Interest: The authors declare no conflict of interest.

Abbreviations

AICART	Aminoimidazole carboxamide ribonucleotide transformylase
ALK	Anaplastic lymphoma kinase
AQ	anthraquinone
ARS	Artesunate
BCR	Breakpoint cluster region
BRAF	v-raf murine sarcoma viral oncogene homolog B1
CA-4	Combretasin A-4
CDK	Cyclin dependent kinase
CNS	Central Nervous System
CSF-1	Colony-stimulating factor
DENV-2	Dengue virus serotype 2
DHA	Dihydroartemisinin
DLC	Drug loading content
DLE	Drug-loading efficiency
DMEM	Dulbecco's Modified Eagle Medium
DOX	Doxorubicin
DPPH	2,2-diphenylpicrylhydrazyl
EAC	Ehrlich Ascites Carcinoma
EC50	Half maximal effective concentration

EGFR	Epidermal growth factor receptor
EMT	Epithelial Mesenchymal transition
ERK	Extracellular signal-regulated kinase
FLT3	Fms-like tyrosine kinase
GI50	Half maximal Growth Inhibition
HDAC	Histone deacetylases
HER	Human epidermal growth factor receptor
HetQ	heterocycle-fused quinone
IC50	Half maximal Inhibitory concentration
JAK2	Janus kinase 2
KDR	Kinase insert domain receptor
LC50	Half maximal Lethal concentration
MEK	Mitogen-activated protein kinase
MG-MID	Mean graph midpoint
MTT	3-(4,5-dimethylthiazolyl-2)-2,5-diphenyltetrazolium bromide
NCI	National Cancer Institute
ND	Not Defined
NQ	Naphthoquinone
NSCLC	Non-small cell lung cancer
P13K	Phosphoinositide3-kinase
PBD	Pyrrolo-benzodiazepines
PGDFR	Platelet-derived growth factor
Raf	Rapidly accelerated fibrosarcoma
Ras	Rat Sarcoma
ROS	Reactive Oxygen Species
SAHA	standard hydroxamic acid
SRB	Sulforhodamine B
TKi	Tyrosine kinase inhibitor
TRK	Tropomyosin Receptor Kinase
VEGFR	vascular endothelial growth factor receptor
XPO1	Exportin 1

References

1. Angre, T.; Kumar, A.; Singh, A.K.; Thareja, S.; Kumar, P. Role of Collagen Regulators in Cancer Treatment: A Comprehensive Review. *Anti-Cancer Agents Med. Chem.* **2022**, *22*, 2956–2984.
2. Sung, H.; Ferlay, J.; Siegel, R.L.; Laversanne, M.; Soerjomataram, I.; Jemal, A.; Bray, F. Global cancer statistics 2020: GLOBOCAN estimates of incidence and mortality worldwide for 36 cancers in 185 countries. *Cancer J. Clin.* **2021**, *71*, 209–249. [[CrossRef](#)] [[PubMed](#)]
3. Gu, L.; Shan, T.; Ma, Y.-X.; Tay, F.R.; Niu, L. Novel biomedical applications of crosslinked collagen. *Trends Biotechnol.* **2019**, *37*, 464–491. [[CrossRef](#)] [[PubMed](#)]
4. Bray, F.; Ferlay, J.; Soerjomataram, I.; Siegel, R.L.; Torre, L.A.; Jemal, A. Global cancer statistics 2018: GLOBOCAN estimates of incidence and mortality worldwide for 36 cancers in 185 countries. *Cancer J. Clin.* **2018**, *68*, 394–424. [[CrossRef](#)] [[PubMed](#)]
5. Singh, A.K.; Kumar, A.; Thareja, S.; Kumar, P. Current insights into the role of BRAF inhibitors in treatment of melanoma. *Anti-Cancer Agents Med. Chem.* **2022**, 1–7. [[CrossRef](#)]
6. Rang, H.; Dale, M.; Ritter, J.; Moore, P. *Edinburgh, Scotland, Pharmacology*, 5th ed.; Churchill Livingstone: London, UK, 2003.
7. Williams David, A.; Lemke Thomson, A. *Foyes Principle of Medicinal Chemistry*; Lippincott, Williams & Wilkins: Philadelphia, FL, USA, 2002.
8. Stefanowicz, P.; Jaremko, Ł.; Jaremko, M.; Lis, T. Crystal-state studies on p-toluenesulfonates of N-oxyimides—A possible structural basis of serine proteases inhibition. *New J. Chem.* **2006**, *30*, 258–265. [[CrossRef](#)]
9. Álvarez-Builla, J.; Barluenga, J. Heterocyclic compounds: An introduction. *Mod Heterocycl Chem* **2011**, *1*, 1–9.
10. Ferreira, P.M.; Maia, H.L.; Monteiro, L.S.S. Synthesis of 2, 3, 5-substituted pyrrole derivatives. *Tetrahedron. Lett.* **2002**, *43*, 4491–4493. [[CrossRef](#)]
11. Kijewska, M.; Sharfalddin, A.A.; Jaremko, Ł.; Cal, M.; Setner, B.; Siczek, M.; Stefanowicz, P.; Hussien, M.A.; Emwas, A.-H.; Jaremko, M. Lossen Rearrangement of p-Toluenesulfonates of N-Oxyimides in Basic Condition, Theoretical Study, and Molecular Docking. *Front. Chem.* **2021**, *9*, 662533. [[CrossRef](#)]
12. Shukla, P.K.; Verma, A.; Mishra, P. Significance of nitrogen heterocyclic nuclei in the search of pharmacological active compounds. In *New Perspective in Agricultural and Human Health*; Shukla, R.P., Mishra, R.S., Tripathi, A.D., Yadav, A.K., Tiwari, M., Mishra, R.R., Eds.; Bharti Publications: Delhi, India, 2017; pp. 100–126.

13. Martins, P.; Jesus, J.; Santos, S.; Raposo, L.R.; Roma-Rodrigues, C.; Baptista, P.V.; Fernandes, A.R. Heterocyclic anticancer compounds: Recent advances and the paradigm shift towards the use of nanomedicine's tool box. *Molecules* **2015**, *20*, 16852–16891. [[CrossRef](#)]
14. Ajani, O.; Audu, O.; Aderohunmu, D.; Owolabi, F.; Olomieja, A. Undeniable pharmacological potentials of quinazoline motifs in therapeutic medicine. *Am. J. Drug Discov. Dev.* **2017**, *7*, 1–24. [[CrossRef](#)]
15. Özkay, Y.; Işıkdag, İ.; İncesu, Z.; Akalın, G. Synthesis of 2-substituted-N-[4-(1-methyl-4, 5-diphenyl-1H-imidazole-2-yl) phenyl] acetamide derivatives and evaluation of their anticancer activity. *Eur. J. Med. Chem.* **2010**, *45*, 3320–3328. [[CrossRef](#)] [[PubMed](#)]
16. Jangale, A.D.; Dalal, D.S. Green synthetic approaches for biologically relevant organic compounds. *Synth. Commun.* **2017**, *47*, 2139–2173. [[CrossRef](#)]
17. Yang, D.; An, B.; Wei, W.; Tian, L.; Huang, B.; Wang, H. Copper-catalyzed domino synthesis of nitrogen heterocycle-fused benzoimidazole and 1, 2, 4-benzothiadiazine 1, 1-dioxide derivatives. *ACS Comb. Sci.* **2015**, *17*, 113–119. [[CrossRef](#)] [[PubMed](#)]
18. Srivastava, M.; Singh, J.; Singh, S.B.; Tiwari, K.; Pathak, V.K.; Singh, J. Synthesis of novel fused heterocycle-oxa-aza-phenanthrene and anthracene derivatives via sequential one-pot synthesis in aqueous micellar system. *Green Chem.* **2012**, *14*, 901–905. [[CrossRef](#)]
19. Czarnik, A.W. Peer Reviewed: Combinatorial Chemistry. *Anal. Chem.* **1998**, *70*, 378–386. [[CrossRef](#)]
20. García-Valverde, M.; Torroba, T. Sulfur-Nitrogen Heterocycles. *Guest editorial; Molecules* **2005**, *10*, 318–320. [[CrossRef](#)]
21. Al-Ghorbani, M.; Bushra, B.A.; Mamatha, S.; Khanum, S.A. Piperazine and morpholine: Synthetic preview and pharmaceutical applications. *Res. J. Pharm. Technol.* **2015**, *8*, 611–628. [[CrossRef](#)]
22. Heravi, M.M.; Zadsirjan, V. Prescribed drugs containing nitrogen heterocycles: An overview. *RSC Adv.* **2020**, *10*, 44247–44311. [[CrossRef](#)]
23. Mendez, D.; Gaulton, A.; Bento, A.P.; Chambers, J.; De Veij, M.; Félix, E.; Magariños, M.P.; Mosquera, J.F.; Mutowo, P.; Nowotka, M. ChEMBL: Towards direct deposition of bioassay data. *Nucleic Acids Res.* **2019**, *47*, 930–940. [[CrossRef](#)]
24. Larkins, E.; Blumenthal, G.M.; Chen, H.; He, K.; Agarwal, R.; Gieser, G.; Stephens, O.; Zahalka, E.; Ringgold, K.; Helms, W. FDA Approval: Alectinib for the Treatment of Metastatic, ALK-Positive Non-Small Cell Lung Cancer Following Crizotinib/Alectinib for ALK-Positive Non-Small Cell Lung Cancer. *Clin. Cancer Res.* **2016**, *22*, 5171–5176. [[CrossRef](#)] [[PubMed](#)]
25. Sun, N.; Ren, C.; Kong, Y.; Zhong, H.; Chen, J.; Li, Y.; Zhang, J.; Zhou, Y.; Qiu, X.; Lin, H. Development of a Brigatinib degrader (SIAIS117) as a potential treatment for ALK positive cancer resistance. *Eur. J. Med. Chem.* **2020**, *193*, 112190. [[CrossRef](#)] [[PubMed](#)]
26. Collier, T.L.; Normandin, M.D.; Stephenson, N.A.; Livni, E.; Liang, S.H.; Wooten, D.W.; Esfahani, S.A.; Stabin, M.G.; Mahmood, U.; Chen, J. Synthesis and preliminary PET imaging of ¹¹C and ¹⁸F isotopologues of the ROS1/ALK inhibitor lorlatinib. *Nat. Commun.* **2017**, *8*, 1–12. [[CrossRef](#)]
27. Sartore-Bianchi, A.; Pizzutillo, E.G.; Marrapese, G.; Tosi, F.; Cerea, G.; Siena, S. Entrectinib for the treatment of metastatic NSCLC: Safety and efficacy. *Expert Rev. Anticancer Ther.* **2020**, *20*, 333–341. [[CrossRef](#)] [[PubMed](#)]
28. Kasamon, Y.L.; Ko, C.W.; Subramaniam, S.; Ma, L.; Yang, Y.; Nie, L.; Shord, S.; Przepiorka, D.; Farrell, A.T.; McKee, A.E. FDA approval summary: Midostaurin for the treatment of advanced systemic mastocytosis. *Oncologist* **2018**, *23*, 1511–1519. [[CrossRef](#)] [[PubMed](#)]
29. Liang, X.; Wu, P.; Yang, Q.; Xie, Y.; He, C.; Yin, L.; Yin, Z.; Yue, G.; Zou, Y.; Li, L. An update of new small-molecule anticancer drugs approved from 2015 to 2020. *Eur. J. Med. Chem.* **2021**, *220*, 113473. [[CrossRef](#)]
30. Tzogani, K.; Røshol, H.; Olsen, H.H.; Aas, I.B.; Dalhus, M.L.; Håkonsen, G.D.; Nilssen, L.S.; Lindberg, V.; Økvist, M.; Bolstad, B. The European Medicines Agency review of Gilteritinib (Xospata) for the treatment of adult patients with relapsed or refractory acute myeloid leukemia with an FLT3 mutation. *Oncologist* **2020**, *25*, e1070–e1076. [[CrossRef](#)] [[PubMed](#)]
31. Gunawardane, R.N.; Nepomuceno, R.R.; Rooks, A.M.; Hunt, J.P.; Ricono, J.M.; Belli, B.; Armstrong, R.C. Transient exposure to quizartinib mediates sustained inhibition of FLT3 signaling while specifically inducing apoptosis in FLT3-activated leukemia cells. *Mol. Cancer Ther.* **2013**, *12*, 438–447. [[CrossRef](#)]
32. Benner, B.; Good, L.; Quiroga, D.; Schultz, T.E.; Kassem, M.; Carson, W.E.; Cherian, M.A.; Sardesai, S.; Wesolowski, R. Pexidartinib, a novel small molecule CSF-1R inhibitor in use for tenosynovial giant cell tumor: A systematic review of pre-clinical and clinical development. *Drug Des. Dev. Ther.* **2020**, *14*, 1693. [[CrossRef](#)]
33. Butterworth, S.; Cross, D.A.; Finlay, M.R.V.; Ward, R.A.; Waring, M.J. The structure-guided discovery of osimertinib: The first US FDA approved mutant selective inhibitor of EGFR T790M. *Medchemcomm* **2017**, *8*, 820–822. [[CrossRef](#)]
34. Zhang, W.; Fan, Y.-F.; Cai, C.-Y.; Wang, J.-Q.; Teng, Q.-X.; Lei, Z.-N.; Zeng, L.; Gupta, P.; Chen, Z.-S. Olmutinib (BI1482694/HM61713), a novel epidermal growth factor receptor tyrosine kinase inhibitor, reverses ABCG2-mediated multidrug resistance in cancer cells. *Front. Pharmacol.* **2018**, *9*, 1097. [[CrossRef](#)] [[PubMed](#)]
35. Singh, H.; Walker, A.J.; Amiri-Kordestani, L.; Cheng, J.; Tang, S.; Balcazar, P.; Barnett-Ringgold, K.; Palmby, T.R.; Cao, X.; Zheng, N. US Food and Drug Administration Approval: Neratinib for the Extended Adjuvant Treatment of Early-Stage HER2-Positive Breast Cancer/FDA Approval Summary: Neratinib. *Clin. Cancer Res.* **2018**, *24*, 3486–3491. [[CrossRef](#)]
36. Lavacchi, D.; Mazzoni, F.; Giaccone, G. Clinical evaluation of dacomitinib for the treatment of metastatic non-small cell lung cancer (NSCLC): Current perspectives. *Drug Des. Dev. Ther.* **2019**, *13*, 3187. [[CrossRef](#)] [[PubMed](#)]
37. Li, X.; Wang, B. Pharmaceutically Acceptable Salt of (e)-n-[4-[[3-chloro-4-(2-Pyridylmethoxy) phenyl] amino]-3-cyano-7-ethoxy-6-quinoly]-3-[(2r)-1-methylpyrrolidin-2-yl] prop-2-enamide, Preparation Method Thereof, and Medical Use Thereof. US Patent Application No. 14/001,778, 2013.

38. Zhou, C.; Xie, L.; Liu, W.; Zhang, L.; Zhou, S.; Wang, L.; Chen, J.; Li, H.; Zhao, Y.; Zhu, B. Absorption, metabolism, excretion, and safety of [¹⁴C] almonertinib in healthy Chinese subjects. *Ann. Transl. Med.* **2021**, *9*, 867. [[CrossRef](#)] [[PubMed](#)]
39. Hao, Z.; Wang, P. Lenvatinib in management of solid tumors. *Oncologist* **2020**, *25*, e302–e310. [[CrossRef](#)]
40. Sochacka-Ćwikła, A.; Mączyński, M.; Regiec, A. FDA-Approved Small Molecule Compounds as Drugs for Solid Cancers from Early 2011 to the End of 2021. *Molecules* **2022**, *27*, 2259. [[CrossRef](#)]
41. Zhang, Y.; Zou, J.-Y.; Wang, Z.; Wang, Y. Fruquintinib: A novel antivascular endothelial growth factor receptor tyrosine kinase inhibitor for the treatment of metastatic colorectal cancer. *Cancer Manag. Res.* **2019**, *11*, 7787. [[CrossRef](#)]
42. Shen, G.; Zheng, F.; Ren, D.; Du, F.; Dong, Q.; Wang, Z.; Zhao, F.; Ahmad, R.; Zhao, J. Anlotinib: A novel multi-targeting tyrosine kinase inhibitor in clinical development. *J. Hematol. Oncol.* **2018**, *11*, 1–11. [[CrossRef](#)]
43. Isaac, K.; Mato, A.R. Acalabrutinib and its therapeutic potential in the treatment of chronic lymphocytic leukemia: A short review on emerging data. *Cancer Manag. Res.* **2020**, *12*, 2079. [[CrossRef](#)]
44. Guo, Y.; Liu, Y.; Hu, N.; Yu, D.; Zhou, C.; Shi, G.; Zhang, B.; Wei, M.; Liu, J.; Luo, L. Discovery of zanubrutinib (BGB-3111), a novel, potent, and selective covalent inhibitor of Bruton's tyrosine kinase. *J. Med. Chem.* **2019**, *62*, 7923–7940. [[CrossRef](#)]
45. Palmer, J.; Mesa, R. The role of fedratinib for the treatment of patients with primary or secondary myelofibrosis. *Ther. Adv. Hematol.* **2020**, *11*, 2040620720925201. [[CrossRef](#)] [[PubMed](#)]
46. Markham, A. Copanlisib: First global approval. *Drugs* **2017**, *77*, 2057–2062. [[CrossRef](#)]
47. Dreyling, M.; Morschhauser, F.; Bouabdallah, K.; Bron, D.; Cunningham, D.; Assouline, S.; Verhoef, G.; Linton, K.; Thieblemont, C.; Vitolo, U. Phase II study of copanlisib, a PI3K inhibitor, in relapsed or refractory, indolent or aggressive lymphoma. *Ann. Oncol.* **2017**, *28*, 2169–2178. [[CrossRef](#)] [[PubMed](#)]
48. Bumber, Y.; Younes, A.; Garcia-Manero, G. Mocetinostat (MGCD0103): A review of an isotype-specific histone deacetylase inhibitor. *Expert Opin. Investig. Drugs* **2011**, *20*, 823–829. [[CrossRef](#)] [[PubMed](#)]
49. Karandish, F.; Haldar, M.K.; You, S.; Brooks, A.E.; Brooks, B.D.; Guo, B.; Choi, Y.; Mallik, S. Prostate-specific membrane antigen targeted polymersomes for delivering mocetinostat and docetaxel to prostate cancer cell spheroids. *ACS Omega* **2016**, *1*, 952–962. [[CrossRef](#)]
50. Rodrigues, D.A.; Sagrillo, F.S.; Fraga, C.A. Duvelisib: A 2018 novel FDA-approved small molecule inhibiting phosphoinositide 3-kinases. *Pharmaceuticals* **2019**, *12*, 69. [[CrossRef](#)]
51. Ibrahim, A.; Hirschfeld, S.; Cohen, M.H.; Griebel, D.J.; Williams, G.A.; Pazdur, R. FDA drug approval summaries: Oxaliplatin. *Oncologist* **2004**, *9*, 8–12. [[CrossRef](#)]
52. Monneret, C. Platinum anticancer drugs. From serendipity to rational design. In *Annales Pharmaceutiques Françaises*; Elsevier: Amsterdam, The Netherlands, 2011; pp. 286–295.
53. Dean, L. Irinotecan therapy and UGT1A1 genotype. In *Medical Genetics Summaries*; National Center for Biotechnology Information (US): Bethesda, MD, USA, 2012; updated 2018.
54. Bailly, C. Irinotecan: 25 years of cancer treatment. *Pharmacol. Res.* **2019**, *148*, 104398. [[CrossRef](#)]
55. El-Subbagh, H.I.; Al-Badr, A.A. Cytarabine. In *Profiles of Drug Substances, Excipients and Related Methodology*; Elsevier: Amsterdam, The Netherlands, 2009; Volume 34, pp. 37–113.
56. Baker, W.J.; Royer Jr, G.L.; Weiss, R.B. Cytarabine and neurologic toxicity. *Oncology* **1991**, *9*, 679–693. [[CrossRef](#)]
57. Noble, S.; Goa, K.L. Gemcitabine. *Drugs* **1997**, *54*, 447–472. [[CrossRef](#)]
58. Paroha, S.; Verma, J.; Dubey, R.D.; Dewangan, R.P.; Molugulu, N.; Bapat, R.A.; Sahoo, P.K.; Kesharwani, P. Recent advances and prospects in gemcitabine drug delivery systems. *Int. J. Pharm.* **2021**, *592*, 120043. [[CrossRef](#)]
59. Ganjoo, K.N.; Patel, S.J. Trabectedin: An anticancer drug from the sea. *Expert Opin. Pharmacother.* **2009**, *10*, 2735–2743. [[CrossRef](#)]
60. Barone, A.; Chi, D.-C.; Theoret, M.R.; Chen, H.; He, K.; Kufryn, D.; Helms, W.S.; Subramaniam, S.; Zhao, H.; Patel, A. FDA Approval Summary: Trabectedin for Unresectable or Metastatic Liposarcoma or Leiomyosarcoma Following an Anthracycline-Containing Regimen. *Clin. Cancer Res.* **2017**, *23*, 7448–7453. [[CrossRef](#)]
61. Brown, A.P.; Morrissey, R.L.; Faircloth, G.T.; Levine, B.S. Preclinical toxicity studies of kahalalide F, a new anticancer agent: Single and multiple dosing regimens in the rat. *Cancer Chemother. Pharmacol.* **2002**, *50*, 333–340. [[CrossRef](#)] [[PubMed](#)]
62. Nastrucci, C.; Cesario, A.; Russo, P. Anticancer drug discovery from the marine environment. *Recent Pat. Anti-Cancer Drug Discov.* **2012**, *7*, 218–232. [[CrossRef](#)]
63. Fenical, W.; Jensen, P.R.; Palladino, M.A.; Lam, K.S.; Lloyd, G.K.; Potts, B.C. Discovery and development of the anticancer agent salinosporamide A (NPI-0052). *Bioorg. Med. Chem.* **2009**, *17*, 2175–2180. [[CrossRef](#)]
64. Greig, S.L. Osimertinib: First global approval. *Drugs* **2016**, *76*, 263–273. [[CrossRef](#)]
65. Watanabe, J.; Minami, M.; Kobayashi, M. Antitumor activity of TZT-1027 (Soblidotin). *Anticancer Res.* **2006**, *26*, 1973–1981. [[PubMed](#)]
66. Syed, Y.Y. Selinexor: First global approval. *Drugs* **2019**, *79*, 1485–1494. [[CrossRef](#)] [[PubMed](#)]
67. Podar, K.; Shah, J.; Chari, A.; Richardson, P.G.; Jagannath, S. Selinexor for the treatment of multiple myeloma. *Expert Opin. Pharmacother.* **2020**, *21*, 399–408. [[CrossRef](#)]
68. Leong, H.; Bonk, M.E. Therapeutics: Bendamustine (Treanda) for chronic lymphocytic leukemia: A brief overview. *Pharm. Ther.* **2009**, *34*, 73.
69. Cohen, M.H.; Williams, G.A.; Sridhara, R.; Chen, G.; Pazdur, R. FDA drug approval summary: Gefitinib (ZD1839)(Iressa[®]) tablets. *Oncologist* **2003**, *8*, 303–306. [[CrossRef](#)]

70. Kim, E.S. Abemaciclib: First global approval. *Drugs* **2017**, *77*, 2063–2070. [[CrossRef](#)] [[PubMed](#)]
71. Voli, L.A.; Mamyrbékova, J.A.; Bazureau, J.-P. Abemaciclib, a recent novel FDA-Approved small molecule inhibiting cyclin-dependant kinase 4/6 for the treatment of metastatic breast cancer: A mini-review. *Open J. Med. Chem.* **2020**, *10*, 128–138. [[CrossRef](#)]
72. Shah, A.; Bloomquist, E.; Tang, S.; Fu, W.; Bi, Y.; Liu, Q.; Yu, J.; Zhao, P.; Palmby, T.R.; Goldberg, K.B. FDA Approval: Ribociclib for the Treatment of Postmenopausal Women with Hormone Receptor-Positive HER2-Negative Advanced or Metastatic Breast Cancer. *Clin. Cancer Res.* **2018**, *24*, 2999–3004. [[CrossRef](#)] [[PubMed](#)]
73. Dimou, A.; Syrigos, K.N.; Saif, M.W. Is there a role for mitomycin C in metastatic colorectal, cancer? Expert opinion on investigational drugs. *Expert Opin. Investig. Drugs* **2010**, *19*, 723–735. [[CrossRef](#)]
74. Benayoun, L.; Schaffer, M.; Bril, R.; Gingis-Velitski, S.; Segal, E.; Nevelsky, A.; Satchi-Fainaro, R.; Shaked, Y. Porfimer-sodium (Photofrin-II) in combination with ionizing radiation inhibits tumor-initiating cell proliferation improves glioblastoma treatment efficacy. *Cancer Biol. Ther.* **2013**, *14*, 64–74. [[CrossRef](#)]
75. Hörmann, V.; Kumi-Diaka, J.; Durity, M.; Rathinavelu, A. Anticancer activities of genistein-topotecan combination in prostate cancer, cells. *J. Cell. Mol. Med.* **2012**, *16*, 2631–2636. [[CrossRef](#)]
76. Shah, A.; Mangaonkar, A. Idelalisib: A novel PI3K δ inhibitor for chronic lymphocytic, leukemia. *Ann. Pharmacother.* **2015**, *49*, 1162–1170. [[CrossRef](#)]
77. Zirlik, K.; Veelken, H. Idelalisib. *Small Mol. Hematol.* **2018**, 243–264. [[CrossRef](#)]
78. Markham, A.; Dhillon, S. Acabrutinib: First global, approval. *Drugs* **2018**, *78*, 139–145. [[CrossRef](#)] [[PubMed](#)]
79. Singh, H.; Brave, M.; Beaver, J.A.; Cheng, J.; Tang, S.; Zahalka, E.; Palmby, T.R.; Venugopal, R.; Song, P.; Liu, Q. Food Drug Administration approval: Cabozantinib for the treatment of advanced renal cell, carcinoma. *Ther. Adv. Urol.* **2017**, *23*, 330–335. [[CrossRef](#)] [[PubMed](#)]
80. Duke, E.S.; Barone, A.K.; Chatterjee, S.; Mishra-Kalyani, P.S.; Shen, Y.L.; Isikwei, E.; Zhao, H.; Bi, Y.; Liu, J.; Rahman, N.A. FDA Approval Summary: Cabozantinib for Differentiated Thyroid, Cancer. *Clin. Cancer Res.* **2022**, *28*, 4173–4177. [[CrossRef](#)] [[PubMed](#)]
81. Arora, S.; Balasubramaniam, S.; Zhang, W.; Zhang, L.; Sridhara, R.; Spillman, D.; Mathai, J.P.; Scott, B.; Golding, S.J.; Coory, M. FDA Approval Summary: Pembrolizumab plus Lenvatinib for Endometrial Carcinoma a Collaborative International Review under Project Orbis. FDA Approval: Pembrolizumab plus, lenvatinib; Project Orbis. *Clin. Cancer Res.* **2020**, *26*, 5062–5067. [[CrossRef](#)]
82. Nair, A.; Reece, K.; Donoghue, M.B.; Yuan, W.; Rodriguez, L.; Keegan, P.; Pazdur, R. FDA supplemental approval summary: Lenvatinib for the treatment of unresectable hepatocellular, carcinoma. *Oncologist* **2021**, *26*, e484–e491. [[CrossRef](#)] [[PubMed](#)]
83. Lu, J. Oncology: Palbociclib: A first-in-class CDK4/CDK6 inhibitor for the treatment of hormone-receptor positive advanced breast cancer. *J. Hematol. Oncol.* **2015**, *8*, 1–3. [[CrossRef](#)]
84. Roskoski, R. Cyclin-dependent protein kinase inhibitors including palbociclib as anticancer drugs. *Pharmacol. Res.* **2016**, *107*, 249–275. [[CrossRef](#)]
85. Wright, C.J.; McCormack, P.L. Trametinib: First global approval. *Drugs* **2013**, *73*, 1245–1254. [[CrossRef](#)]
86. Zeiser, R.; Andrlóvá, H.; Meiss, F. Trametinib (GSK1120212). *Small Mol. Oncol.* **2018**, 91–100. [[CrossRef](#)]
87. Odogwu, L.; Mathieu, L.; Blumenthal, G.; Larkins, E.; Goldberg, K.B.; Griffin, N.; Bijwaard, K.; Lee, E.Y.; Philip, R.; Jiang, X. FDA approval summary: Dabrafenib and trametinib for the treatment of metastatic non-small cell lung cancers harboring BRAF V600E mutations. *Oncologist* **2018**, *23*, 740–745. [[CrossRef](#)]
88. Dungo, R.T.; Keating, G.M. Afatinib: First global approval. *Drugs* **2013**, *73*, 1503–1515. [[CrossRef](#)] [[PubMed](#)]
89. Helena, A.Y.; Pao, W. Targeted therapies: Afatinib—New therapy option for EGFR-mutant lung cancer. *Nat. Rev. Clin. Oncol.* **2013**, *10*, 551.
90. Ballantyne, A.D.; Garnock-Jones, K.P. Dabrafenib: First global approval. *Drugs* **2013**, *73*, 1367–1376. [[CrossRef](#)]
91. Menzies, A.M.; Long, G.V.; Murali, R. Dabrafenib and its potential for the treatment of metastatic melanoma. *Drug Des. Dev. Ther.* **2012**, *6*, 391.
92. Dhillon, S. Gilteritinib: First global approval. *Drugs* **2019**, *79*, 331–339. [[CrossRef](#)]
93. Perl, A.E.; Martinelli, G.; Cortes, J.E.; Neubauer, A.; Berman, E.; Paolini, S.; Montesinos, P.; Baer, M.R.; Larson, R.A.; Ustun, C. Gilteritinib or chemotherapy for relapsed or refractory FLT3-mutated AML. *N. Engl. J. Med.* **2019**, *18*, 1728–1740. [[CrossRef](#)]
94. Markham, A. Alpelisib: First global approval. *Drugs* **2019**, *79*, 1249–1253. [[CrossRef](#)]
95. Shirley, M. Encorafenib and binimetinib: First global approvals. *Drugs* **2018**, *78*, 1277–1284. [[CrossRef](#)]
96. Tran, B.; Cohen, M.S. The discovery and development of binimetinib for the treatment of melanoma. *Expert Opin. Drug Discov.* **2020**, *15*, 745–754. [[CrossRef](#)]
97. Kazandjian, D.; Blumenthal, G.M.; Chen, H.-Y.; He, K.; Patel, M.; Justice, R.; Keegan, P.; Pazdur, R. FDA approval summary: Crizotinib for the treatment of metastatic non-small cell lung cancer with anaplastic lymphoma kinase rearrangements. *Oncologist* **2014**, *19*, e5–e11. [[CrossRef](#)]
98. O'Bryant, C.L.; Wenger, S.D.; Kim, M.; Thompson, L.A. Crizotinib: A new treatment option for ALK-positive non-small cell lung cancer. *Ann. Pharmacother.* **2013**, *47*, 189–197. [[CrossRef](#)]
99. Slayton, R.E.; Park, R.C.; Silverberg, S.G.; Shingleton, H.; Creasman, W.T.; Blessing, J.A. Vincristine, dactinomycin, and cyclophosphamide in the treatment of malignant germ cell tumors of the ovary. A Gynecologic Oncology Group Study (a final report). *Cancer* **1985**, *56*, 243–248. [[CrossRef](#)] [[PubMed](#)]

100. Cohen, M.H.; Johnson, J.R.; Chen, Y.-F.; Sridhara, R.; Pazdur, R. FDA drug approval summary: Erlotinib (Tarceva®) tablets. *Oncologist* **2005**, *10*, 461–466. [[CrossRef](#)] [[PubMed](#)]
101. Cameron, F.; Sanford, M. Ibrutinib: First global approval. *Drugs* **2014**, *74*, 263–271. [[CrossRef](#)] [[PubMed](#)]
102. de Claro, R.A.; McGinn, K.M.; Verdun, N.; Lee, S.-L.; Chiu, H.-J.; Saber, H.; Brower, M.E.; Chang, C.G.; Pfuma, E.; Habtemariam, B. FDA approval: Ibrutinib for patients with previously treated mantle cell lymphoma and previously treated chronic lymphocytic leukemia. *Clin. Cancer Res.* **2015**, *21*, 3586–3590. [[CrossRef](#)] [[PubMed](#)]
103. Ryan, Q.; Ibrahim, A.; Cohen, M.H.; Johnson, J.; Ko, C.-W.; Sridhara, R.; Justice, R.; Pazdur, R. FDA drug approval summary: Lapatinib in combination with capecitabine for previously treated metastatic breast cancer that overexpresses HER-2. *Oncologist* **2008**, *13*, 1114–1119. [[CrossRef](#)] [[PubMed](#)]
104. Scott, L. Larotrectinib: First global approval. *Drugs* **2019**, *79*, 201–206. [[CrossRef](#)]
105. Federman, N.; McDermott, R. Larotrectinib, a highly selective tropomyosin receptor kinase (TRK) inhibitor for the treatment of TRK fusion cancer. *Expert Rev. Clin. Pharmacol.* **2019**, *12*, 931–939. [[CrossRef](#)]
106. Neerman, M.F.; Chen, H.-T.; Parrish, A.R.; Simanek, E.E. Reduction of drug toxicity using dendrimers based on melamine. *Mol. Pharm.* **2004**, *1*, 390–393. [[CrossRef](#)]
107. Weinstein, G.D. Drugs five years later: Methotrexate. *Ann. Intern. Med.* **1977**, *86*, 199–204. [[CrossRef](#)]
108. Moshikur, R.M.; Chowdhury, M.R.; Wakabayashi, R.; Tahara, Y.; Moniruzzaman, M.; Goto, M.J. Ionic liquids with methotrexate moieties as a potential anticancer prodrug: Synthesis, characterization and solubility evaluation. *J. Mol. Liq.* **2019**, *278*, 226–233. [[CrossRef](#)]
109. DeRemer, D.L.; Ustun, C.; Natarajan, K. Nilotinib: A second-generation tyrosine kinase inhibitor for the treatment of chronic myelogenous leukemia. *Clin. Ther.* **2008**, *30*, 1956–1975. [[CrossRef](#)] [[PubMed](#)]
110. Harris, M.G.; Coleman, S.G.; Faulds, D.; Chrisp, P. Nilutamide: A review of its pharmacodynamic and pharmacokinetic properties, and therapeutic efficacy in prostate cancer. *Drugs Aging* **1993**, *3*, 9–25. [[CrossRef](#)] [[PubMed](#)]
111. Kim, G.; Ison, G.; McKee, A.E.; Zhang, H.; Tang, S.; Gwise, T.; Sridhara, R.; Lee, E.; Tzou, A.; Philip, R. FDA Approval Summary: Olaparib Monotherapy in Patients with Deleterious Germline BRCA-Mutated Advanced Ovarian Cancer Treated with Three or More Lines of Chemotherapy/Olaparib for Advanced Ovarian Cancer with BRCA Mutation. *Clin. Cancer Res.* **2015**, *21*, 4257–4261. [[CrossRef](#)] [[PubMed](#)]
112. Caulfield, S.E.; Davis, C.C.; Byers, K.F. Olaparib: A novel therapy for metastatic breast cancer in patients with a BRCA1/2 mutation. *J. Adv. Pract. Oncol.* **2019**, *10*, 167. [[PubMed](#)]
113. Lagoja, I.M. Pyrimidine as constituent of natural biologically active compounds. *Chem. Biodivers.* **2005**, *2*, 1–50. [[CrossRef](#)]
114. Albratty, M.; Alhazmi, H.A. Novel pyridine and pyrimidine derivatives as promising anticancer agents: A review. *Arab. J. Chem.* **2022**, *15*, 103846. [[CrossRef](#)]
115. Fathalla, O.A.; Mohamed, N.A.; El-Serwy, W.S.; AbdelHamid, H.F.; El-Moez, A.; Sherein, I.; Soliman, A.-m.M. Synthesis of some new pyrimidine derivatives and evaluation of their anticancer and antibacterial activities. *Res. Chem. Intermed.* **2013**, *39*, 821–841. [[CrossRef](#)]
116. Ahmed, M.H.; El-Hashash, M.A.; Marzouk, M.I.; El-Naggar, A.M. Synthesis and antitumor activity of some nitrogen heterocycles bearing pyrimidine moiety. *J. Heterocycl. Chem.* **2020**, *57*, 3412–3427. [[CrossRef](#)]
117. Gupta, S.; Bartwal, G.; Singh, A.; Tanwar, J.; Khurana, J. Design, synthesis and biological evaluation of spiro-isoquinoline-pyrimidine derivatives as anticancer agents against MCF-7 cancer cell lines. *Results Chem.* **2022**, *4*, 100386. [[CrossRef](#)]
118. Al-Issa, S. Synthesis and anticancer activity of some fused pyrimidines and related heterocycles. *Saudi Pharm. J.* **2013**, *21*, 305–316. [[CrossRef](#)] [[PubMed](#)]
119. Osmaniye, D.; Hıdır, A.; Sağlık, B.N.; Levent, S.; Özkay, Y.; Kaplancıklı, Z.A. Synthesis of New Pyrimidine-Triazole Derivatives and Investigation of Their Anticancer Activities. *Chem. Biodivers.* **2022**, *19*, e202200216. [[CrossRef](#)]
120. Qin, W.-W.; Sang, C.-Y.; Zhang, L.-L.; Wei, W.; Tian, H.-Z.; Liu, H.-X.; Chen, S.-W.; Hui, L. Synthesis and biological evaluation of 2, 4-diaminopyrimidines as selective Aurora A kinase inhibitors. *Eur. J. Med. Chem.* **2015**, *95*, 174–184. [[CrossRef](#)] [[PubMed](#)]
121. Venturini Filho, E.; Pina, J.W.; Antoniazzi, M.K.; Loureiro, L.B.; Ribeiro, M.A.; Pinheiro, C.B.; Guimarães, C.J.; de Oliveira, F.C.; Pessoa, C.; Taranto, A.G. Synthesis, docking, machine learning and antiproliferative activity of the 6-ferrocene/heterocycle-2-aminopyrimidine and 5-ferrocene-1H-Pyrazole derivatives obtained by microwave-assisted Atwal reaction as potential anticancer agents. *Bioorg. Med. Chem. Lett.* **2021**, *48*, 128240. [[CrossRef](#)]
122. Mohi El-Deen, E.M.; Anwar, M.M.; El-Gwaad, A.A.A.; Karam, E.A.; El-Ashrey, M.K.; Kassab, R.R. Novel Pyridothienopyrimidine Derivatives: Design, Synthesis and Biological Evaluation as Antimicrobial and Anticancer Agents. *Molecules* **2022**, *27*, 803. [[CrossRef](#)] [[PubMed](#)]
123. Al-Anazi, M.; Khairuddean, M.; Al-Najjar, B.O.; Alidmat, M.M.; Kamal, N.N.S.N.M.; Muhamad, M. Synthesis, anticancer activity and docking studies of pyrazoline and pyrimidine derivatives as potential epidermal growth factor receptor (EGFR) inhibitors. *Arab. J. Chem.* **2022**, *15*, 103864. [[CrossRef](#)]
124. El-Metwally, S.A.; Abou-El-Regal, M.M.; Eissa, I.H.; Mehany, A.B.; Mahdy, H.A.; Elkady, H.; Elwan, A.; Elkaeed, E.B. Discovery of thieno [2, 3-d] pyrimidine-based derivatives as potent VEGFR-2 kinase inhibitors and anti-cancer agents. *Bioorg. Chem.* **2021**, *112*, 104947. [[CrossRef](#)]

125. Madia, V.N.; Nicolai, A.; Messore, A.; De Leo, A.; Ialongo, D.; Tudino, V.; Saccoliti, F.; De Vita, D.; Scipione, L.; Artico, M.; et al. Design, synthesis and biological evaluation of new pyrimidine derivatives as anticancer agents. *Molecules* **2021**, *26*, 771. [[CrossRef](#)]
126. Marella, A.; Tanwar, O.P.; Saha, R.; Ali, M.R.; Srivastava, S.; Akhter, M.; Shaquiquzzaman, M.; Alam, M.M. Quinoline: A versatile heterocyclic. *Saudi Pharm. J.* **2013**, *21*, 1–12. [[CrossRef](#)]
127. Hamdy, R.; Elseginy, S.A.; Ziedan, N.I.; Jones, A.T.; Westwell, A.D. New quinoline-based heterocycles as anticancer agents targeting bcl-2. *Molecules* **2019**, *24*, 1274. [[CrossRef](#)]
128. Jin, X.-Y.; Chen, H.; Li, D.-D.; Li, A.-L.; Wang, W.-Y.; Gu, W. Design, synthesis, and anticancer evaluation of novel quinoline derivatives of ursolic acid with hydrazide, oxadiazole, and thiadiazole moieties as potent MEK inhibitors. *J. Enzym. Inhib. Med. Chem.* **2019**, *34*, 955–972. [[CrossRef](#)] [[PubMed](#)]
129. Katariya, K.D.; Shah, S.R.; Reddy, D. Anticancer, antimicrobial activities of quinoline based hydrazone analogues: Synthesis, characterization and molecular docking. *Bioorg. Chem.* **2020**, *94*, 103406. [[CrossRef](#)] [[PubMed](#)]
130. George, R.F.; Samir, E.M.; Abdelhamed, M.N.; Abdel-Aziz, H.A.; Abbas, S.E. Synthesis and anti-proliferative activity of some new quinoline based 4, 5-dihydropyrazoles and their thiazole hybrids as EGFR inhibitors. *Bioorg. Chem.* **2019**, *83*, 186–197. [[CrossRef](#)] [[PubMed](#)]
131. Köprülü, T.K.; Ökten, S.; Atalay, V.E.; Tekin, Ş.; Çakmak, O. Biological activity and molecular docking studies of some new quinolines as potent anticancer agents. *Med. Oncol.* **2021**, *38*, 1–11. [[CrossRef](#)] [[PubMed](#)]
132. Ramya, P.S.; Guntuku, L.; Angapelly, S.; Karri, S.; Digwal, C.S.; Babu, B.N.; Naidu, V.; Kamal, A. Curcumin inspired 2-chloro/phenoxy quinoline analogues: Synthesis and biological evaluation as potential anticancer agents. *Bioorg. Med. Chem. Lett.* **2018**, *28*, 892–898. [[CrossRef](#)]
133. Upadhyay, K.D.; Dodia, N.M.; Khunt, R.C.; Chaniara, R.S.; Shah, A.K. Synthesis and biological screening of pyrano [3, 2-c] quinoline analogues as anti-inflammatory and anticancer agents. *ACS Med. Chem. Lett.* **2018**, *9*, 283–288. [[CrossRef](#)] [[PubMed](#)]
134. Hagra, M.; El Deeb, M.A.; Elzahabi, H.S.; Elkaeed, E.B.; Mehany, A.B.; Eissa, I.H. Discovery of new quinolines as potent colchicine binding site inhibitors: Design, synthesis, docking studies, and anti-proliferative evaluation. *J. Enzym. Inhib. Med. Chem.* **2021**, *36*, 640–658. [[CrossRef](#)]
135. Mirzaei, S.; Hadizadeh, F.; Eivand, F.; Mosaffa, F.; Ghodsi, R. Synthesis, structure-activity relationship and molecular docking studies of novel quinoline-chalcone hybrids as potential anticancer agents and tubulin inhibitors. *J. Mol. Struct.* **2020**, *1202*, 127310. [[CrossRef](#)]
136. Chate, A.V.; Kamdi, S.P.; Bhagat, A.N.; Jadhav, C.K.; Nipte, A.; Sarkate, A.P.; Tiwari, S.V.; Gill, C.H. Design, Synthesis and SAR Study of Novel Spiro [Pyrimido[5,4-b]Quinoline-10,5'-Pyrrolo[2,3-d]Pyrimidine] Derivatives as Promising Anticancer Agents. *J. Heterocycl. Chem.* **2018**, *55*, 2297–2302. [[CrossRef](#)]
137. Ziarani, G.; Moradi, R.; Lashgari, N.; Kruger, H.G. *Metal-Free Synthetic Organic Dyes*; Elsevier: Amsterdam, The Netherlands, 2018.
138. Murali, K.; Sparkes, H.A.; Prasad, K.J.R. Synthesis of hetero annulated isoxazolo-, pyrido- and pyrimido carbazoles: Screened for in vitro antitumor activity and structure activity relationships, a novel 2-amino-4-(3'-bromo-4'-methoxyphenyl)-8-chloro-11H-pyrimido [4, 5-a] carbazole as an antitumor agent. *Eur. J. Med. Chem.* **2017**, *128*, 319–331.
139. Wang, Y.-Q.; Li, X.-H.; He, Q.; Chen, Y.; Xie, Y.-Y.; Ding, J.; Miao, Z.-H.; Yang, C.-H. Design, synthesis and biological evaluation of substituted 11H-benzo [a] carbazole-5-carboxamides as novel antitumor agents. *Eur. J. Med. Chem.* **2011**, *46*, 5878–5884. [[CrossRef](#)]
140. Debray, J.; Zeghida, W.; Baldeyrou, B.; Mahieu, C.; Lansiaux, A.; Demeunynck, M. Montmorillonite K-10 catalyzed cyclization of N-ethoxycarbonyl-N'-arylguanidines: Access to pyrimido [4,5-c] carbazole and pyrimido [5,4-b] indole derivatives. *Bioorg. Med. Chem. Lett.* **2010**, *20*, 4244–4247. [[CrossRef](#)] [[PubMed](#)]
141. Sun, L.; Wu, Y.; Liu, Y.; Chen, X.; Hu, L. Novel carbazole sulfonamide derivatives of antitumor agent: Synthesis, antiproliferative activity and aqueous solubility. *Bioorg. Med. Chem. Lett.* **2017**, *27*, 261–265. [[CrossRef](#)] [[PubMed](#)]
142. Arya, K.R.; Rajendra Prasad, K.J. Rational eco-compatible synthesis and biological screening of new highly functionalized pyrido [2, 3-a] carbazole derivatives: A novel class of antioxidant and anticancer agents. *Synth. Commun.* **2018**, *48*, 1465–1481. [[CrossRef](#)]
143. Padmaja, P.; Rao, G.K.; Indrasena, A.; Reddy, B.V.S.; Patel, N.; Shaik, A.B.; Reddy, N.; Dubey, P.K.; Bhadra, M.P. Synthesis and biological evaluation of novel pyrano [3,2-c] carbazole derivatives as anti-tumor agents inducing apoptosis via tubulin polymerization inhibition. *Org. Biomol. Chem.* **2015**, *13*, 1404–1414. [[CrossRef](#)]
144. Patel, M.; Pandey, N.; Timaniya, J.; Parikh, P.; Chauhan, A.; Jain, N.; Patel, K. Coumarin-carbazole based functionalized pyrazolines: Synthesis, characterization, anticancer investigation and molecular docking. *RSC Adv.* **2021**, *11*, 27627–27644. [[CrossRef](#)]
145. Huang, W.; Gao, Z.; Zhang, Z.; Fang, W.; Wang, Z.; Wan, Z.; Shi, L.; Wang, K.; Ke, S. Selective and effective anticancer agents: Synthesis, biological evaluation and structure-activity relationships of novel carbazole derivatives. *Bioorg. Chem.* **2021**, *113*, 104991. [[CrossRef](#)]
146. Vairavelu, L.; Zeller, M.; Prasad, K.R. Solvent-free synthesis of heteroannulated carbazoles: A novel class of anti-tumor agents. *Bioorg. Chem.* **2014**, *54*, 12–20. [[CrossRef](#)]
147. Altaf, A.A.; Shahzad, A.; Gul, Z.; Rasool, N.; Badshah, A.; Lal, B.; Khan, E. A review on the medicinal importance of pyridine derivatives. *J. Drug Des. Med. Chem.* **2015**, *1*, 1–11.
148. Gomha, S.M.; Abdelrazek, F.M.; Abdelrahman, A.H.; Metz, P. Synthesis of some new pyridine-based heterocyclic compounds with anticipated antitumor activity. *J. Heterocycl. Chem.* **2018**, *55*, 1729–1737. [[CrossRef](#)]

149. Fayed, E.A.; Sabour, R.; Harras, M.F.; Mehany, A. Design, synthesis, biological evaluation and molecular modeling of new coumarin derivatives as potent anticancer agents. *Med. Chem. Res.* **2019**, *28*, 1284–1297. [[CrossRef](#)]
150. Nagender, P.; Kumar, R.N.; Reddy, G.M.; Swaroop, D.K.; Poornachandra, Y.; Kumar, C.G.; Narsaiah, B. Synthesis of novel hydrazone and azole functionalized pyrazolo [3, 4-b] pyridine derivatives as promising anticancer agents. *Bioorg. Med. Chem. Lett.* **2016**, *26*, 4427–4432. [[CrossRef](#)] [[PubMed](#)]
151. El-Naggar, M.; Almahli, H.; Ibrahim, H.S.; Eldehna, W.M.; Abdel-Aziz, H.A. Pyridine-ureas as potential anticancer agents: Synthesis and in vitro biological evaluation. *Molecules* **2018**, *23*, 1459. [[CrossRef](#)]
152. Dinda, J.; Nandy, A.; Rana, B.K.; Bertolasi, V.; Saha, K.D.; Bielawski, C.W. Cytotoxicity of silver (I), gold (I) and gold (III) complexes of a pyridine wingtip substituted annelated N-heterocyclic carbene. *RSC Adv.* **2014**, *4*, 60776–60784. [[CrossRef](#)]
153. El-Gohary, N.; Gabr, M.; Shaaban, M. Synthesis, molecular modeling and biological evaluation of new pyrazolo [3, 4-b] pyridine analogs as potential antimicrobial, antitumor-sensing and anticancer agents. *Bioorg. Chem.* **2019**, *89*, 102976. [[CrossRef](#)] [[PubMed](#)]
154. Sangani, C.B.; Makawana, J.A.; Zhang, X.; Teraiya, S.B.; Lin, L.; Zhu, H.-L. Design, synthesis and molecular modeling of pyrazole–quinoline–pyridine hybrids as a new class of antimicrobial and anticancer agents. *Eur. J. Med. Chem.* **2014**, *76*, 549–557. [[CrossRef](#)]
155. Elzahabi, H.S. Synthesis, characterization of some benzazoles bearing pyridine moiety: Search for novel anticancer agents. *Eur. J. Med. Chem.* **2011**, *46*, 4025–4034. [[CrossRef](#)]
156. Zheng, S.; Zhong, Q.; Mottamal, M.; Zhang, Q.; Zhang, C.; LeMelle, E.; McFerrin, H.; Wang, G. Design, synthesis, and biological evaluation of novel pyridine-bridged analogues of combretastatin-A4 as anticancer agents. *J. Med. Chem.* **2014**, *57*, 3369–3381. [[CrossRef](#)] [[PubMed](#)]
157. Abbas, I.; Gomha, S.; Elaasser, M.; Bauomi, M. Synthesis and biological evaluation of new pyridines containing imidazole moiety as antimicrobial and anticancer agents. *Turk. J. Chem.* **2015**, *39*, 334–346. [[CrossRef](#)]
158. Ivasechko, I.; Yushyn, I.; Roszczenko, P.; Senkiv, J.; Finiuk, N.; Lesyk, D.; Holota, S.; Czarnomysy, R.; Klyuchivska, O.; Khylyuk, D. Development of Novel Pyridine-Thiazole Hybrid Molecules as Potential Anticancer Agents. *Molecules* **2022**, *27*, 6219. [[CrossRef](#)]
159. Debus, H. Ueber die einwirkung des ammoniaks auf glyoxal. *Ann. Chem. Pharm.* **1858**, *107*, 199–208. [[CrossRef](#)]
160. Liu, L.-X.; Wang, X.-Q.; Zhou, B.; Yang, L.-J.; Li, Y.; Zhang, H.-B.; Yang, X.-D. Synthesis and antitumor activity of novel N-substituted carbazole imidazolium salt derivatives. *Sci. Rep.* **2015**, *5*, 1–20. [[CrossRef](#)] [[PubMed](#)]
161. Ruzi, Z.; Nie, L.; Bozorov, K.; Zhao, J.; Aisa, H.A. Synthesis and anticancer activity of ethyl 5-amino-1-N-substituted-imidazole-4-carboxylate building blocks. *Arch. Pharm.* **2021**, *354*, 2000470. [[CrossRef](#)] [[PubMed](#)]
162. Singh, R.; Kumar, R.; Pandrala, M.; Kaur, P.; Gupta, S.; Tailor, D.; Malhotra, S.V.; Salunke, D.B. Facile synthesis of C6-substituted benz [4,5] imidazo [1,2-a] quinoxaline derivatives and their anticancer evaluation. *Arch. Der Pharm.* **2021**, *354*, 2000393. [[CrossRef](#)]
163. Yang, X.-D.; Wan, W.-C.; Deng, X.-Y.; Li, Y.; Yang, L.-J.; Li, L.; Zhang, H.-B. Design, synthesis and cytotoxic activities of novel hybrid compounds between 2-phenylbenzofuran and imidazole. *Bioorg. Med. Chem. Lett.* **2012**, *22*, 2726–2729. [[CrossRef](#)]
164. Song, W.-J.; Yang, X.-D.; Zeng, X.-H.; Xu, X.-L.; Zhang, G.-L.; Zhang, H.-B. Synthesis and cytotoxic activities of novel hybrid compounds of imidazole scaffold-based 2-substituted benzofurans. *RSC Adv.* **2012**, *2*, 4612–4615. [[CrossRef](#)]
165. Khayyat, A.N.; Mohamed, K.O.; Malebari, A.M.; El-Malah, A. Design, Synthesis, and Antiproliferative Activities of Novel Substituted Imidazole-Thione Linked Benzotriazole Derivatives. *Molecules* **2021**, *26*, 5983. [[CrossRef](#)]
166. Singh, A.K.; Kumar, A.; Singh, H.; Sonawane, P.; Paliwal, H.; Thareja, S.; Pathak, P.; Grishina, M.; Jaremko, M.; Emwas, A.-H. Concept of hybrid drugs and recent advancements in anticancer hybrids. *Pharmaceuticals* **2022**, *15*, 1071. [[CrossRef](#)]
167. Kalra, S.; Joshi, G.; Kumar, M.; Arora, S.; Kaur, H.; Singh, S.; Munshi, A.; Kumar, R. Anticancer potential of some imidazole and fused imidazole derivatives: Exploring the mechanism via epidermal growth factor receptor (EGFR) inhibition. *RSC Med. Chem.* **2020**, *11*, 923–939. [[CrossRef](#)]
168. Taheri, B.; Taghavi, M.; Zarei, M.; Chamkouri, N.; Mojaddami, A. Imidazole and carbazole derivatives as potential anticancer agents: Molecular docking studies and cytotoxic activity evaluation. *Bul. Chem. Soc. Ethiop.* **2020**, *34*, 377–384. [[CrossRef](#)]
169. Oskuei, S.R.; Mirzaei, S.; Jafari-Nik, M.R.; Hadizadeh, F.; Eisvand, F.; Mosaffa, F.; Ghodsi, R. Design, synthesis and biological evaluation of novel imidazole-chalcone derivatives as potential anticancer agents and tubulin polymerization inhibitors. *Bioorg. Chem.* **2021**, *112*, 104904. [[CrossRef](#)] [[PubMed](#)]
170. Wang, X.-Q.; Liu, L.-X.; Li, Y.; Sun, C.-J.; Chen, W.; Li, L.; Zhang, H.-B.; Yang, X.-D. Design, synthesis and biological evaluation of novel hybrid compounds of imidazole scaffold-based 2-benzylbenzofuran as potent anticancer agents. *Eur. J. Med. Chem.* **2013**, *62*, 111–121. [[CrossRef](#)]
171. Du, Q.R.; Li, D.D.; Pi, Y.Z.; Li, J.R.; Sun, J.; Fang, F.; Zhong, W.Q.; Gong, H.B.; Zhu, H.L. Novel 1,3,4-oxadiazole thioether derivatives targeting thymidylate synthase as dual anticancer/antimicrobial agents. *Bioorg. Med. Chem.* **2013**, *21*, 2286–2297. [[CrossRef](#)] [[PubMed](#)]
172. Shrivastava, N.; Naim, M.J.; Alam, M.J.; Nawaz, F.; Ahmed, S.; Alam, O. Benzimidazole scaffold as anticancer agent: Synthetic approaches and structure–activity relationship. *Arch. Pharm.* **2017**, *350*, e201700040. [[CrossRef](#)] [[PubMed](#)]
173. Rawat, S.; Ghate, M. Potential Anticancer Agents From Benzimidazole Derivatives. *Nveo-Nat. Volatiles Essent. Oils J. NVEO* **2021**, *8*, 4109–4120.

174. Nicolai, A.; Madia, V.N.; Messori, A.; De Vita, D.; De Leo, A.; Ialongo, D.; Tudino, V.; Tortorella, E.; Scipione, L.; Taurone, S.; et al. Anti-Tumoral Effects of a (1 H-Pyrrol-1-yl) Methyl-1 H-Benzimidazole Carbamate Ester Derivative on Head and Neck Squamous Carcinoma Cell Lines. *Pharmaceuticals* **2021**, *14*, 564. [[CrossRef](#)]
175. Shao, K.P.; Zhang, X.Y.; Chen, P.J.; Xue, D.Q.; He, P.; Ma, L.Y.; Zheng, J.X.; Zhang, Q.R.; Liu, H.M. Synthesis and biological evaluation of novel pyrimidine-benzimidazol hybrids as potential anticancer agents. *Bioorg. Med. Chem. Lett.* **2014**, *24*, 3877–3881. [[CrossRef](#)] [[PubMed](#)]
176. Husain, A.; Rashid, M.; Shaharyar, M.; Siddiqui, A.A.; Mishra, R. Benzimidazole clubbed with triazolo-thiadiazoles and triazolo-thiadiazines: New anticancer agents. *Eur. J. Med. Chem.* **2013**, *62*, 785–798. [[CrossRef](#)]
177. Sana, S.; Reddy, V.G.; Reddy, T.S.; Tokala, R.; Kumar, R.; Bhargava, S.K.; Shankaraiah, N. Cinnamide derived pyrimidine-benzimidazole hybrids as tubulin inhibitors: Synthesis, in silico and cell growth inhibition studies. *Bioorg. Chem.* **2021**, *110*, 104765. [[CrossRef](#)]
178. Sireesha, R.; Sreenivasulu, R.; Chandrasekhar, C.; Jadav, S.S.; Pavani, Y.; Rao, M.V.B.; Subbarao, M. Design, synthesis, anti-cancer evaluation and binding mode studies of benzimidazole/benzoxazole linked β -carboline derivatives. *J. Mol. Struct.* **2021**, *1226*, 129351. [[CrossRef](#)]
179. Shi, L.; Wu, T.-T.; Wang, Z.; Xue, J.-Y.; Xu, Y.-G. Discovery of quinazolin-4-amines bearing benzimidazole fragments as dual inhibitors of c-Met and VEGFR-2. *Bioorg. Med. Chem.* **2014**, *22*, 4735–4744. [[CrossRef](#)] [[PubMed](#)]
180. Romero-Castro, A.; León-Rivera, I.; Avila-Rojas, L.C.; Navarrete-Vázquez, G.; Nieto-Rodríguez, A. Synthesis and preliminary evaluation of selected 2-aryl-5(6)-nitro-1H-benzimidazole derivatives as potential anticancer agents. *Arch. Pharm. Chemi.* **2011**, *34*, 181–189. [[CrossRef](#)] [[PubMed](#)]
181. Sivaramakarthykeyan, R.; Iniyaval, S.; Saravanan, V.; Lim, W.-M.; Mai, C.-W.; Ramalingan, C. Molecular hybrids integrated with benzimidazole and pyrazole structural motifs: Design, synthesis, biological evaluation, and molecular docking studies. *ACS Omega* **2020**, *5*, 10089–10098. [[CrossRef](#)] [[PubMed](#)]
182. Perin, N.; Hok, L.; Beč, A.; Persoons, L.; Vanstreels, E.; Daelemans, D.; Vianello, R.; Hranjec, M. N-substituted benzimidazole acrylonitriles as in vitro tubulin polymerization inhibitors: Synthesis, biological activity and computational analysis. *Eur. J. Med. Chem.* **2021**, *211*, 113003. [[CrossRef](#)] [[PubMed](#)]
183. Wu, L.-T.; Jiang, Z.; Shen, J.-J.; Yi, H.; Zhan, Y.-C.; Sha, M.-Q.; Wang, Z.; Xue, S.-T.; Li, Z.-R. Design, synthesis and biological evaluation of novel benzimidazole-2-substituted phenyl or pyridine propyl ketene derivatives as antitumour agents. *Eur. J. Med. Chem.* **2016**, *114*, 328–336. [[CrossRef](#)]
184. Holiyachi, M.; Shastri, S.L.; Chougala, B.M.; Shastri, L.A.; Joshi, S.D.; Dixit, S.R.; Nagarajaiah, H.; Sunagar, V.A. Design, Synthesis and Structure-Activity Relationship Study of Coumarin Benzimidazole Hybrid as Potent Antibacterial and Anticancer Agents. *Chem. Sel.* **2016**, *1*, 4638–4644. [[CrossRef](#)]
185. Tahlan, S.; Ramasamy, K.; Lim, S.M.; Shah, S.A.A.; Mani, V.; Narasimhan, B. Design, synthesis and therapeutic potential of 3-(2-(1H-benzo [d] imidazol-2-ylthio) acetamido)-N-(substituted phenyl) benzamide analogues. *Chem. Cent. J.* **2018**, *12*, 1–12. [[CrossRef](#)] [[PubMed](#)]
186. Yuan, X.; Yang, Q.; Liu, T.; Li, K.; Liu, Y.; Zhu, C.; Zhang, Z.; Li, L.; Zhang, C.; Xie, M. Design, synthesis and in vitro evaluation of 6-amide-2-aryl benzoxazole/benzimidazole derivatives against tumor cells by inhibiting VEGFR-2 kinase. *Eur. J. Med. Chem.* **2019**, *179*, 147–165. [[CrossRef](#)] [[PubMed](#)]
187. Zhou, C.; Gan, L.; Zhang, Y.; Zhang, F.; Wang, G.; Jin, L.; Geng, R. Review on supermolecules as chemical drugs. *Sci. China Ser. B Chem.* **2009**, *52*, 415–458. [[CrossRef](#)]
188. Juan-Juan, C.; Yan, W.; Hui-Zhen, Z.; Cheng-He, Z.; Rong-Xia, G.; Qing-Gang, J. Recent advances in researches of triazole-based supramolecular chemistry and medicinal drugs. *Chem. J. Chin. Univ. Chin.* **2011**, *32*, 1970–1985.
189. Kurumurthy, C.; Rao, P.S.; Rao, P.S.; Narsaiah, B.; Velatooru, L.; Pamanji, R.; Rao, J.V. Synthesis of novel alkyltriazole tagged pyrido [2, 3-d] pyrimidine derivatives and their anticancer activity. *Eur. J. Med. Chem.* **2011**, *46*, 3462–3468. [[CrossRef](#)]
190. Al-Blewi, F.; Shaikh, S.A.; Naqvi, A.; Aljohani, F.; Aouad, M.R.; Ihmaid, S.; Rezki, N. Design and synthesis of novel imidazole derivatives possessing triazole pharmacophore with potent anticancer activity, and in silico ADMET with GSK-3 β molecular docking investigations. *Int. J. Mol. Sci.* **2021**, *22*, 1162. [[CrossRef](#)] [[PubMed](#)]
191. Bozorov, K.; Zhao, J.; Aisa, H.A. 1, 2, 3-Triazole-containing hybrids as leads in medicinal chemistry: A recent overview. *Bioorg. Med. Chem.* **2019**, *27*, 3511–3531. [[CrossRef](#)] [[PubMed](#)]
192. Djemoui, A.; Naouri, A.; Ouahrani, M.R.; Djemoui, D.; Lahcene, S.; Lahrech, M.B.; Boukenna, L.; Albuquerque, H.M.; Saher, L.; Rocha, D.H. A step-by-step synthesis of triazole-benzimidazole-chalcone hybrids: Anticancer activity in human cells+. *J. Mol. Struct.* **2020**, *1204*, 127487. [[CrossRef](#)]
193. Suryanarayana, K.; Robert, A.R.; Kerru, N.; Pooventhiran, T.; Thomas, R.; Maddila, S.; Jonnalagadda, S.B. Design, synthesis, anticancer activity and molecular docking analysis of novel dinitrophenylpyrazole bearing 1, 2, 3-triazoles. *J. Mol. Struct.* **2021**, *1243*, 130865. [[CrossRef](#)]
194. Chandrashekar, M.; Nayak, V.L.; Ramakrishna, S.; Mallavadhani, U.V. Novel triazole hybrids of myrrhanone C, a natural polygodane triterpene: Synthesis, cytotoxic activity and cell based studies. *Eur. J. Med. Chem.* **2016**, *114*, 293–307. [[CrossRef](#)] [[PubMed](#)]

195. Najafi, Z.; Mahdavi, M.; Safavi, M.; Saeedi, M.; Alinezhad, H.; Pordeli, M.; Kabudanian Ardestani, S.; Shafiee, A.; Foroumadi, A.; Akbarzadeh, T. Synthesis and In Vitro Cytotoxic Activity of Novel Triazole-Isoxazole Derivatives. *J. Heterocycl. Chem.* **2015**, *52*, 1743–1747. [[CrossRef](#)]
196. Duan, Y.C.; Ma, Y.C.; Zhang, E.; Shi, X.J.; Wang, M.M.; Ye, X.W.; Liu, H.M. Design and synthesis of novel 1,2,3-triazole-dithiocarbamate hybrids as potential anticancer agents. *Eur. J. Med. Chem.* **2013**, *62*, 11–19. [[CrossRef](#)]
197. Kumbhare, R.M.; Dadmal, T.L.; Ramaiah, M.J.; Kishore, K.S.; Pushpa Valli, S.N.; Tiwari, S.K.; Appalanaidu, K.; Rao, Y.K.; Bhadra, M.P. Synthesis and anticancer evaluation of novel triazole linked N-(pyrimidin-2-yl)benzo[d]thiazol-2-amine derivatives as inhibitors of cell survival proteins and inducers of apoptosis in MCF-7 breast cancer cells. *Bioorg. Med. Chem. Lett.* **2015**, *25*, 654–658. [[CrossRef](#)]
198. Ma, L.Y.; Wang, B.; Pang, L.P.; Zhang, M.; Wang, S.Q.; Zheng, Y.C.; Shao, K.P.; Xue, D.Q.; Liu, H.M. Design and synthesis of novel 1,2,3-triazole-pyrimidine-urea hybrids as potential anticancer agents. *Sci. Rep.* **2015**, *25*, 1124–1128. [[CrossRef](#)]
199. Bush, K.; Bradford, P.A. β -Lactams and β -Lactamase Inhibitors: An Overview. *Cold Spring Harb. Perspect. Med.* **2016**, *6*, 1–22. [[CrossRef](#)] [[PubMed](#)]
200. Banik, I.; Becker, F.F.; Banik, B.K. Stereoselective synthesis of β -lactams with polyaromatic imines: Entry to new and novel anticancer agents. *J. Med. Chem.* **2003**, *46*, 12–15. [[CrossRef](#)] [[PubMed](#)]
201. Borazjani, N.; Behzadi, M.; Dadkhah Aseman, M.; Jarrahpour, A.; Rad, J.A.; Kianpour, S.; Iraj, A.; Nabavizadeh, S.M.; Ghanbari, M.M.; Batta, G. Cytotoxicity, anticancer, and antioxidant properties of mono and bis-naphthalimido β -lactam conjugates. *Med. Chem. Res.* **2020**, *29*, 1355–1375. [[CrossRef](#)]
202. Payili, N.; Yennam, S.; Rekula, S.R.; Naidu, C.G.; Bobde, Y.; Ghosh, B. Design, Synthesis, and Evaluation of the Anticancer Properties of Novel Quinone Bearing Carbamyl β -Lactam Hybrids. *J. Heterocycl. Chem.* **2018**, *55*, 1358–1365. [[CrossRef](#)]
203. Ranjbari, S.; Behzadi, M.; Sepehri, S.; Dadkhah Aseman, M.; Jarrahpour, A.; Mohkam, M.; Ghasemi, Y.; Reza Akbarizadeh, A.; Kianpour, S.; Atioğlu, Z.; et al. Investigations of antiproliferative and antioxidant activity of β -lactam morpholino-1,3,5-triazine hybrids. *Bioorg. Med. Chem.* **2020**, *28*, 115408. [[CrossRef](#)] [[PubMed](#)]
204. Olazaran, F.n.E.; Rivera, G.; Pérez-Vázquez, A.M.; Morales-Reyes, C.M.; Segura-Cabrera, A.; Balderas-Rentería, I. Biological Evaluation in vitro and in silico of Azetidino-2-one Derivatives as Potential Anticancer Agents. *ACS Med. Chem. Lett.* **2017**, *8*, 32–37. [[CrossRef](#)]
205. Rashidi, M.; Islami, M.R.; Esmaili-Mahani, S. Design and stereoselective synthesis of novel β -lactone and β -lactams as potent anticancer agents on breast cancer cells. *Tetrahedron* **2018**, *74*, 835–841. [[CrossRef](#)]
206. Fu, D.-J.; Fu, L.; Liu, Y.-C.; Wang, J.-W.; Wang, Y.-Q.; Han, B.-K.; Li, X.-R.; Zhang, C.; Li, F.; Song, J. Structure-activity relationship studies of β -lactam-azide analogues as orally active antitumor agents targeting the tubulin colchicine site. *Sci. Rep.* **2017**, *7*, 1–12. [[CrossRef](#)]
207. Gupta, A.; Halve, A. [Beta]-lactams: A mini review of their biological activity. *Int. J. Pharm. Sci. Res.* **2015**, *6*, 978.
208. Banik, B.K.; Banik, I.; Becker, F.F. Asymmetric synthesis of anticancer β -lactams via Staudinger reaction: Utilization of chiral ketene from carbohydrate. *Eur. J. Med. Chem.* **2010**, *45*, 846–848. [[CrossRef](#)]
209. Carr, M.; Greene, L.M.; Knox, A.J.; Lloyd, D.G.; Zisterer, D.M.; Meegan, M.J. Lead identification of conformationally restricted β -lactam type combretastatin analogues: Synthesis, antiproliferative activity and tubulin targeting effects. *Eur. J. Med. Chem.* **2010**, *45*, 5752–5766. [[CrossRef](#)]
210. Higashio, Y.; Shoji, T. Heterocyclic compounds such as pyrrole, pyridines, pyrrolidine, piperidine, indole, imidazol and pyrazines. *Appl. Catal. A Gen.* **2004**, *260*, 251–259. [[CrossRef](#)]
211. Singla, R.; Prakash, K.; Gupta, K.B.; Upadhyay, S.; Dhiman, M.; Jaitak, V. Identification of novel indole based heterocycles as selective estrogen receptor modulator. *Bioorg. Chem.* **2018**, *79*, 72–88. [[CrossRef](#)]
212. Cihan-Üstündağ, G.; Şatana, D.; Özhan, G.; Çapan, G. Indole-based hydrazide-hydrazones and 4-thiazolidinones: Synthesis and evaluation as antitubercular and anticancer agents. *J. Enzym. Inhib. Med. Chem.* **2016**, *31*, 369–380. [[CrossRef](#)] [[PubMed](#)]
213. He, Z.; Qiao, H.; Yang, F.; Zhou, W.; Gong, Y.; Zhang, X.; Wang, H.; Zhao, B.; Ma, L.; Liu, H.-m. Novel thiosemicarbazone derivatives containing indole fragment as potent and selective anticancer agent. *Eur. J. Med. Chem.* **2019**, *184*, 111764. [[CrossRef](#)] [[PubMed](#)]
214. Prakash, B.; Amuthavalli, A.; Edison, D.; Sivaramkumar, M.; Velmurugan, R. Novel indole derivatives as potential anticancer agents: Design, synthesis and biological screening. *Med. Chem. Res.* **2018**, *27*, 321–331. [[CrossRef](#)]
215. Ali, I.; Mukhtar, S.D.; Hsieh, M.F.; Allothman, Z.A.; Alwarthan, A. Facile synthesis of indole heterocyclic compounds based micellar nano anti-cancer drugs. *RSC Adv.* **2018**, *8*, 37905–37914. [[CrossRef](#)] [[PubMed](#)]
216. Chen, K.; Zhang, Y.L.; Fan, J.; Ma, X.; Qin, Y.J.; Zhu, H.L. Novel nicotinoyl pyrazoline derivatives bearing N-methyl indole moiety as antitumor agents: Design, synthesis and evaluation. *Eur. J. Med. Chem.* **2018**, *156*, 722–737. [[CrossRef](#)]
217. Lafayette, E.A.; de Almeida, S.M.V.; Cavalcanti Santos, R.V.; de Oliveira, J.F.; Amorim, C.; da Silva, R.M.F.; Pitta, M.; Pitta, I.D.R.; de Moura, R.O.; de Carvalho Júnior, L.B.; et al. Synthesis of novel indole derivatives as promising DNA-binding agents and evaluation of antitumor and antitopoisomerase I activities. *Eur. J. Med. Chem.* **2017**, *136*, 511–522. [[CrossRef](#)]
218. Song, Y.; Feng, S.; Feng, J.; Dong, J.; Yang, K.; Liu, Z.; Qiao, X. Synthesis and biological evaluation of novel pyrazoline derivatives containing indole skeleton as anti-cancer agents targeting topoisomerase II. *Eur. J. Med. Chem.* **2020**, *200*, 112459. [[CrossRef](#)]

219. Bakherad, Z.; Safavi, M.; Sepehri, S.; Fassihi, A.; Sadeghi-Aliabadi, H.; Bakherad, M.; Rastegar, H.; Larijani, B.; Saghaie, L.; Mahdavi, M. Preparation of some novel imidazopyridine derivatives of indole as anticancer agents: One-pot multicomponent synthesis, biological evaluation and docking studies. *Res. Chem. Intermed.* **2019**, *45*, 5261–5290. [[CrossRef](#)]
220. Eldehna, W.M.; Hassan, G.S.; Al-Rashood, S.T.; Alkahtani, H.M.; Almehizia, A.A.; Al-Ansary, G.H. Marine-Inspired Bis-indoles Possessing Antiproliferative Activity against Breast Cancer; Design, Synthesis, and Biological Evaluation. *Mar. Drugs* **2020**, *18*, 190. [[CrossRef](#)] [[PubMed](#)]
221. Sreenivasulu, R.; Tej, M.B.; Jadav, S.S.; Sujitha, P.; Kumar, C.G.; Raju, R.R. Synthesis, anticancer evaluation and molecular docking studies of 2,5-bis(indolyl)-1,3,4-oxadiazoles, Nortopsentin analogues. *J. Mol. Struct.* **2020**, *1208*, 127875. [[CrossRef](#)]
222. Naim, M.J.; Alam, O.; Nawaz, F.; Alam, M.J.; Alam, P. Current status of pyrazole and its biological activities. *J. Pharm. Bioallied Sci.* **2016**, *8*, 2–17. [[PubMed](#)]
223. Abdelgawad, N.; Ismail, M.F.; Hekal, M.H.; Marzouk, M.I. Design, synthesis, and evaluation of some novel heterocycles bearing pyrazole moiety as potential anticancer agents. *J. Heterocycl. Chem.* **2019**, *56*, 1771–1779. [[CrossRef](#)]
224. Nassar, I.F.; El Farargy, A.F.; Abdelrazek, F.M.; Ismail, N.S. Design, synthesis and anticancer evaluation of novel pyrazole, pyrazolo [3, 4-d] pyrimidine and their glycoside derivatives. *Nucleosides Nucleotides Nucleic Acids* **2017**, *36*, 275–291. [[CrossRef](#)] [[PubMed](#)]
225. El-Sayed, A.A.; Amr, A.E.E.; El-Ziaty, A.K.; Elsayed, E.A. Cytotoxic Effects of Newly Synthesized Heterocyclic Candidates Containing Nicotinonitrile and Pyrazole Moieties on Hepatocellular and Cervical Carcinomas. *Molecules* **2019**, *24*, 1965. [[CrossRef](#)]
226. Omran, D.M.; Ghaly, M.A.; El-Messery, S.M.; Badria, F.A.; Abdel-Latif, E.; Shehata, I.A. Targeting hepatocellular carcinoma: Synthesis of new pyrazole-based derivatives, biological evaluation, DNA binding, and molecular modeling studies. *Bioorg. Chem.* **2019**, *88*, 102917. [[CrossRef](#)] [[PubMed](#)]
227. Zhu, S.-L.; Wu, Y.; Liu, C.-J.; Wei, C.-Y.; Tao, J.-C.; Liu, H.-M. Design and stereoselective synthesis of novel isosteviol-fused pyrazolines and pyrazoles as potential anticancer agents. *Eur. J. Med. Chem.* **2013**, *65*, 70–82. [[CrossRef](#)] [[PubMed](#)]
228. Alam, R.; Alam, M.A.; Panda, A.K. Design, Synthesis, and Cytotoxicity Evaluation of 3-(5-(3-(aryl)-1-phenyl-1H-pyrazol-4-yl)-1-phenyl-4, 5-dihydro-1H-pyrazol-3-yl) pyridine and 5-(3-(aryl)-1-phenyl-1H-pyrazol-4-yl)-3-(pyridin-3-yl)-4, 5-dihydropyrazole-1-carbaldehyde Derivatives as Potential Anticancer Agents. *J. Heterocycl. Chem.* **2017**, *54*, 1812–1821.
229. Harras, M.F.; Sabour, R. Design, synthesis and biological evaluation of novel 1,3,4-trisubstituted pyrazole derivatives as potential chemotherapeutic agents for hepatocellular carcinoma. *Bioorg. Chem.* **2018**, *78*, 149–157. [[CrossRef](#)] [[PubMed](#)]
230. Liu, D.C.; Gao, M.J.; Huo, Q.; Ma, T.; Wang, Y.; Wu, C.Z. Design, synthesis, and apoptosis-promoting effect evaluation of novel pyrazole with benzo[d]thiazole derivatives containing aminoguanidine units. *J. Enzym. Inhib. Med. Chem.* **2019**, *34*, 829–837. [[CrossRef](#)] [[PubMed](#)]
231. Afifi, O.S.; Shaaban, O.G.; Abd El Razik, H.A.; Shams El-Dine, S.E.-D.A.; Ashour, F.A.; El-Tombary, A.A.; Abu-Serie, M.M. Synthesis and biological evaluation of purine-pyrazole hybrids incorporating thiazole, thiazolidinone or rhodanine moiety as 15-LOX inhibitors endowed with anticancer and antioxidant potential. *Bioorg. Chem.* **2019**, *87*, 821–837. [[CrossRef](#)] [[PubMed](#)]
232. Bakhotmah, D.A.; Ali, T.E.; Assiri, M.A.; Yahia, I.S. Synthesis of Some Novel 2-[Pyrano[2,3-c]Pyrazoles-4-Ylidene]Malononitrile Fused with Pyrazole, Pyridine, Pyrimidine, Diazepine, Chromone, Pyrano[2,3-c]Pyrazole and Pyrano[2,3-d]Pyrimidine Systems as Anticancer Agents. *Polycycl. Aromat. Compd.* **2022**, *42*, 2136–2150. [[CrossRef](#)]
233. Hameed, A.; Al-Rashida, M.; Uroos, M.; Ali, S.A.; Arshia Ishtiaq, M.; Khan, K.M. Quinazoline and quinazolinone as important medicinal scaffolds: A comparative patent review (2011–2016). *Expert Opin. Ther. Pat.* **2018**, *28*, 281–297. [[CrossRef](#)]
234. Ghorab, M.M.; Alsaied, M.S.; Al-Dosari, M.S.; El-Gazzar, M.G.; Parvez, M.K. Design, Synthesis and Anticancer Evaluation of Novel Quinazoline-Sulfonamide Hybrids. *Molecules* **2016**, *21*, 189. [[CrossRef](#)] [[PubMed](#)]
235. Chang, J.; Ren, H.; Zhao, M.; Chong, Y.; Zhao, W.; He, Y.; Zhao, Y.; Zhang, H.; Qi, C. Development of a series of novel 4-anilinoquinazoline derivatives possessing quinazoline skeleton: Design, synthesis, EGFR kinase inhibitory efficacy, and evaluation of anticancer activities in vitro. *Eur. J. Med. Chem.* **2017**, *138*, 669–688. [[CrossRef](#)] [[PubMed](#)]
236. Ahmed, M.F.; Khalifa, A.S.; Eed, E.M. Discovery of New Quinazoline-Based Anticancer Agents as VEGFR-2 Inhibitors and Apoptosis Inducers. *Russ. J. Bioorg. Chem.* **2022**, *48*, 739–748. [[CrossRef](#)]
237. ElZahabi, H.S.A.; Nafie, M.S.; Osman, D.; Elghazawy, N.H.; Soliman, D.H.; El-Helby, A.A.H.; Arafa, R.K. Design, synthesis and evaluation of new quinazolin-4-one derivatives as apoptotic enhancers and autophagy inhibitors with potent antitumor activity. *Eur. J. Med. Chem.* **2021**, *222*, 113609. [[CrossRef](#)]
238. Abdelsalam, E.A.; Zaghary, W.A.; Amin, K.M.; Abou Taleb, N.A.; Mekawey, A.A.I.; Eldehna, W.M.; Abdel-Aziz, H.A.; Hammad, S.F. Synthesis and in vitro anticancer evaluation of some fused indazoles, quinazolines and quinolines as potential EGFR inhibitors. *Bioorg. Chem.* **2019**, *89*, 102985. [[CrossRef](#)]
239. Hoan, D.Q.; Hoa, L.T.; Huan, T.T.; Dinh, N.H. Synthesis and Transformation of 4-(1-Chloro-1-nitroethyl)-6, 7-dimethoxy-2-methylquinazoline: Spectral Characterization and Anti-cancer Properties of some Novel Quinazoline Derivatives. *J. Heterocycl. Chem.* **2020**, *57*, 1720–1728. [[CrossRef](#)]
240. Wang, Z.; Liu, L.; Dai, H.; Si, X.; Zhang, L.; Li, E.; Yang, Z.; Chao, G.; Zheng, J.; Ke, Y.; et al. Design, synthesis and biological evaluation of novel 2,4-disubstituted quinazoline derivatives targeting H1975 cells via EGFR-PI3K signaling pathway. *Bioorg. Med. Chem.* **2021**, *43*, 116265. [[CrossRef](#)]
241. Zayed, M.F.; Rateb, H.S.; Ahmed, S.; Khaled, O.A.; Ibrahim, S.R.M. Quinazolinone-Amino Acid Hybrids as Dual Inhibitors of EGFR Kinase and Tubulin Polymerization. *Molecules* **2018**, *23*, 1699. [[CrossRef](#)] [[PubMed](#)]

242. Abuelizz, H.A.; Marzouk, M.; Ghabbour, H.; Al-Salahi, R. Synthesis and anticancer activity of new quinazoline derivatives. *Saudi Pharm. J.* **2017**, *25*, 1047–1054. [[CrossRef](#)] [[PubMed](#)]
243. Poudapally, S.; Battu, S.; Velatooru, L.R.; Bethu, M.S.; Janapala, V.R.; Sharma, S.; Sen, S.; Pottabathini, N.; Iska, V.B.R.; Katangoor, V. Synthesis and biological evaluation of novel quinazoline-sulfonamides as anti-cancer agents. *Bioorg. Med. Chem. Lett.* **2017**, *27*, 1923–1928. [[CrossRef](#)]
244. Ewes, W.A.; Elmorsy, M.A.; El-Messery, S.M.; Nasr, M.N.A. Synthesis, biological evaluation and molecular modeling study of [1,2,4]-Triazolo[4,3-c]quinazolines: New class of EGFR-TK inhibitors. *Bioorg. Med. Chem.* **2020**, *28*, 115373. [[CrossRef](#)] [[PubMed](#)]
245. Tariq, S.; Somakala, K.; Amir, M. Quinoxaline: An insight into the recent pharmacological advances. *Eur. J. Med. Chem.* **2018**, *143*, 542–557. [[CrossRef](#)]
246. Srivastava, S.; Banerjee, J.; Srestha, N. Quinoxaline as a potent heterocyclic moiety. *IOSR J. Pharm.* **2014**, *4*, 17–27. [[CrossRef](#)]
247. El Newahie, A.M.; Ismail, N.S.; Abou El Ella, D.A.; Abouzid, K.A.M. Quinoxaline-Based Scaffolds Targeting Tyrosine Kinases and Their Potential Anticancer Activity. *Arch. Pharm.* **2016**, *349*, 309–326. [[CrossRef](#)] [[PubMed](#)]
248. Ismail, M.M.; Amin, K.M.; Noaman, E.; Soliman, D.H.; Ammar, Y.A. New quinoxaline 1, 4-di-N-oxides: Anticancer and hypoxia-selective therapeutic agents. *Eur. J. Med. Chem.* **2010**, *45*, 2733–2738. [[CrossRef](#)] [[PubMed](#)]
249. Abbas, H.-A.S.; Al-Marhabi, A.R.; Eissa, S.I.; Ammar, Y.A. Molecular modeling studies and synthesis of novel quinoxaline derivatives with potential anticancer activity as inhibitors of c-Met kinase. *Bioorg. Med. Chem.* **2015**, *23*, 6560–6572. [[CrossRef](#)]
250. Desplat, V.; Vincenzi, M.; Lucas, R.; Moreau, S.; Savrimoutou, S.; Pinaud, N.; Lesbordes, J.; Peyrilles, E.; Marchivie, M.; Routier, S. Synthesis and evaluation of the cytotoxic activity of novel ethyl 4-[4-(4-substitutedpiperidin-1-yl)] benzyl-phenylpyrrolo [1, 2-a] quinoxaline-carboxylate derivatives in myeloid and lymphoid leukemia cell lines. *Eur. J. Med. Chem.* **2016**, *113*, 214–227. [[CrossRef](#)] [[PubMed](#)]
251. El Newahie, A.M.; Nissan, Y.M.; Ismail, N.S.; Abou El Ella, D.A.; Khojah, S.M.; Abouzid, K.A.M. Design and synthesis of new quinoxaline derivatives as anticancer agents and apoptotic inducers. *Molecules* **2019**, *24*, 1175. [[CrossRef](#)] [[PubMed](#)]
252. Ahmed, E.A.; Mohamed, M.F.; Omran, A.; Salah, H. Synthesis, EGFR-TK inhibition and anticancer activity of new quinoxaline derivatives. *Synth. Commun.* **2020**, *50*, 2924–2940. [[CrossRef](#)]
253. Alsaif, N.A.; Dahab, M.A.; Alanazi, M.M.; Obaidullah, A.J.; Al-Mehizia, A.A.; Alanazi, M.M.; Aldawas, S.; Mahdy, H.A.; Elkady, H. New quinoxaline derivatives as VEGFR-2 inhibitors with anticancer and apoptotic activity: Design, molecular modeling, and synthesis. *Bioorg. Chem.* **2021**, *110*, 104807. [[CrossRef](#)]
254. El-Adl, K.; Sakr, H.M.; Yousef, R.G.; Mehany, A.B.; Metwaly, A.M.; Elhendawy, M.A.; Radwan, M.M.; ElSohly, M.A.; Abulkhair, H.S.; Eissa, I.H. Discovery of new quinoxaline-2 (1H)-one-based anticancer agents targeting VEGFR-2 as inhibitors: Design, synthesis, and anti-proliferative evaluation. *Bioorg. Chem.* **2021**, *114*, 105105. [[CrossRef](#)]
255. Hajri, M.; Esteve, M.-A.; Khoumeri, O.; Abderrahim, R.; Terme, T.; Montana, M.; Vanelle, P. Synthesis and evaluation of in vitro antiproliferative activity of new ethyl 3-(arylethynyl) quinoxaline-2-carboxylate and pyrido [4, 3-b] quinoxalin-1 (2H)-one derivatives. *Eur. J. Med. Chem.* **2016**, *124*, 959–966. [[CrossRef](#)] [[PubMed](#)]
256. Karthikeyan, C.; Solomon, V.R.; Lee, H.; Trivedi, P.J.B.; Nutrition, P. Design, synthesis and biological evaluation of some isatin-linked chalcones as novel anti-breast cancer agents: A molecular hybridization approach. *Biomed. Prev. Nutr.* **2013**, *3*, 325–330. [[CrossRef](#)]
257. Eldehna, W.M.; El Hassab, M.A.; Abo-Ashour, M.F.; Al-Warhi, T.; Elaasser, M.M.; Safwat, N.A.; Suliman, H.; Ahmed, M.F.; Al-Rashood, S.T.; Abdel-Aziz, H.A. Development of isatin-thiazolo [3, 2-a] benzimidazole hybrids as novel CDK2 inhibitors with potent in vitro apoptotic anti-proliferative activity: Synthesis, biological and molecular dynamics investigations. *Bioorg. Chem.* **2021**, *110*, 104748. [[CrossRef](#)]
258. Abdel-Aziz, H.A.; Eldehna, W.M.; Keeton, A.B.; Piazza, G.A.; Kadi, A.A.; Attwa, M.W.; Abdelhameed, A.S.; Attia, M.I. Development, Therapy: Isatin-benzoazine molecular hybrids as potential antiproliferative agents: Synthesis and in vitro pharmacological profiling. *Drug Des. Dev. Ther.* **2017**, *11*, 2333. [[CrossRef](#)]
259. Meleddu, R.; Petrikaite, V.; Distinto, S.; Arridu, A.; Angius, R.; Serusi, L.; Škarnulytė, L.; Endriulaitytė, U.; Paškevičiūtė, M.; Cottiglia, F. Investigating the anticancer activity of isatin/dihydropyrazole hybrids. *ACS Med. Chem. Lett.* **2018**, *10*, 571–576. [[CrossRef](#)] [[PubMed](#)]
260. Eldehna, W.M.; Altoukhy, A.; Mahrous, H.; Abdel-Aziz, H.A. Design, synthesis and QSAR study of certain isatin-pyridine hybrids as potential anti-proliferative agents. *Eur. J. Med. Chem.* **2015**, *90*, 684–694. [[CrossRef](#)] [[PubMed](#)]
261. Al-Wabli, R.I.; Almomen, A.A.; Almutairi, M.S.; Keeton, A.B.; Piazza, G.A.; Attia, M.I. Development, Therapy: New Isatin–Indole Conjugates: Synthesis, Characterization, and a Plausible Mechanism of Their in vitro Antiproliferative Activity. *Drug Des. Dev. Ther.* **2020**, *14*, 483. [[CrossRef](#)]
262. Panga, S.; Podila, N.K.; Asres, K.; Ciddi, V. Synthesis and anticancer activity of new isatin-benzoic acid conjugates. *Ethiop. Pharm. J.* **2016**, *31*, 75–92. [[CrossRef](#)]
263. Ferguson, L.; Bhakta, S.; Fox, K.R.; Wells, G.; Brucoli, F. Synthesis and Biological Evaluation of a Novel C8-Pyrrolobenzodiazepine (PBD) Adenosine Conjugate. A Study on the Role of the PBD Ring in the Biological Activity of PBD-Conjugates. *Molecules* **2020**, *25*, 1243. [[CrossRef](#)] [[PubMed](#)]
264. Bose, D.S.; Idrees, M.; Todewale, I.K.; Jakka, N.; Rao, J.V. Hybrids of privileged structures benzothiazoles and pyrrolo [2, 1-c][1, 4] benzodiazepin-5-one, and diversity-oriented synthesis of benzothiazoles. *Eur. J. Med. Chem.* **2012**, *50*, 27–38. [[CrossRef](#)] [[PubMed](#)]

265. Kamal, A.; Ramakrishna, G.; Nayak, V.L.; Raju, P.; Rao, A.S.; Viswanath, A.; Vishnuvardhan, M.; Ramakrishna, S.; Srinivas, G. Design and synthesis of benzo [c, d] indolone-pyrrolobenzodiazepine conjugates as potential anticancer agents. *Bioorg. Med. Chem.* **2012**, *20*, 789–800. [[CrossRef](#)]
266. Chen, C.-Y.; Lee, P.-H.; Lin, Y.-Y.; Yu, W.-T.; Hu, W.-P.; Hsu, C.-C.; Lin, Y.-T.; Chang, L.-S.; Hsiao, C.-T.; Wang, J.; et al. Synthesis, DNA-binding abilities and anticancer activities of triazole-pyrrolo [2, 1-c][1, 4] benzodiazepines hybrid scaffolds. *Bioorg. Med. Chem. Lett.* **2013**, *23*, 6854–6859. [[CrossRef](#)]
267. Abu-Zied, K.M.; Mohamed, T.K.; Al-Duaij, O.K.; Zaki, M.E. A simple approach to fused pyrido [2, 3-d] pyrimidines incorporating khellinone and trimethoxyphenyl moieties as new scaffolds for antibacterial and antifungal agents. *Heterocycl. Commun.* **2014**, *20*, 93–102. [[CrossRef](#)]
268. Robins, R.K.; Hitchings, G.H. Studies on condensed pyrimidine systems. XIX. A new synthesis of pyrido [2, 3-d] pyrimidines. The condensation of 1, 3-diketones and 3-ketoaldehydes with 4-aminopyrimidines. *J. Am. Chem. Soc.* **1958**, *80*, 3449–3457. [[CrossRef](#)]
269. Kumar, R.N.; Dev, G.J.; Ravikumar, N.; Swaroop, D.K.; Debanjan, B.; Bharath, G.; Narsaiah, B.; Jain, S.N.; Rao, A.G. Synthesis of novel triazole/isoxazole functionalized 7-(trifluoromethyl) pyrido [2, 3-d] pyrimidine derivatives as promising anticancer and antibacterial agents. *Bioorg. Med. Chem. Lett.* **2016**, *26*, 2927–2930. [[CrossRef](#)]
270. Hou, J.; Wan, S.; Wang, G.; Zhang, T.; Li, Z.; Tian, Y.; Yu, Y.; Wu, X.; Zhang, J. Design, synthesis, anti-tumor activity, and molecular modeling of quinazoline and pyrido [2, 3-d] pyrimidine derivatives targeting epidermal growth factor receptor. *Eur. J. Med. Chem.* **2016**, *118*, 276–289. [[CrossRef](#)]
271. Banda, V.; Gaddameedi Jitender, D.; Gautham Santhosh, K.; Pillalamarri Sambasiva, R.; Chavva, K.; Rajesh, P.; Janapala Venkateswara, R.; Banda, N. Studies on Synthesis of Novel Pyrido [2, 3-d] pyrimidine Derivatives and Their Anticancer Activity. *J. Heterocycl. Chem.* **2018**, *55*, 2538–2544. [[CrossRef](#)]
272. Behalo, M.S.; Mele, G.J. Synthesis and evaluation of pyrido [2, 3-d] pyrimidine and 1, 8-naphthyridine derivatives as potential antitumor agents. *J. Heterocycl. Chem.* **2017**, *54*, 295–300. [[CrossRef](#)]
273. Elzahabi, H.S.; Nossier, E.S.; Khalifa, N.M.; Alasfoury, R.A.; El-Manawaty, M.A.; Chemistry, M. Anticancer evaluation and molecular modeling of multi-targeted kinase inhibitors based pyrido [2, 3-d] pyrimidine scaffold. *J. Enzyme. Inhib. Med. Chem.* **2018**, *33*, 546–557. [[CrossRef](#)]
274. Faidallah, H.M.; Rostom, S.A.; Khan, K.A. Synthesis of some polysubstituted nicotinonitriles and derived pyrido [2, 3-d] pyrimidines as in vitro cytotoxic and antimicrobial candidates. *J. Chem.* **2016**, *2016*, 1–12. [[CrossRef](#)]
275. Al-Warhi, T.; Sallam, A.-A.M.; Hemeda, L.R.; El Hassab, M.A.; Aljaeed, N.; Alotaibi, O.J.; Doghish, A.S.; Noshay, M.; Eldehna, W.M.; Ibrahim, M.H. Identification of Novel Cyanopyridones and Pyrido [2, 3-D] Pyrimidines as Anticancer Agents with Dual VEGFR-2/HER-2 Inhibitory Action: Synthesis, Biological Evaluation and Molecular Docking Studies. *Pharmaceuticals* **2022**, *15*, 1262. [[CrossRef](#)]
276. Ding, J.; Liu, T.; Zeng, C.; Li, B.; Ai, Y.; Zhang, X.; Zhong, H. Design, synthesis, and anti-breast-cancer activity evaluation of pyrrolo (pyrido)[2, 3-d] pyrimidine derivatives. *Chem. Heterocycl. Compd.* **2022**, *58*, 438–448. [[CrossRef](#)]

Disclaimer/Publisher’s Note: The statements, opinions and data contained in all publications are solely those of the individual author(s) and contributor(s) and not of MDPI and/or the editor(s). MDPI and/or the editor(s) disclaim responsibility for any injury to people or property resulting from any ideas, methods, instructions or products referred to in the content.